Probabilistic Methods in Geotechnical Engineering

Edited by Gordon A. Fenton

Workshop presented at
ASCE GeoLogan'97 Conference, Logan, Utah

July 15, 1997

Sponsored by ASCE Geotechnical Safety and Reliability Committee

Foreword

Uncertainty is a fact of life in geotechnical and geoenvironmental engineering practice. Nature in its complexity offers soil profiles often very different from those assumed in analysis and design; loads and environmental conditions likewise defy accurate prediction; and limited sampling, measurement errors and shortcomings of analysis procedures further complicate the engineer's task. Probabilistic methods, complementing conventional analyses, provide the means for quantifying and communicating degrees of uncertainty, evaluating data acquisition strategies, and assessing hazard mitigation measures. The methods range from probabilistic site characterization, which involves quantifying the variability and heterogeneity of stratigraphy and material properties, to risk-based decision analysis, which provides a framework for identifying the kinds and degrees of risk involved in a project, and the consequences should "failure" occur, and evaluating the effectiveness of alternative actions (in site exploration, design, construction, or monitoring) aimed at controlling or reducing risks.

These lecture notes for the Workshop on Probabilistic Methods in Geotechnical Engineering present basic concepts of probabilistic modeling, along with many examples of how they can be used to deal with uncertainties inherent in site characterization and geotechnical performance prediction, safety assessment and monitoring. The notes progress through increasingly complex methodology, starting with the basics of event and fault trees, through single and multiple random variables, to fundamentals of random fields and geostatistics. Among the applications considered: rock slope maintenance, clay barrier containment, proof testing of piles, and predicting differential settlement. Appended to the notes are some excerpts, rich with references, from the 1995 National Research Council Report on Probabilistic Methods in Geotechnical Engineering.

The workshop notes were prepared by the individual lecturers, Professors T.H. Wu, Robert Gilbert, Wilson Tang and Gordon Fenton, all members of the ASCE-GT Safety and Reliability Committee. Although efforts were made to obtain coherence and continuity of coverage, it is expected that the notes will benefit from further editing based on the experience gained at the workshop and attendees' and readers' comments, and can subsequently serve as the basis for similar committee-sponsored educational and professional activities. Many thanks, on behalf of the Committee, to the contributors and to the workshop participants.

Erik H. Vanmarcke
Chair, Safety and Reliability Committee,
Geotechnical Engineering Division, ASCE

Logan, Utah
July, 1997

Table of Contents

Page

Chapter 1

Events, Event and Fault Trees, Bayes' Theorem

by Tien H. Wu

1.1 Definitions

Events and Probabilities

Events are outcomes, or combinations of outcomes, arising from an 'experiment'. 'Experiment' is used here in a general sense; an example is whether a slope fails or not. One possible outcome of this experiment, or event, is failure of the slope. A random event is one whose occurrence is not known with certainty but can only be associated with a probability that the event will occur. An example is the probability that the slope will fail. Events are generally denoted using capital letters, for example failure will be denoted F and non-failure by its complement $\bar{F}$. The probability that an event F will occur is denoted by P [F].

Example 1: Failure of a rock slope

Consider several maintenance activities, M_i, for a rock slope. Example events are that a maintenance activity is effective, E, or ineffective, $\bar{E}$. In either case, E or $\bar{E}$, there is a probability that the slope will fail, which is also an event, denoted by F. The consequence of failure, C_k is another example of an event. Some possible consequences are damage or remediation costs (C_1 in dollars), service disruption (C_2 in days), etc. Each consequence is a random event with an associated probability. For example the probabilities that C_2 = 3 days or that $C_1 > \$100,000$ are written P [C_2 = 3] and P $\left[C_1 > \$100,000\right]$, respectively. Probabilities are numbers between 0 and 1 with larger likelihoods of occurrence being closer to 1.

Combination of events

The conditional event, $A \mid B$, is the event that A occurs given that event B has occurred. As an example, the event of slope failure, F, given a maintenance activity is effective, E, is written $F \mid E$. Intuitively, we should be better able to estimate the probability of event F, if we are given some condition, such as that the maintenance activity is effective. The intersection of events, written $A \cap B$, means that both A and B occur, while the union of events, written $A \cup B$, means that either A or B or both occur. An example of intersection, also called joint occurrence, is that a slope fails and the cost C_2 = 3 days. An example of union is the cost C_1 = \$5000, or C_2 = 3 days, or both.

Event Tree

An event tree is a graphical description of all possible subsequent events following an initial event. Fig. 1.1 shows an event tree for rock slope failure. Each branch of the tree is associated with an event. Maintenance activity 1 is the initial event; it is either effective (E) or ineffective ($\bar{E}$). An effective maintenance activity is expected to reduce the probability of failure of the slope but

cannot eliminate entirely the possibility of failure. Thus, the branch representing the event that the maintenance activity was effective, E, has two sub-branches representing failure (F) or non-failure ($\bar{F}$) with associated probabilities. The failure event, F, has a set of possible consequences, C_j, each with an associated probability. The tree can be used to assess either the overall probability of failure or the probabilities of the consequence, which is often expressed as a dollar cost.

Note that each event, or branch in the event tree, is conditional on the sequence of events leading up to that branch. Fig. 1.1 shows the conditions leading up to a branch of the tree. The probabilities are therefore conditional probabilities. The event E arising from maintenance activity M_1 can be explicitly written as $E \mid M_1$. Similarly, the probability of the consequence, C_1, shown in the upper right branch, is P $\left[C_1 > c \mid M_1 \cap E \cap F\right]$ which is the probability that the cost C_1 is greater than some specified amount c given that maintenance activity M_1 was employed, that it was effective, but that failure occurred.

Each branch of the tree can lead to any number of possible subsequent events; Fig. 1.1 shows only a small subset of events leading from mitigation measure M_1. One advantage of the event tree is that it forces the careful identification of all possible events leading to failure and/or serviceability problems. Once the tree has been constructed, one can proceed to evaluate the conditional probability of each event (branch).

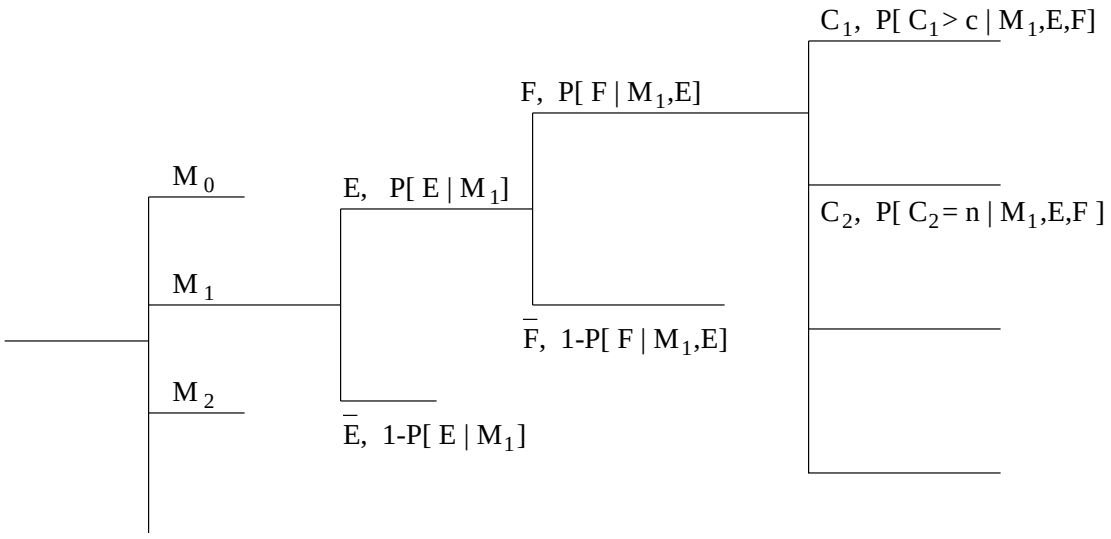

Figure 1.1 Example event tree

Fault Tree

Where the causes, or events, that could lead to failure are complex, a fault tree may be constructed to identify and describe the various events and their relation to failure. A fault tree is a decomposition of the top event, such as failure, into a combination of subevents. A simplified example is given in Fig. 1.2. The top event, slope failure, could result from a rock fall *or* a wedge slide; this is shown by the symbol (+). Assume that a wedge slide could occur only if there is a high pore pressure along a weak plane. Then both a weak plane *and* high pore pressure must occur and this is shown by the symbol (·). If high pore pressure would occur when there is heavy rainfall *or* when the drains are ineffective, then the subevents are connected by a (+).

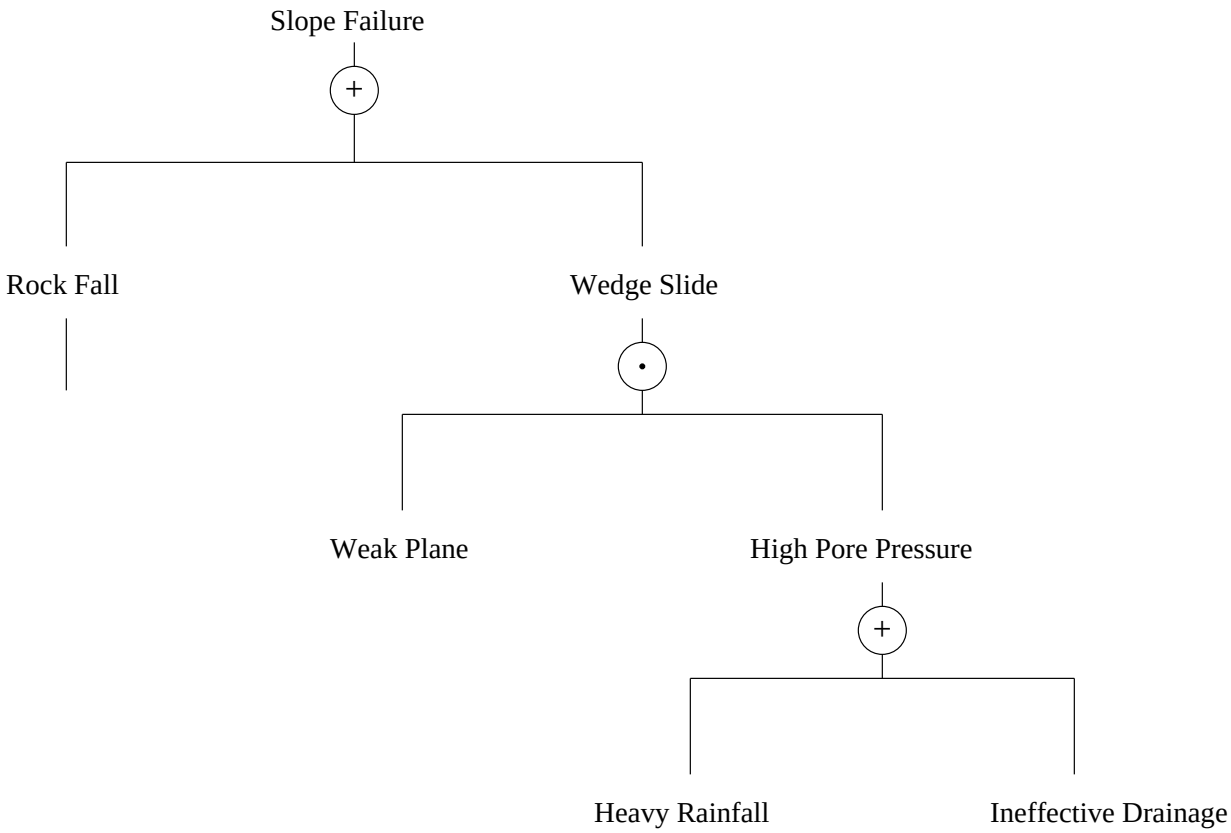

Figure 1.2 Example fault tree

1.2 Fundamental Relations

When events are considered in combination, there are some simple formulae that allow us to compute probabilities;

$$\mathrm{P}[A \cap B] = \mathrm{P}\left[A \mid B\right] \cdot \mathrm{P}[B] = \mathrm{P}\left[B \mid A\right] \cdot \mathrm{P}[A] \tag{1.1}$$

$$\mathrm{P}[A \cup B] = \mathrm{P}[A] + \mathrm{P}[B] - \mathrm{P}[A \cap B] \tag{1.2}$$

The probability of an event, $\mathrm{P}[A]$, lies between 0 and 1,

$$0 \leq \mathrm{P}[A] \leq 1 \tag{1.3}$$

while the probability of a certain event, $[\Omega]$, is

$$\mathrm{P}[\Omega] = \mathrm{P}\left[A \cup \bar{A}\right] = 1 \tag{1.4}$$

If all possible causes, B_i, of an event, which may be slope failure, are identified and the probabilities of failure given each cause are determined, they can be combined using the *Total Probability Theorem* to give

$$\mathrm{P}[A] = \mathrm{P}\left[A \mid B_1\right] \mathrm{P}[B_1] + \mathrm{P}\left[A \mid B_2\right] \mathrm{P}[B_2] + \cdots + \mathrm{P}\left[A \mid B_n\right] \mathrm{P}[B_n] \tag{1.5}$$

which gives the probability of the event in question by using the probabilities that each 'cause' B_i occurs. The events B_i are mutually exclusive and collectively exhaustive.

Example 1 (continued). The above relations can be used to evaluate probabilities of combination of events in the event tree shown in Fig. 1.1. If one were interested in the probability of failure given that the maintenance activity M_1 was undertaken, then one could combine the conditional probability of failure arising from all branches from M_1;

$$\begin{aligned} \mathrm{P}\left[F \mid M_1\right] &= \mathrm{P}\left[F \mid E \cap M_1\right] \mathrm{P}\left[E \mid M_1\right] + \mathrm{P}\left[F \mid \bar{E} \cap M_1\right] \mathrm{P}\left[\bar{E} \mid M_1\right] \\ &= \mathrm{P}\left[F \mid E \cap M_1\right] \mathrm{P}\left[E \mid M_1\right] + \mathrm{P}\left[F \mid \bar{E} \cap M_1\right] \left(1 - \mathrm{P}\left[E \mid M_1\right]\right) \end{aligned} \quad (1.6)$$

where the branches leading from event $\bar{E}$ are similar to those leading from event E. Likewise, the overall probability of failure for uncertain maintenance activities is obtained by a summation of all the M_i's;

$$\mathrm{P}\left[F\right] = \sum_{i=1}^{n} \mathrm{P}\left[F \mid M_i\right] \mathrm{P}\left[M_i\right] \quad (1.7)$$

Suppose that the following probabilities have been estimated;

- the probability that maintenance activity M_1 is effective is $\mathrm{P}\left[E \mid M_1\right] = 0.7$,
- the probability of failure given that maintenance activity M_1 was used and is effective is $\mathrm{P}\left[F \mid E \cap M_1\right] = 0.1$,
- the probability of failure given that maintenance activity M_1 was used and is not effective is $\mathrm{P}\left[F \mid \bar{E} \cap M_1\right] = 1.0$,

then the probability of failure given M_1 is taken from Eq. (1.6),

$$\mathrm{P}\left[F \mid M_1\right] = (0.1)(0.7) + (1.0)(1 - 0.7) = 0.37$$

Furthermore, if the probability that the cost $C_1 > c$ given failure is $\mathrm{P}\left[C_1 > c \mid F \cap M_1\right] = 0.2$ while the probability that the cost $C_1 > c$ given that the system does not fail is $\mathrm{P}\left[C_1 > c \leq c \mid \bar{F} \cap M_1\right] = 0.0$, for some value c, then the probability that the cost $C_1 > c$ given that maintenance activity M_1 was employed is

$$\begin{aligned} \mathrm{P}\left[C_1 > c \mid M_1\right] &= \mathrm{P}\left[C_1 > c \mid F \cap M_1\right] \mathrm{P}\left[F \mid M_1\right] + \mathrm{P}\left[C_1 > c \mid \bar{F} \cap M_1\right] \mathrm{P}\left[\bar{F} \mid M_1\right] \\ &= (0.2)(0.37) + (0.0)(1 - 0.37) = 0.074 \end{aligned}$$

1.3 Random Variables

Random variables are variables whose values are not known with certainty. A probability is associated with the event that a random variable will have a given value. Consider first the case of a discrete random variable, which takes values from a discrete set of possibilities. For example, the number of slope failures can be represented by the random variable N. The event $N = 3$ corresponds to the event that there are 3 slope failures. The associated set of probabilities is called the *probability mass function* (pmf), $p_N(n) = \mathrm{P}\left[N = n\right]$, $n = 0, 1, 2, \ldots$

If the random variable is continuous, probabilities can be derived from a continuous function called the *probability density function* (pdf), denoted $f_X(x)$. Unlike the *mass* function, the *density*

function is not in itself a probability – it must be multiplied by a length measure before becoming a probability, hence the use of the word *density*. Thus, for continuous random variables, probabilities are associated with intervals. The probability that the continuous random variable X lies between x and $x + dx$ is $f_X(x)\,dx$. An example is that the shear strength of a soil lies between 90 and 100 kPa. Note that the probability that a sample has strength exactly 98.00 . . . kPa is vanishingly small. Since $f_X(x)$ generally varies with x, the probability that X lies between a and b must be obtained as a sum of probabilities;

$$\mathrm{P}\,[a < X \leq b] = \int_a^b f_X(x)\,dx$$

In Example 1, the remediation cost, C_1, in dollars is treated as a continuous random variable, while the delay cost, C_2, in days is treated as a discrete random variable.

Methods for establishing pmf and pdf from data are described in Section 2.4.3. When sufficient data are not available, subjective probability based on judgement may be used. An example is the probability that a slope will fail in a certain mode. To estimate the annual probability of failure in mode 1, one might count the annual number failures in mode 1 that have occurred over a large number of similar rock slopes over a year and divide this number by the total number of rock slopes considered. This would lead to an estimate of the pmf $p_{N_{F_1}}(n)$, where F_1 denotes a mode 1 failure. Unfortunately, this requires records of failures on many similar slopes. Such records are often not available, as in the present example. Alternatively, if enough information is available on the properties of the rock mass and the loads acting on it, then the failure probability $\mathrm{P}\,[F_1]$ can be estimated as described in Chapter 2. When the required information is not available, it is necessary to estimate the probabilities using engineering judgement based on experience and observation in the field.

Subjective probability plays an important role in engineering because it provides a rational procedure for incorporating the engineer's experience and judgement into the design process. It is an expression of the 'degree of belief', or, according to de Fenetti (1970), "... having obtained the information that some events have occurred, what are we entitled to say about ... events not yet known." Formal methods for encoding subjective probability are available (e.g. Hampton *et al.*, 1973, Morris, 1974, Spetzler and Stael von Holstein, 1975).

Example 2: Subjective Probability

Subjective probability was used in a project to choose the optimum maintenance activities by Roberds (1991). The following are examples from Roberds' paper. Fig. 1.3a shows the pmf, $p_{N_{F_1}}(n \mid M_0) = \mathrm{P}\left[N_{F_1} = n \mid M_0\right]$, that represents the subjective probability of number of failures in mode 1 on a specific slope for a given period if no maintenance (M_0) were implemented. Mode 1 denotes isolated rock falls. Estimates of $p_{N_{F_i}}(n \mid M_0)$ were also made for modes 2, 3, etc., which are small individual wedge slides, large individual wedge slides, etc. Fig 1.3b shows the pdf, $f_{E_1}(e \mid M_1)$, which represents the subjective probability density of the effectiveness, E_1, of the maintenance activity, M_1, in reducing the number of failures in mode 1. M_1 denotes scaling and E_1 is expressed as the reduction, as a fraction, of the number of failures from the case of no maintenance activity, $N_{F_1} \mid M_0$. Estimates of $f_{E_j}(e \mid M_1)$ for the effectiveness of other maintenance activities, where are M_2 = isolated rock bolts, M_3 = rock bolts with mesh and shotcrete, etc.

Fig. 1.3c shows the subjective probability $f_{C_1}(c \mid F_1 \cap M_0)$ of the consequence C_1 given a failure in mode 1 with no maintenance activity. C_1 denotes remediation cost in dollars. Estimates of $f_{C_k}(c \mid F_j \cap M_0)$ were also made for other costs, C_k, for example C_2 = service disruption in days, C_3 = number of injuries, etc.

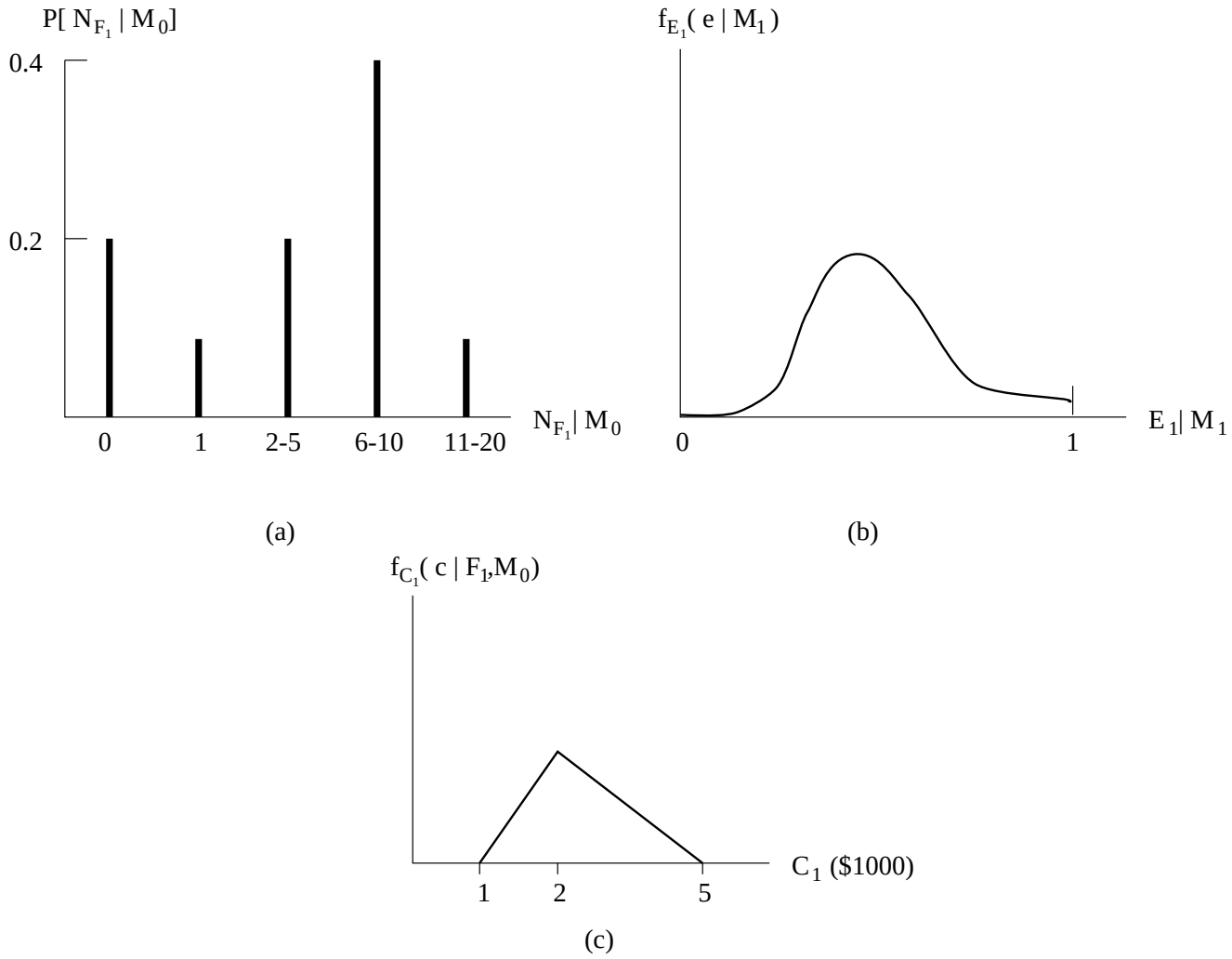

Figure 1.3 Subjective probabilities

1.4 Decisions under Uncertainty

A very important application of probability analysis is to evaluate and compare different design or maintenance options. Engineering decisions are usually made in the face of some uncertainty, since future events, such as the magnitude of a potential earthquake or intensity of a future rainstorm, cannot be predicted with certainty. In Example 1, the number of failures on the different slopes and the effectiveness of the different maintenance activities are all uncertain and are described by probabilities. Consequently, the outcome of any design or maintenance option cannot be predicted with certainty. Use of probability methods in decision making allows the various uncertainties and their effects to be accounted for in a systematic manner. For example, in Fig. 1.1, the consequences C_k of any maintenance activity M_i are given as probability distributions. The decision on which maintenance activity to adopt can be based on the most likely outcomes, or the expected value of the consequences that follow from the different maintenance options. Expected value denotes the mean value of the pdf of the consequence. When the events M_i denote options in a decision-making process, the tree is called a decision tree.

Example 3: Maintenance Strategy for Rock Slopes

Consider now maintenance activities, M_i, for rock slopes with F_j, $j = 1, 2, \ldots$ possible modes of failure and associated consequences C_k, all of which will be random variables. For each possible failure mode there may be several possible consequences, as illustrated in Fig. 1.4.

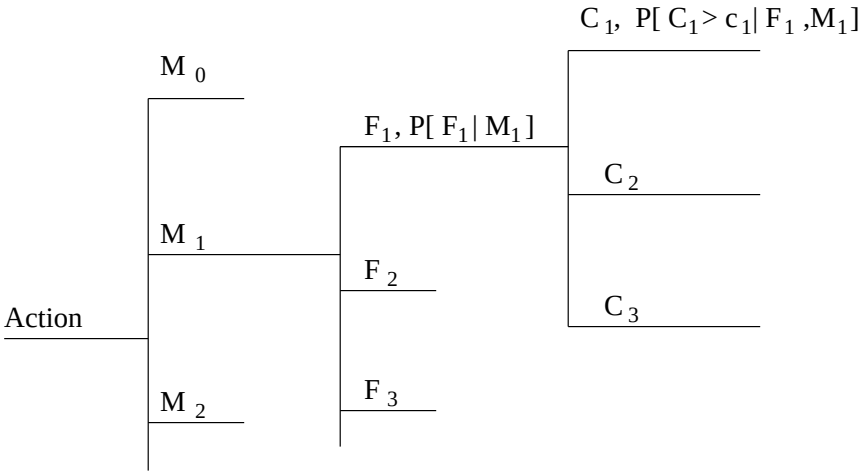

Figure 1.4 Event tree for rock slope maintenance activities

For a given maintenance activity, the probabilities associated with the consequence cost (C_1) can be determined by summing, over all failure modes, the cost probability of each mode, weighted by the probability of occurrence of that mode; using Eq. (1.5),

$$\mathrm{P}\left[C_1 > c \,|\, M_i\right] = \sum_j \mathrm{P}\left[C_1 > c \,|\, F_j \cap M_i\right] \mathrm{P}\left[F_j \,|\, M_i\right] \tag{1.8}$$

where it is assumed that a rock slope can fail in only one mode at a time, i.e. modes are disjoint or mutually exclusive. If a slope can fail in more than one mode at a time then the probabilities of the different joint occurrences must be assessed. For example, if a slope can fail in modes 1, 2, or both, then the possible joint occurrences are the combination of events: $A_1 = F_1 \cap \bar{F}_2$ (mode 1 *alone*), $A_2 = \bar{F}_1 \cap F_2$ (mode 2 *alone*), and $A_{12} = F_1 \cap F_2$ (both modes). These constitute distinct and disjoint events in Eq. (1.8). In this case, if all other modes are disjoint, the cost probability would be calculated as

$$\begin{aligned}\mathrm{P}\left[C_1 > c \,|\, M_i\right] = {} & \mathrm{P}\left[C_1 > c \,|\, A_1 \cap M_i\right] \mathrm{P}\left[A_1 \,|\, M_i\right] \\ & + \mathrm{P}\left[C_1 > c \,|\, A_2 \cap M_i\right] \mathrm{P}\left[A_2 \,|\, M_i\right] \\ & + \mathrm{P}\left[C_1 > c \,|\, A_{12} \cap M_i\right] \mathrm{P}\left[A_{12} \,|\, M_i\right] \\ & + \sum_{j=3} \mathrm{P}\left[C_1 > c \,|\, F_j \cap M_i\right] \mathrm{P}\left[F_j \,|\, M_i\right]\end{aligned} \tag{1.9}$$

In general, all the *conditions* appearing in the sum on the right hand side must be disjoint and collectively exhaustive, according to the Total Probability Theorem.

Once the probability distribution of the implementation costs of each maintenance activity has been obtained, the expected cost can be computed (see Section 2.4.3) and compared with expected

costs of other maintenance activities, including no action, M_0. Then decisions can be made after a comparison of the expected costs.

Problems involving real slopes may be more complicated than the simplified examples given above. A portion of the event tree for the rock slope problem described by Roberds (1991) is shown in Fig. 1.5. In this case it was necessary to estimate the number of slope failures and multiply this by the consequence of one failure. For example, the consequence, C_1, or failures in mode 1, given maintenance activity M_1 is

$$C_1 \mid F_1 \cap M_1 = \{N_{F_1} \mid M_1\}\{C_1 \mid F_1 \cap M_1\} \tag{1.10}$$

The number of failures given maintenance activity 1, $N_{F_1} \mid M_1$, was obtained by applying the effectiveness E of M_1 to $N_{F_1} \mid M_0$. The consequence, C_1, of M_1 for all failure modes is obtained by summation

$$C_1 \mid M_1 = \sum_j \{N_{F_j} \mid M_1\}\{C_1 \mid F_j \cap M_1\} \tag{1.11}$$

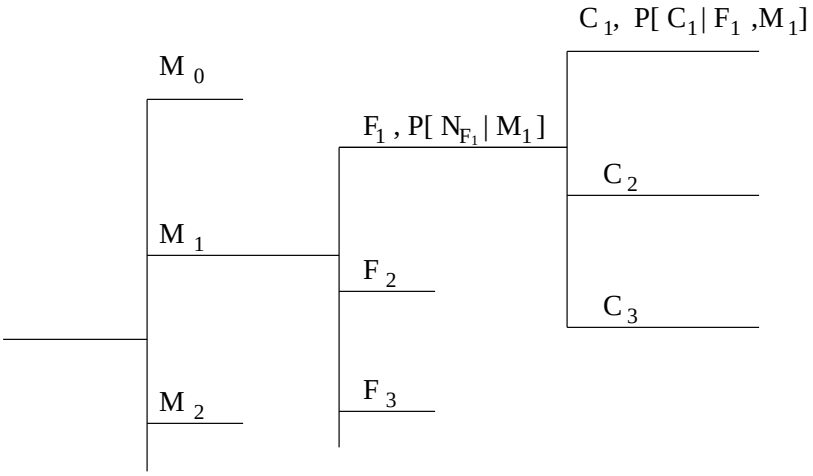

Figure 1.5 Event tree for rock slope maintenance strategies (after Roberds, 1991)

This was done for all consequences and all maintenance activities. Examples of the pmf of N_{F_1} and the pdf's of E and C are shown in Fig. 1.2. Because of the complicated pdf's, the probability distributions of consequences were obtained by Monte Carlo simulation. The results are given in Table 1.1, which gives the implementation costs, I_i, the consequences, $C_k \mid M_i$, and the total equivalent cost $U \mid M_i$ of each maintenance activity M_i. The total equivalent cost is the result of combining the different types of consequences. The equivalent costs show that maintenance activity M_3, rock bolts with mesh and shotcrete has the lowest expected equivalent cost and should be chosen. Further considerations on the choice of the maintenance activity are described in the paper. Roberds also shows that this method can be extended to all the slopes in a given stretch of roadway.

For more details on the event tree approach to risk assessment and probabilistic design optimization, the interested reader should consult Ang and Tang (1984, pp 498-509), Roberds (1991), or Vanmarcke (1974 and 1989).

Table 1.1 Implementation costs, consequences, and total equivalent costs for alternative preventative maintenance activities (from Roberds, 1991)

Costs & Consq.			**Preventative Maintenance Activities**						
		M_0	M_1	M_2	M_3	M_4	M_5	M_6	M_7
I_i	min	0	1	5	20	100	50	10	10
($1000)	mode	0	2	10	50	200	100	25	15
	max	0	5	50	100	500	150	50	20
$C_1 \mid M_i$	5%	0	0	0	0	0	0	0	0
($1000)	mean	25	14	19	7	5	14	21	12
	95%	66	54	64	37	29	54	59	35
$C_2 \mid M_i$	5%	0	0	0	0	0	0	0	0
($days$)	mean	4.7	2.7	3.7	1.3	0.9	2.0	4.2	2.4
	95%	14	10	13	7.9	5.9	8.1	12	7.6
$C_3 \mid M_i$	5%	0	0	0	0	0	0	0	0
($person$)	mean	2.3	1.1	1.8	0.5	0.4	1.3	2.3	0.6
	95%	7.0	4.4	6.1	2.8	2.8	5.3	7.0	2.3
$C_4 \mid M_i$	5%	0	0	0	0	0	0	0	0
($\$million$)	mean	2.7	0.9	1.6	0.5	0.3	1.1	2.0	2.0
	95%	8.9	4.4	6.1	2.7	2.3	4.8	7.2	6.5
$U\{M_i\}$	5%	0	0	0	0	0.2	0.1	0	0
($\$million$)	mean	3.1	1.1	1.9	0.6	0.7	1.4	2.3	2.2
	95%	9.9	5.0	7.0	3.2	3.0	5.5	7.9	6.8

Notes: 1) Implementation costs are in terms of triangular pdf (min - most likely or mode - max), with insignificant correlation.
2) Consequences and total equivalent costs are in terms of 5% - expected value - 95%, and are correlated (both among consequences and among activities).

1.5 Bayes' Theorem and Updating

Bayes' theorem allows the updating of probabilities given additional information or observations. For example, if the event Z is observed, then the updated probability that the event A occurs given that Z occurred is

$$\mathrm{P}\left[A \mid Z\right] = \frac{\mathrm{P}\left[Z \mid A\right] \mathrm{P}\left[A\right]}{\mathrm{P}\left[Z\right]} \tag{1.12}$$

We often say that $\mathrm{P}\left[A \mid Z\right]$ is the updated, or *posterior*, probability of the event A. The probability before obtaining data Z, $\mathrm{P}\left[A\right]$, is called the *prior* probability.

Bayes' Theorem provides a formal approach to the introduction of new information to update probabilities and combining different types of information, including judgement. In applications, Eq. (1.12) is usually written as

$$\mathrm{P}''\left[\theta = \theta_j \mid Z\right] = K\,\mathrm{P}\left[Z \mid \theta = \theta_i\right] \mathrm{P}'\left[\theta = \theta_i\right] \tag{1.13}$$

for discrete random variables, where θ is the state of nature, P′[$\theta = \theta_i$] and P″[$\theta = \theta_j \mid Z$] are the prior and posterior probabilities, respectively, $\mathrm{P}\left[Z \mid \theta = \theta_i\right]$ is the likelihood of getting the observation or data Z given the state of nature is θ_i, and K is a normalization constant.

For continuous random variables, Eq. (1.12) becomes

$$f''(\theta) = k\, L(\theta)\, f'(\theta) \tag{1.14}$$

where $f'(\theta)$ and $f''(\theta)$ are the prior and posterior probabilities, respectively, $L(\theta)$ is the likelihood function, and k is a normalization constant. The uncertain state of nature θ is represented by a parameter of the pmf or pdf that describes the random variable under consideration.

Example 4:

Returning to the number of slope failures in Example 2, assume that the subjective probability of number of failures, $p_N(n)$, in Fig. 1.3a, which is also the prior probability, can be represented by a Poisson distribution (see Section 2.4.2, Table 2.5) with a mean rate of occurrence of $\nu = 1/\text{year}$ and a variance of 1. Here, ν is the parameter θ in Eq. (1.14) that represents the uncertain state of nature. Now consider the case in which observations were made for a year and 1 failure occurred. This data point is insufficient for deriving the distribution $p_N(n)$. Nevertheless, it is a valuable addition to the subjective probability and is used to obtain a posterior probability. Calculations can be simplified if $L(\nu)$ and $f'(\nu)$ have certain forms that allow close-form solutions to be obtained for $f''(\nu)$ (Ang and Tang, 1975, pp 351–354). Using the method of conjugate distributions, ν is assumed to have a Gamma distribution with prior parameters $r' = 1$ and $k' = 1$. Following the examples in Ang and Tang, we obtain $r'' = 2$ and $k'' = 2$. This gives a mean value of $\nu'' = 1/\text{year}$ and $\mathrm{Var}[\nu] = 0.5$. Note that the posterior mean rate remains the same because the observations gave the same rate. However, the posterior variance of ν is 0.5 which reflects a reduction in uncertainty due to the observation. The posterior distribution $f''(\nu)$ can be used to derive a posterior distribution $p''_N(n)$ (see Benjamin and Cornell, 1970, pp 632–635), which can be used to revise the implementation costs of the maintenance activities. For other examples of probabilistic updating, see Tang, 1971, and Wu *et al.*, 1987.

Chapter 2

Basic Random Variables

by Robert B. Gilbert

2.1 Introduction

In the last chapter, you learned how to work with events and their associated probabilities of occurrence. In this chapter, we will introduce a tool that is useful for evaluating the probability of an event: the random variable. First, we will provide graphical and numerical methods to represent, understand and quantify variability. Next, we will present the random variable as a theoretical tool for modeling variability. Finally, we will demonstrate how random variable models can be used in design by introducing the reliability-based design approach.

2.2 Graphical Analysis of Variability

Variability often leads to uncertainty. We do not know what the unit weight of a soil is at a particular location unless we have measured it at that location. This uncertainty arises because the unit weight varies from point to point in the soil. For example, unit weight measurements from a boring are presented in Table 2.1. This boring was drilled offshore in the Gulf of Mexico at the location of an oil production platform. The soil consists of a normally consolidated clay over the length of the boring. The unit weight varies with depth, and ranges from 95 to 125 pcf.

In this section, we will present five graphical methods for analyzing variability: histograms, frequency plots, frequency density plots, cumulative frequency plots and scatter plots.

2.2.1 Histograms

A histogram is obtained by dividing the data range into bins, and then counting the number of values in each bin. The unit weight data are divided into 4-pcf wide intervals from 90 to 130 pcf in Table 2.2. For example, there are zero values between 90 and 94 pcf (Table 2.1), two values between 94 and 98 pcf, etc. A bar-chart plot of the number of occurrences in each interval is called a *histogram*. The histogram for unit weight is shown on Fig. 2.1.

The histogram conveys important information about variability in the data set. It shows the range of the data, the most frequently occurring values, and the amount of scatter about the middle values in the set.

There are several issues to consider in determining the number of intervals for a histogram. First, the number of intervals should depend on the number of data points. As the number of data points increases, the number of intervals should also increase. Second, the number of intervals can affect

Table 2.1 Total Unit Weight Data from Offshore Boring

Number	Depth (ft)	Total Unit Weight, x (pcf)	$(x-\hat{\mu}_x)^2$ (pcf)^2	$(x-\hat{\mu}_x)^3$ (pcf)^3	Sorted Values: Depth (ft)	Sorted Values: Total Unit Weight (pcf)
1	0.5	105	7.2	-19.4	172.0	95
2	1.0	119	128.0	1447.7	7.5	96
3	1.5	117	86.7	807.6	5.0	99
4	5.0	99	75.5	-655.7	22.0	99
5	6.5	101	44.7	-299.1	45.0	99
6	7.5	96	136.6	-1596.5	102.0	99
7	16.5	114	39.8	251.5	19.0	100
8	19.0	100	59.1	-454.3	27.5	100
9	22.0	99	75.5	-655.7	37.5	100
10	25.0	102	32.3	-184.0	50.0	100
11	27.5	100	59.1	-454.3	81.5	100
12	31.0	101	44.7	-299.1	121.5	100
13	34.5	101	44.7	-299.1	6.5	101
14	37.5	100	59.1	-454.3	31.0	101
15	40.0	101	44.7	-299.1	34.5	101
16	45.0	99	75.5	-655.7	40.0	101
17	50.0	100	59.1	-454.3	62.0	101
18	60.5	103	22.0	-103.0	122.0	101
19	62.0	101	44.7	-299.1	132.0	101
20	71.5	106	2.8	-4.8	25.0	102
21	72.0	109	1.7	2.3	91.5	102
22	81.5	100	59.1	-454.3	112.0	102
23	82.0	104	13.6	-50.1	152.5	102
24	91.5	102	32.3	-184.0	60.5	103
25	101.5	106	2.8	-4.8	82.0	104
26	102.0	99	75.5	-655.7	142.5	104
27	112.0	102	32.3	-184.0	322.0	104
28	121.5	100	59.1	-454.3	0.5	105
29	122.0	101	44.7	-299.1	162.0	105
30	132.0	101	44.7	-299.1	71.5	106
31	142.5	104	13.6	-50.1	101.5	106
32	152.5	102	32.3	-184.0	272.0	106
33	162.0	105	7.2	-19.4	201.5	107
34	172.0	95	161.0	-2042.3	281.5	108
35	191.5	116	69.1	574.4	72.0	109
36	201.5	107	0.5	-0.3	251.5	109
37	211.5	112	18.6	80.2	271.5	109
38	241.5	114	39.8	251.5	261.8	110
39	251.5	109	1.7	2.3	292.0	111
40	261.8	110	5.3	12.4	211.5	112
41	271.5	109	1.7	2.3	311.5	112
42	272.0	106	2.8	-4.8	341.5	112
43	281.5	108	0.1	0.0	411.5	112
44	292.0	111	11.0	36.3	432.0	112
45	301.5	125	299.7	5188.9	331.5	113
46	311.5	112	18.6	80.2	342.0	113
47	322.0	104	13.6	-50.1	16.5	114
48	331.5	113	28.2	149.9	241.5	114
49	341.5	112	18.6	80.2	371.5	114
50	342.0	113	28.2	149.9	391.5	114
51	352.0	116	69.1	574.4	402.0	114
52	361.5	124	266.1	4340.7	381.5	115
53	362.0	117	86.7	807.6	392.0	115
54	371.5	114	39.8	251.5	412.0	115
55	381.5	115	53.5	391.0	421.5	115
56	391.5	114	39.8	251.5	442.0	115
57	392.0	115	53.5	391.0	191.5	116
58	402.0	114	39.8	251.5	352.0	116
59	411.5	112	18.6	80.2	1.5	117
60	412.0	115	53.5	391.0	362.0	117
61	421.5	115	53.5	391.0	1.0	119
62	432.0	112	18.6	80.2	451.5	119
63	442.0	115	53.5	391.0	361.5	124
64	451.5	119	128.0	1447.7	301.5	125
	$\sum$	6892	3254	7034		

how the data are perceived. If too few or too many intervals are used, then the distribution of scatter in the data will not be clear. Unfortunately, there are no set rules for determining the appropriate number of intervals to use. Experimentation with different intervals is one approach. In addition, the following equation provides an empirical guide

$$k = 1 + 3.3 \log_{10}(n)$$

where k is the number of intervals and n is the number of data points. As an example, k is equal to 7 for the unit weight data set with n equal to 64.

Table 2.2 Frequency Plot Data for Total Unit Weight

Interval			Frequency of	Frequency	Cumulative
Lower Bound (1)	Upper Bound (2)	Number of Occurrences (3)	Occurrences (%) (4)	Density (%/pcf) (5)	Frequency (%) (6)
90	94	0	0	0.00	0
94	98	2	3	0.78	3
98	102	21	33	8.20	36
102	106	9	14	3.52	50
106	110	6	9	2.34	59
110	114	13	20	5.08	80
114	118	9	14	3.52	94
118	122	2	3	0.78	97
122	126	2	3	0.78	100
126	130	0	0	0.00	100
	$\sum$	64	100	25	

Column 4 = Column 3/($\sum$ Column 3)
Column 5 = Column 4/(Column 2 − Column 1)
Column 6 = Running Total of Column 4

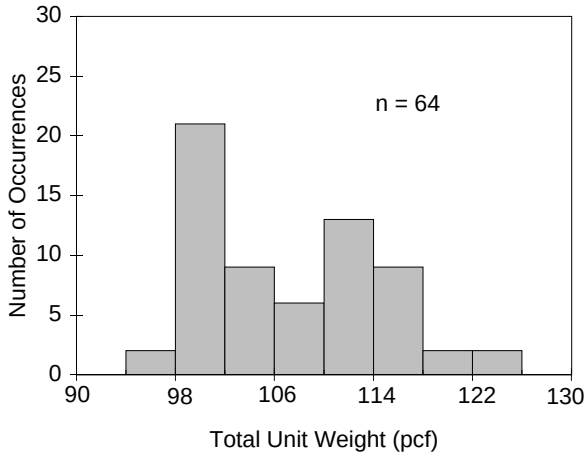

Figure 2.1 Histogram of total unit weight

2.2.2 Frequency Plot

The frequency of occurrence in each histogram interval is obtained by dividing the number of occurrences by the total number of data points. A bar-chart plot of the frequency of occurrence in each interval is called a *frequency plot*. The interval frequencies for the unit weight data are calculated in Table 2.2, and the resulting frequency plot is shown on Fig. 2.2.

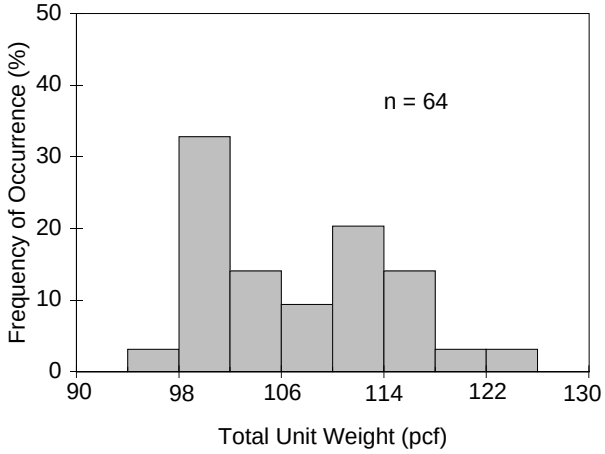

Figure 2.2 Frequency plot of total unit weight

Note that the histogram and frequency plot have the same shape and convey the same information. The frequency plot is simply a normalized version of the histogram. Because it is normalized, the frequency plot is useful in comparing different data sets.

Example frequency plots are shown on Figs. 2.2 through 2.5. Fig. 2.2 shows the unit weight data, which vary spatially.

Fig. 2.3 shows an example of data that vary with time. The data are monthly average pumping rate measurements versus time for the leak detection system in a hazardous waste landfill. The data vary from month to month due to varying rates of leachate generation and waste placement.

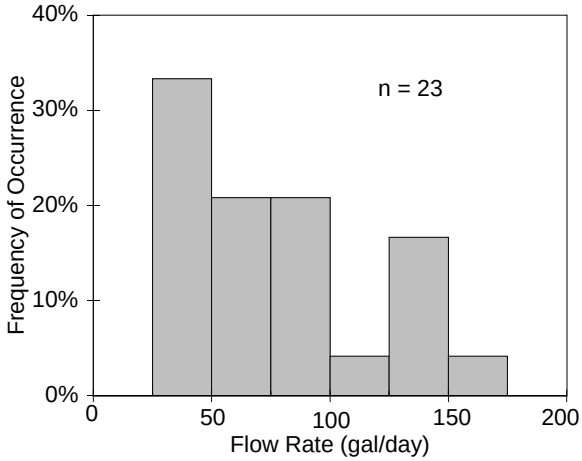

Figure 2.3 Frequency plot of monthly average flow rate for leak detection system

Fig. 2.4 shows an example of data that vary between construction projects. The data are the ratios of actual to estimated cost for the remediation of Superfund (environmentally contaminated) sites. The data vary between sites due to variations in site conditions, weather, contractors, technology and regulatory constraints. Note that the majority of projects have cost ratios greater than 1.0.

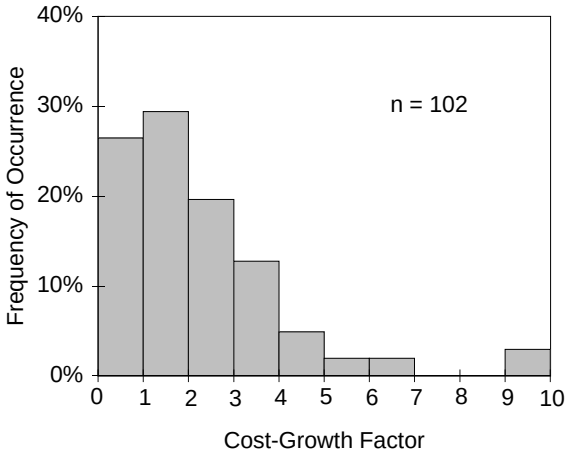

Figure 2.4 Frequency plot of cost-growth factor

Fig. 2.5 shows an example of data that vary between geotechnical testing laboratories. The data are the measured friction angles for specimens of loose Ottawa sand. Although Ottawa sand is a uniform material and there were only minor variations in the specimen densities, there is significant variability in the test results. Most of this variability is attributed to differences in test equipment and procedures between the various laboratories.

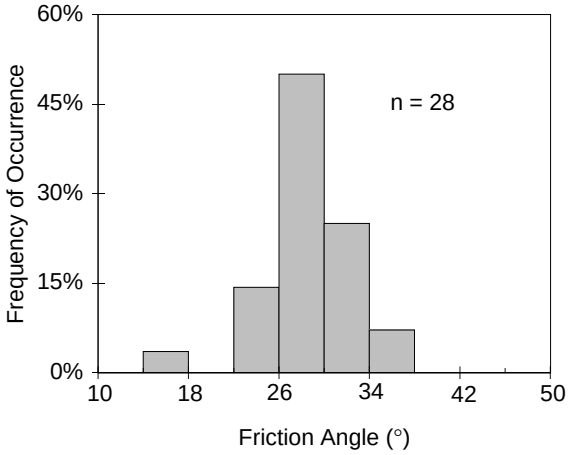

Figure 2.5 Frequency plot of friction angle

2.2.3 Frequency Density Plot

Another plot related to the histogram is the frequency density plot. The frequency density is obtained by dividing the interval frequencies by the interval widths. A bar-chart plot of the frequency density is called the *frequency density plot*. The objective in dividing the frequency by the interval width is to normalize the histogram further: the area below the frequency density plot (obtained by multiplying the bar heights by their widths) is equal to 100%. This normalization will be useful in fitting theoretical random variable models to the data, which will be discussed later in this chapter.

The frequency densities for the unit weight data are calculated in Table 2.2. Note that the units for the frequency density are % per the units for the data, which are % per pcf in the case of the unit weight data. The resulting frequency density plot is shown on Fig. 2.6.

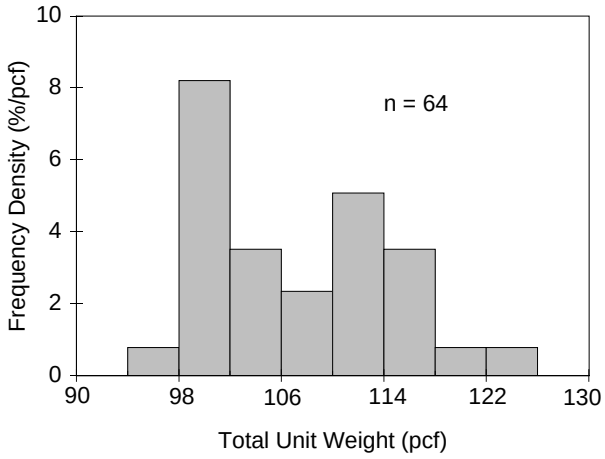

Figure 2.6 Frequency density plot of total unit weight

2.2.4 Cumulative Frequency Plot

The cumulative frequency plot is the final graphical tool that we will present for variability analysis. Cumulative frequency is the frequency of data points that have values less than or equal to the upper bound of an interval in the frequency plot. The cumulative frequency is obtained by summing up (or accumulating) the interval frequencies for all intervals below the upper bound. A plot of cumulative frequency versus the upper bound is called the *cumulative frequency plot*.

The cumulative frequencies for the unit weight data are calculated in Table 2.2. For example, the cumulative frequency for an upper bound of 102 pcf is equal to 0% + 3% + 33% = 36%. The resulting cumulative frequency plot is shown on Fig. 2.7.

A percentile value for the data set corresponds to the corresponding value with that cumulative frequency. For example, the 50th percentile value for the unit weight data set is 106 pcf (50 percent of the values are less than or equal to 106 pcf), while the 90th percentile value is equal to 117 pcf (Fig. 2.7).

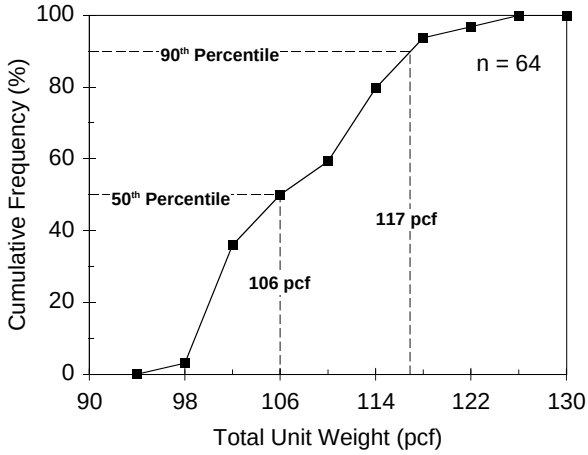

Figure 2.7 Cumulative frequency plot of total unit weight

2.2.5 Data Transformations

In some cases, it is useful to transform the data before plotting it. One example is a data set of measured hydraulic conductivity values for a compacted clay liner. The frequency plot for these data is shown on Fig. 2.8. It does not convey much about the data set because the hydraulic conductivity values range over several orders of magnitude. A more useful representation of the data is to develop a frequency plot for the logarithm of hydraulic conductivity, as shown on Fig. 2.9. Now it can be seen that the most likely interval is between $10^{-8.4}$ and $10^{-8.2}$ cm/s, and that most of the data are less than or equal to 10^{-7} cm/s.

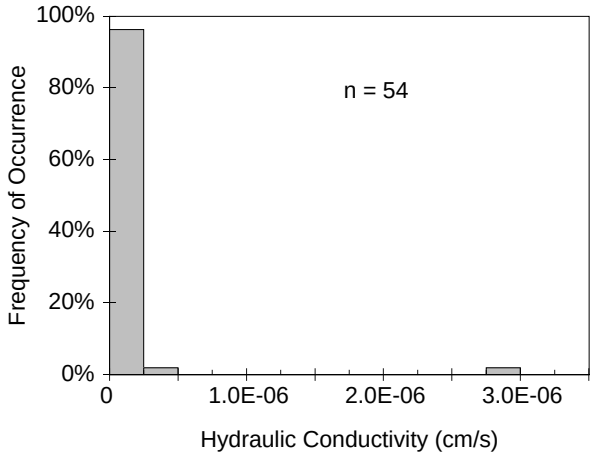

Figure 2.8 Frequency plot of hydraulic conductivity

A second example of data for which a transformation is useful are undrained shear strength data for a normally consolidated clay. A frequency plot of these data from an offshore boring in the Gulf of Mexico are shown in Fig. 2.10. The data exhibit substantial variability with depth, ranging from 500 to 5,000 psf. However, this frequency plot is misleading because much of the variability can be attributed to the shear strength increasing with depth. In order to demonstrate this trend, a *scatter*

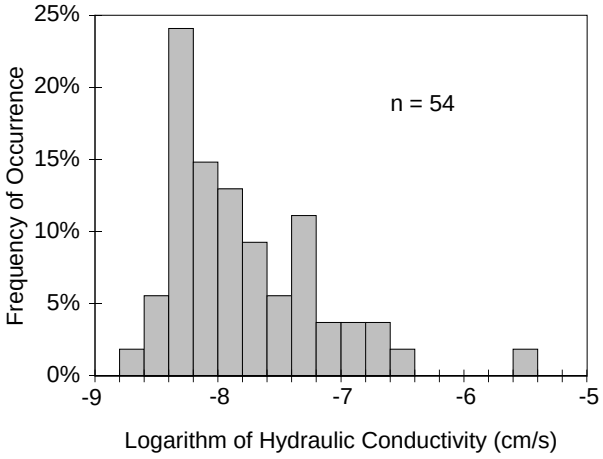

Figure 2.9 Frequency plot of log-hydraulic conductivity

plot of the undrained shear strength versus depth is shown on Fig. 2.11. A more useful measure of undrained strength is to normalize it by depth, as shown in Fig. 2.12. This scatter plot shows that the trend with depth has now been removed from the data, and the variability in the shear strength to depth ratio is much smaller than that in the undrained shear strength alone. A frequency plot of the shear strength to depth ratio is shown on Fig. 2.13.

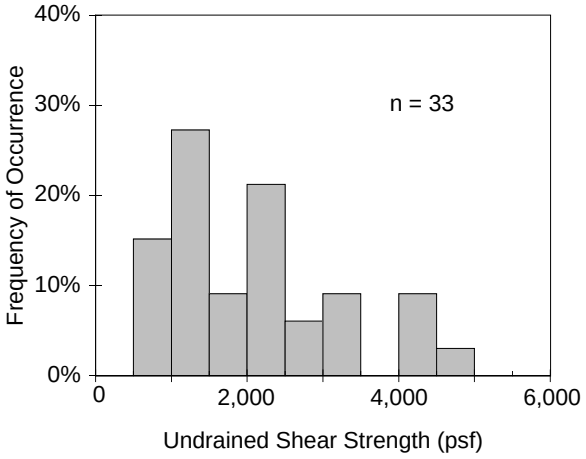

Figure 2.10 Frequency plot of undrained shear strength

2.3 Quantitative Analysis of Variability

In addition to graphical analyses, the variability in a data set can also be analyzed quantitatively. The statistics of a data set (also known as the sample statistics where the data set is the sample) provide quantitative measures of variability. Features of interest include the central tendency of the data, dispersion or scatter in the data, skewness in the data, and correlation or dependence between data points. Common statistical quantities are presented in this section.

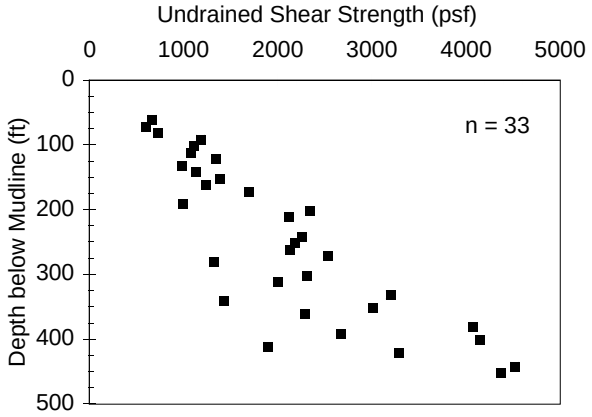

Figure 2.11 Scatter plot of undrained shear strength

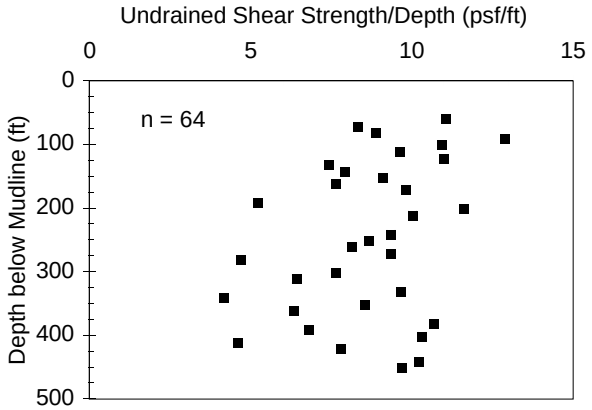

Figure 2.12 Scatter plot of shear strength to depth ratio

2.3.1 Central Tendency

The most common measure for the center of a data set is the average value, which is also called the sample mean. The *sample mean* is obtained as follows

$$\hat{\mu}_X = \frac{1}{n}\sum_{i=1}^{n} x_i$$

where $\hat{\mu}_X$ is the sample mean, x_i is each data value, and n is the total number of data points. For example, the sample mean of the unit weight data set in Table 2.1 is given by $6,892/64$ = 108 pcf.

The sample median and mode are other measures of central tendency for a data set. The *sample median* is the 50th percentile value, while the *sample mode* is the most likely value. For example, the sample median for the unit weight data set equals 106 pcf (Fig. 2.7), while the sample mode equals 100 pcf (Fig. 2.2). The sample mode depends on the interval width used in the frequency plot, and a data set may have more than one mode.

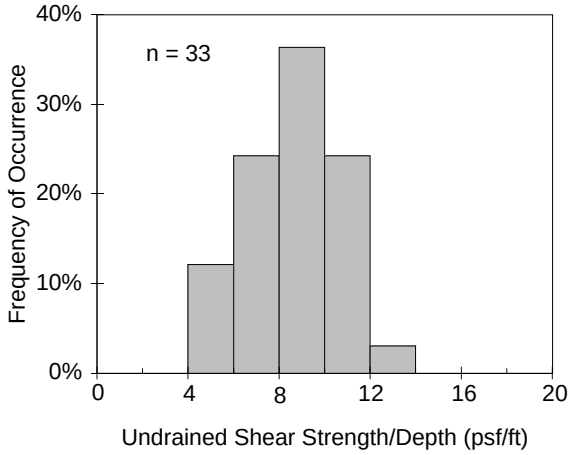

Figure 2.13 Frequency plot of shear strength to depth ratio

Sample means, medians and modes for the data sets described previously are summarized in Table 2.3. Note that the mean, median and mode are not equal unless the data distribution (the frequency plot) is symmetrical and has a single mode (peak).

Table 2.3 Summary Statistics for Different Data Sets

Data Set	Figure	Sample Mean	Sample Median	Sample Mode	Sample Standard Deviation	Sample COV	Sample Skewness Coefficient
Unit Weight	Fig 2.2	108 pcf	106 pcf	100 pcf	7.19 pcf	0.067	0.31
LDS Flow	Fig 2.3	77.8 gal/d	67.0 gal/d	37.5 gal/d	43.1 gal/d	0.55	0.63
Cost Ratio	Fig 2.4	2.22	1.74	1.5	1.93	0.87	2.1
Test Error	Fig 2.5	29°	29°	28°	16°	0.55	-0.01
K, cm/s	Fig 2.8	8.78×10^{-8}	1×10^{-8}	1.25×10^{-7}	4.08×10^{-7}	4.7	7.1
log(K)	Fig 2.9	-7.81	-8.00	-8.30	0.613	0.078	1.4
USS	Fig 2.10	2070 psf	2000 psf	1250 psf	1100 psf	0.53	0.81
USS/Depth	Fig 2.13	8.63 psf/ft	8.90 psf/ft	9.00 psf/ft	2.11 psf/ft	0.24	-0.4

2.3.2 Dispersion or Scatter

The amount of scatter in a data set is most easily measured by the sample range. The *sample range* is simply the maximum value in the data set minus the minimum value. For the unit weight data set, the range is 125 – 95 = 30 pcf (Table 2.1).

The sample variance is a measure of dispersion about the mean value of the data set. The *sample variance* is obtained as follows

$$\hat{\sigma}_X^2 = \frac{1}{n-1}\sum_{i=1}^{n}(x_i - \hat{\mu}_X)^2$$

where $\hat{\sigma}_X^2$ is the sample variance. The sample variance is the average of the square of the distance between individual data points and the sample mean. Its value will always be greater than or equal to zero. For the unit weight data set, the sample variance is given by $3,254/(64-1) = 51.7$ pcf^2 (Table 2.1).

The *sample standard deviation*, $\hat{\sigma}_X$, is the square root of the sample variance, while the *sample coefficient of variation* (c.o.v.), $\hat{\delta}_X$, is the standard deviation divided by the mean value

$$\hat{\delta}_X = \frac{\hat{\sigma}_X}{|\hat{\mu}_X|}$$

Since the standard deviation has the same units as the mean value, the c.o.v. is a dimensionless measure of dispersion. The sample standard deviation and c.o.v. for the unit weight data set are equal to 7.19 pcf and $7.19/108 = 0.067$, respectively.

Statistical measures of dispersion for the various data sets are summarized in Table 2.3. Note the large range of c.o.v. values, with a minimum of 0.067 and a maximum of 4.7. Also, note how accounting for the trend in undrained shear strength with depth (Fig. 2.11) reduces the sample c.o.v. from 0.53 to 0.24.

2.3.3 Skewness

Since the sample variance is the average of the square distance from the sample mean, data values the same distance above and below the sample mean contribute equally. Therefore, the sample variance provides no indication of how symmetrically the data are dispersed about the mean. The sample skewness, which is essentially the average of the cubed distance from the sample mean, provides a measure of symmetry for a data set. The *sample skewness coefficient*, a dimensionless measure of skewness, is given by the following

$$\hat{\psi} = \left[\frac{n}{(n-1)(n-2)}\right] \frac{\sum_{i=1}^{n}(x_i - \hat{\mu}_x)^3}{\hat{\sigma}_x^3}$$

where $\hat{\psi}$ is the sample skewness coefficient. A skewness coefficient of zero means that the data values are distributed symmetrically about the mean value. A positive skewness coefficient indicates that the data are skewed about the mean to the right (toward larger values), while a negative skewness coefficient indicates that the data are skewed to the left (toward smaller values). The sample skewness coefficient for the unit weight data is equal to $\left(\frac{64}{(63)(62)}\right)\left(\frac{7,034}{7.19^3}\right) = 0.31$ (Table 2.1), indicating that the data are skewed toward larger values (Fig. 2.2).

Skewness coefficients for the other data sets are summarized in Table 2.3. Most of the data are positively skewed. Note how taking the logarithm of hydraulic conductivity reduces the skewness coefficient from 7.1 to 1.4 (Table 2.3).

2.3.4 Correlation or Dependence

Two variables may be related to one another, as indicated by a scatter plot, such as that shown on Fig. 2.11. The sample correlation coefficient is a measure of the degree of linear dependence between two variables. The *sample correlation coefficient*, $\hat{\rho}$ is given by the following

$$\hat{\rho}_{XY} = \frac{\sum_{i=1}^{n} [(x_i - \hat{\mu}_X)(y_i - \hat{\mu}_Y)]}{\sqrt{\sum_{i=1}^{n}(x_i - \hat{\mu}_X)^2 \sum_{j=1}^{n}(y_j - \hat{\mu}_Y)^2}}$$

where x_i and y_i are paired observations of the two variables. The sample correlation coefficient ranges between -1.0 and 1.0, that is $-1.0 \leq \hat{\rho} \leq 1.0$. A value of zero for $\hat{\rho}$ indicates no linear dependence between the two variables. A negative value of $\hat{\rho}$ indicates that one variable tends to decrease as the other increases, while a positive value indicates that one variable tends to increase as the other increases. The closer the absolute value of $\hat{\rho}$ is to 1.0, the stronger the linear relationship between the two variables.

For example, the sample correlation coefficient between undrained shear strength and depth is calculated in Table 2.4. The sample correlation coefficient is equal to

$$\hat{\rho} = \frac{3.64 \times 10^6}{\sqrt{(.473 \times 10^6)(38.8 \times 10^6)}} = 0.85$$

This positive value near one indicates that the undrained shear strength tends to increase linearly with increasing depth (Fig. 2.11).

2.4 Theoretical Random Variable Models

A random variable is a mathematical model to represent a quantity that varies. Specifically, a random variable model describes the possible values that the quantity can take on and the respective probabilities for each of these values. Since the frequency plot for a data set indicates the probability of different values occurring (e.g., Fig. 2.2), a random variable model is just a mathematical representation of the information contained in a frequency plot.

Why is a theoretical random variable model needed to describe a data set? First, a data set is limited in size. For example, if another sample of 64 unit weight measurements were obtained, we would get a different frequency plot than that shown on Fig. 2.2 and different sample statistics than those summarized in Table 2.3. We would need to measure the unit weight at every point in the soil in order to obtain the "true" frequencies and statistics. A random variable is a theoretical model of these "true" frequencies and statistics. Second, in most engineering problems we are interested in combinations of variable quantities. For example, a pile foundation will undergo large displacements if the applied load exceeds the pile capacity. We need to consider variability both in the load and the capacity to design this foundation. Random variable models provide a mathematical framework for working with and combining multiple quantities that vary.

After a brief section on terminology, discrete and continuous models for random variables will be discussed in the following sections.

Table 2.4 Correlation Between Undrained Strength and Depth

	x Depth (ft)	y USS (psf)	$(x-\hat{\mu}_X)^2$ (ft^2)	$(y-\hat{\mu}_Y)^2$ (psf^2)	$(x-\hat{\mu}_X)(y-\hat{\mu}_Y)$ (ft-psf)
	60.5	670	35519	1954912	263506
	72.0	600	31316	2155558	259815
	82.0	730	27877	1790731	223428
	91.5	1180	24795	788867	139856
	101.5	1110	21746	918112	141297
	112.0	1080	18759	976503	135345
	122.0	1340	16120	530249	92453
	132.0	980	13680	1184140	127278
	142.5	1130	11335	880185	99882
	152.5	1390	9305	459931	65420
	162.0	1240	7563	685885	72022
	172.0	1690	5923	143021	29106
	191.5	1000	3302	1141012	61382
	201.5	2340	2253	73885	12901
	211.5	2120	1404	2685	-1941
	241.5	2260	56	36794	-1432
	251.5	2180	6	12503	284
	261.8	2130	165	3821	794
	271.5	2540	508	222612	10633
	281.5	1320	1059	559776	24343
	301.5	2310	2760	58476	12704
	311.5	2000	3911	4649	-4264
	331.5	3200	6812	1281012	93416
	341.5	1430	8563	407276	59055
	352.0	3010	10616	887021	97042
	361.5	2290	12664	49203	24963
	381.5	4080	17566	4047412	266639
	391.5	2670	20317	362185	85781
	402.0	4150	23420	4333967	318594
	411.5	1900	26418	28285	27336
	421.5	3290	29769	1492840	210808
	442.0	4520	37263	6011412	473290
	451.5	4370	41021	5298367	466202
$\sum$	8216.0	68250	473789	38783291	3640666
ave	249.0	2068			

2.4.1 Terminology

Random variables are generally denoted by capital letters, such as X representing unit weight. If a random variable takes on a specific value, say if it is measured, then it is no longer random and it will be designated with a lowercase letter. Therefore, x represents an observation or *realization* of X.

The range of possible values that X can take on constitutes the *sample space* for X. For example, the unit weight for a soil could be any value greater than zero. By definition, the probability of the sample space, e.g., P $\left[X > 0 \text{ pcf}\right]$, is equal to 1.0. The event that X takes on specific values is a subset of this sample space. An example is the event that the unit weight is less than 100 pcf, which has a corresponding probability, P $\left[X < 100 \text{ pcf}\right]$. The *probability distribution* for a random variable is a function describing the probability that it takes on different values, e.g., P $[X = x]$.

2.4.2 Discrete Random Variables

Discrete random variables can only take on discrete values within the sample space. For example, consider the number of projects awarded to a consulting firm in the next month, X. If the firm has submitted five proposals, then X could be any of the following possible values: 0, 1, 2, 3, 4, 5.

The *probability mass function* (PMF) for a discrete random variable describes its probability distribution. An example probability mass function is shown on Fig. 2.14. This PMF indicates that the probability of 0 successful proposals is given by P [X = 0] = 0.116, the probability of 1 successful proposal is given by P [X = 1] = 0.312, etc. Note that the individual probabilities for X between 0 and 5 sum to 1.0 since this range constitutes all possible values for X. The probability that X is between two values can also be obtained from the PMF. For example, the probability that X is greater than 1, P [$X > 1$], is equal to 0.336 + 0.181 + 0.049 + 0.005 = 0.571. The PMF for X is denoted by the following mathematical form for notational convenience: P [$X = x$] = $p_X(x)$.

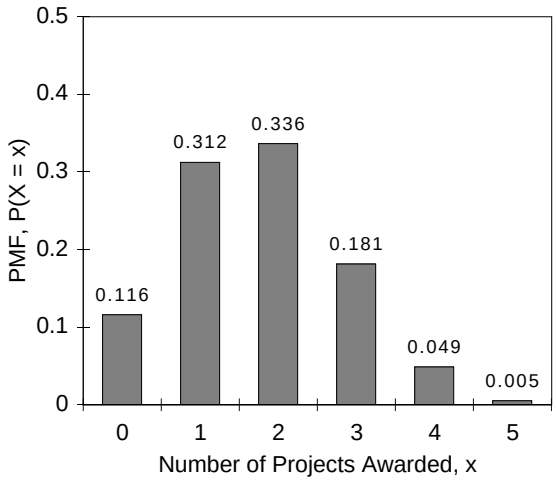

Figure 2.14 Probability mass function for number of successful proposals

The *cumulative distribution function* (CDF) describes the probability that the random variable takes on a value less than or equal to a given value. It is obtained as follows

$$F_X(x) = \text{P}[X \leq x] = \sum_{\text{all } x_i \leq x} p_X(x_i)$$

For example, the CDF evaluated at 1 for the random variable on Fig. 2.14 is given by $F_X(1)$ = 0.116 + 0.312 = 0.428. The resulting CDF for this example is shown on Fig. 2.15. Note that the PMF and the CDF contain the same information (each can be developed from the other) plotted in a different way.

The PMF and CDF are theoretical versions of the frequency plot and the cumulative frequency plot, respectively, for a data set. There are also theoretical versions of the sample statistics (in these notes, the sample statistics are identified by a hat, for example $\hat{\mu}$ is the sample statistic, or estimate, of the distribution mean μ). The *mean value* for a discrete random variable is obtained as follows

$$\mu_X = \sum_{\text{all } x_i} x_i p_X(x_i)$$

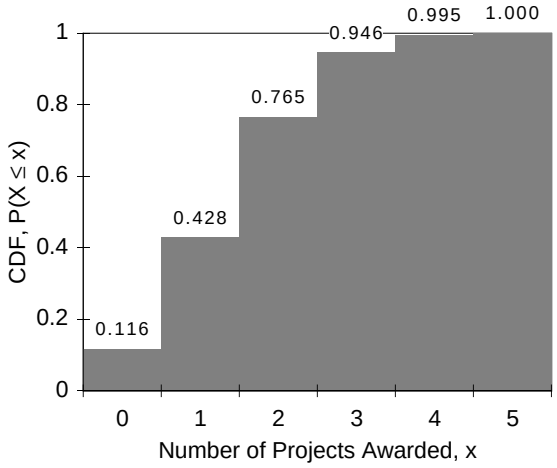

Figure 2.15 Cumulative distribution function for number of successful proposals

where μ_X is the mean value of X. Note that the mean value is a weighted average of X, where each x_i is weighted by its probability of occurrence. The median is the value of X for which there is an equal likelihood above and below, that is $F_X(x_{\text{median}}) = 0.5$. The mode is the value of X that is most likely, that is $p_X(x_{\text{mode}})$ is a maximum. For the number of awarded projects (Fig. 2.14), $\mu_X = 1.75$, x_{median} = between 1 and 2, and $x_{\text{mode}} = 2$.

Similarly, the *variance* is obtained as follows

$$\sigma_X^2 = \sum_{\text{all } x_i} (x_i - \mu_X)^2 p_X(x_i)$$

where σ_X is the *standard deviation* of X. The c.o.v. of X, δ_X, is the ratio of the standard deviation to the mean value

$$\delta_X = \frac{\sigma_X}{|\mu_X|}$$

Finally, the *skewness coefficient* is obtained as follows

$$\psi_X = \frac{1}{\sigma_X^3} \sum_{\text{all } x_i} (x_i - \mu_X)^3 p_X(x_i)$$

For the number of awarded projects (Fig. 2.14), $\sigma_X = 1.07$, $\delta_X = 0.61$ and $\psi_X = 0.28$.

An important tool when working with random variables is expectation. The *expectation* of a quantity is the weighted average of that quantity, where the possible values are weighted by their corresponding probabilities of occurrence. For example, the expected value of X, denoted $\mathrm{E}[X]$, is given by the following

$$\mathrm{E}[X] = \sum_{\text{all } x_i} x_i p_X(x_i)$$

Note that the mean of X, μ_X, is equal to its expected value, $\mathrm{E}[X]$. The expected value of any function of X, denoted $g(X)$, can be obtained similarly

$$\mathrm{E}[g(X)] = \sum_{\text{all } x_i} g(x_i) p_X(x_i)$$

For example, the variance of X is equal to the expected value of $g(X) = (X - \mu_X)^2$.

Expectation is a useful tool in working with multiple random variables and functions of random variables, as you will see in later chapters. It is also a useful tool in decision making, as discussed in the previous chapter. As a simple, practical example of expectation, consider the random variable describing the number of projects awarded to a consulting firm in the next month (Fig. 2.14). If the revenue of each project is \$50,000, then the expected revenue in the next month is obtained as follows

$$\begin{aligned} \text{E}\left[\text{revenue}\right] = \text{E}\left[\$50,000X\right] &= \$0(0.116) + \$50,000(0.312) \\ &+ \$100,000(0.336) + \$150,000(0.181) \\ &+ \$200,000(0.049) + \$250,000(0.005) \\ &= \$87,500 \end{aligned}$$

We could also evaluate the expected profit. If at least \$50,000 of new revenue is required to operate the office each month, 20% profit is realized on the next \$100,000, and 30% profit is realized for revenue above \$150,000, then the expected profit is calculated as follows

$$\begin{aligned} \text{E}\left[\text{profit}\right] &= \$0(0.116) + \$0(0.312) \\ &+ \$10,000(0.336) + \$20,000(0.181) \\ &+ \$35,000(0.049) + \$50,000(0.005) \\ &= \$8,945 \end{aligned}$$

Clearly, this office needs to find more sole-sourced projects, or cut its overhead.

Several of the most common models for discrete random variables are summarized in Table 2.5. The PMF shown on Fig. 2.14 is an example of a binomial distribution with $n = 5$ (there are a maximum of five projects that could be awarded) and $p = 0.35$ (the probability of winning an individual project is assumed to be 35 percent).

Table 2.5 Common Models for Discrete Random Variables

Distribution	PDF	Mean	Variance	Explanation	Example
Binomial	$p_X(x) = \dfrac{n!}{x!(n-x)!}\, p^x(1-p)^{n-x}$ $x = 0, 1, \ldots, n$	np	$np(1-p)$	X represents number of occurrences in n independent trials, where p is probability of occurrence per trial	flood occurrences
Geometric	$p_X(x) = p(1-p)^{x-1}$ $x = 1, 2, \ldots$	$\dfrac{1}{p}$	$\dfrac{1-p}{p^2}$	X represents the number of independent trials to the next occurrence, where p is probability of occurrence per trial	flood return period
Poisson	$p_X(x) = \dfrac{(\nu t)^x}{x!}\, e^{-\nu t}$ $x = 0, 1, \ldots$	νt	νt	X represents the number of independent occurrences in an interval of time t, where ν is the average occurrence rate	earthquake occurrences

2.4.3 Continuous Random Variables

Continuous random variables can take on any value within the sample space. Total unit weight is an example of a continuous random variable; it can take on any value greater than zero.

The *probability density function* (PDF) for a continuous random variable describes its probability distribution. An example PDF is shown on Fig. 2.16. While the PDF is similar to the PMF in the information that it conveys, there is significant difference in these two functions. For a continuous random variable, there is an infinite number of possible values within the sample space. Hence, unlike a discrete random variable, it is not possible to define the probability of the event that X is equal to a given value x, since this probability is vanishingly small. Instead, we can define the probability that X is within a very small interval. This probability is proportional to the PDF. For example, the probability that the unit weight is within a small interval about 110 pcf is greater than the probability that it is within a small interval about 125 pcf (Fig. 2.16). The PDF is denoted mathematically as $f_X(x)$.

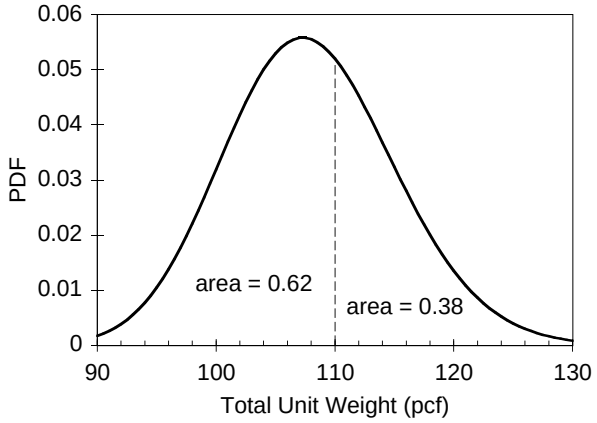

Figure 2.16 Probability density function for unit weight

As with a discrete random variable, the *cumulative distribution function* (CDF) for a continuous variable describes the probability that the variable takes on a value less than or equal to a given value. It is obtained as follows

$$F_X(x) = \mathrm{P}[X \leq x] = \int_{-\infty}^{x} f_X(\xi)\, d\xi$$

Note that the CDF is the area under the PDF. For example the CDF evaluated at 110 pcf for the unit weight is equal to 0.62 (Fig. 2.16). A plot of the CDF for unit weight is shown on Fig. 2.17.

Since the probability of the sample space is equal to 1.0, the area under the PDF must equal 1.0. Recall that the area under a frequency density plot for a data set is also equal to 1.0. Therefore, theoretical PDFs can be fit to model a data set by overlaying a theoretical PDF on top of a frequency density plot. For example, Fig. 2.18 shows the theoretical PDF for the unit weight (Fig. 2.16) overlain on the frequency density plot (Fig. 2.6).

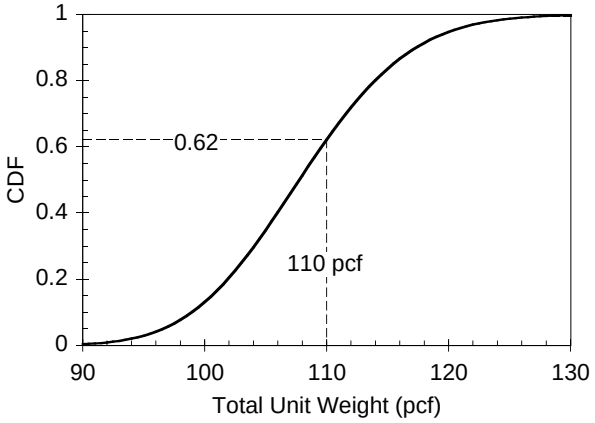

Figure 2.17 Cumulative distribution function for unit weight

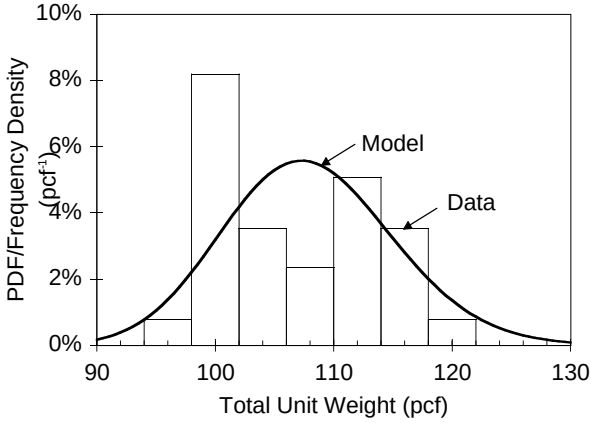

Figure 2.18 Probability density function and frequency density plot for unit weight

The expectation for a continuous random variable is defined in the same way as for a discrete random variable; it is a weighted average, in which values are weighted by their likelihood. However, since there is an infinite number of possible values in the sample space, the process of summing up values weighted by their likelihoods is an integration

$$\mathrm{E}\left[g(X)\right] = \int_{-\infty}^{\infty} g(x) f_X(x)\, dx$$

Similarly, the *mean*, *variance* and *skewness* for a continuous random variable are found as follows

$$\mu_X = \mathrm{E}\left[X\right] = \int_{-\infty}^{\infty} x f_X(x)\, dx$$

$$\sigma_X^2 = \mathrm{E}\left[(X - \mu_X)^2\right] = \int_{-\infty}^{\infty} (x - \mu_X)^2 f_X(x)\, dx$$

$$\psi_X = \frac{\mathrm{E}\left[(X-\mu_X)^3\right]}{\sigma_X^3} = \frac{\int_{-\infty}^{\infty}(x-\mu_X)^3 f_X(x)\,dx}{\sigma_X^3}$$

Common models for continuous random variables are summarized in Table 2.6. The normal distribution and the related lognormal distribution are the most common random variable models, and they will be discussed further in this section.

Table 2.6 Common Models for Continuous Random Variables

Distribution	PDF	Mean	Variance	Explanation	Example
Uniform	$f_X(x) = \frac{1}{b-a}, \quad a \le x \le b$	$\frac{a+b}{2}$	$\frac{(b-a)^2}{12}$		test bias
Triangular	$f_X(x) = \begin{cases} \frac{2}{b-a}\left(\frac{x-a}{u-a}\right) & a \le x \le u \\ \frac{2}{b-a}\left(\frac{b-x}{b-u}\right) & u \le x \le b \end{cases}$	$\frac{a+b+u}{3}$	$\frac{1}{18}(a^2+b^2+u^2 - au-bu-ab)$		construction cost
Exponential	$f_X(x) = \nu e^{-\nu x}, \quad x \ge 0$	$\frac{1}{\nu}$	$\frac{1}{\nu^2}$	X represents the time between independent occurrences, where ν is the ave. occurrence rate	earthquake return period
Normal	$f_X(x) = \frac{1}{\sigma\sqrt{2\pi}} e^{-\frac{1}{2}\left(\frac{x-\mu}{\sigma}\right)^2}$ $-\infty < x < \infty$	μ	σ^2	X represents the sum of many random variables	soil strength
Lognormal	$f_X(x) = \frac{1}{x\sigma_{\ln X}\sqrt{2\pi}} e^{-\frac{1}{2}\left(\frac{\ln x-\mu_{\ln X}}{\sigma_{\ln X}}\right)^2}$ $x \ge 0$	$e^{\mu_{\ln X}+\frac{1}{2}\sigma^2_{\ln X}}$	$\mu_X^2(e^{\sigma^2_{\ln X}} - 1)$	X represents the product of many random variables	hydraulic conductivity

The *normal distribution* (also known as the *Gaussian distribution*) is the classic bell-shaped curve that arises frequently in data sets. For example, the undrained shear strength to depth ratio data from Fig. 2.13 are fit well by a normal distribution (Fig. 2.19). The normal distribution is common in nature because it results if individual random variables are summed together. Hence, data sets ranging from course grades (the summation of scores from individual tests, homework problems and projects) to the height of people (the summation of gene pools over many generations) to the undrained shear strength of soil (the summation of shear resistance between individual particles) all tend toward normal distributions.

The normal distribution has several interesting properties. First, it is a symmetrical distribution (ψ is zero for a normal PDF). Second, its tails decay in an exponential manner. There is a 68-percent chance that a normal variable will be within ± 1 standard deviation from the mean value, a 95-percent chance that it will be within $\mu \pm 2\sigma$, and a 99.7-percent chance that it will be within $\mu \pm 3\sigma$. Therefore, it is very unlikely (less than one-percent chance) to observe a value outside of ± 3 standard deviations from the mean value. Finally, a linear function of a normally distributed variable also has a normal distribution. If $Y = aX + b$ and X has a normal distribution, then Y also has a normal distribution with mean $\mu_Y = a\mu_X + b$ and standard deviation $\sigma_Y = a\sigma_X$.

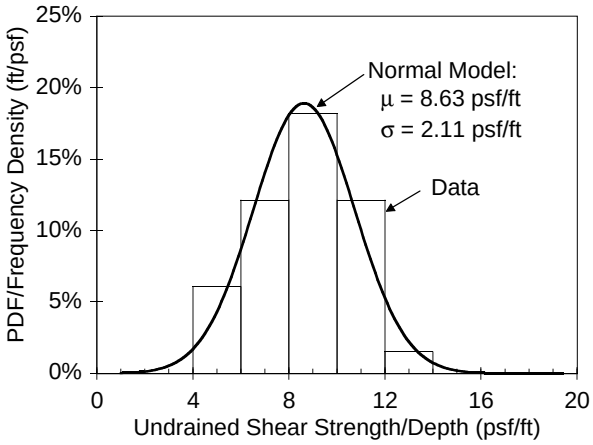

Figure 2.19 Probability density function for strength ratio

The CDF for a normal distribution (the integral of the PDF) cannot be derived analytically. However, it is widely tabulated and available on most spreadsheet programs. The first step in using these tables is to normalize X by subtracting its mean value and dividing by its standard deviation:

$$Z = \frac{X - \mu_X}{\sigma_X}$$

where Z is the normalized version of X; it has mean zero and unit variance. The tables then list the CDF evaluated at x as a function of z: $F_X(x) = \Phi(z)$ where Φ is called the standard normal function. The standard normal values, as a function of z, are provided in Table 2.7. The function `NORMSDIST(z)` in Microsoft Excel® also gives the standard normal function, $\Phi(z)$.

As an example of working with the standard normal function, consider the undrained shear strength to depth ratio data on Fig. 2.19. The probability that this ratio is less than 12 psf/ft is calculated as follows

$$\mathrm{P}\left[X \leq 12 \text{ psf/ft}\right] = F_X(x = 12) = \Phi\left(\frac{x - \mu_X}{\sigma_X}\right) = \Phi\left(\frac{12 - 8.63}{2.11}\right) = \Phi(1.60) = 0.945$$

Similarly, the probability that the ratio is greater than 12 psf/ft can be calculated as follows since the total area under the PDF is equal to 1.0

$$\mathrm{P}\left[X > 12 \text{ psf/ft}\right] = 1 - \mathrm{P}\left[X \leq 12\right] = 1 - 0.945 = 0.055$$

The probability that the strength ratio is less than 4 psf/ft is calculated as follows

$$\mathrm{P}\left[X \leq 4 \text{ psf/ft}\right] = F_X(x = 4) = \Phi\left(\frac{4 - 8.63}{2.11}\right) = \Phi(-2.19)$$

Although Table 2.7 does not list $\Phi(z)$ values for $z < 0$, these probabilities can be calculated as follows, since the normal distribution is symmetrical

$$\mathrm{P}\left[X \leq 4 \text{ psf/ft}\right] = \Phi(-2.19) = 1 - \Phi(2.19) = 1 - 0.986 = 0.014$$

Table 2.7 Tabulated Values for Standard Normal Distribution

z	Φ(z)	z	Φ(z)	z	Φ(z)	z	Φ(z)	z	Φ(z)	z	Φ(z)	z	Φ(z)
0.00	0.50000	0.50	0.69146	1.00	0.84134	1.50	0.93319	2.00	0.97725	2.50	0.99379	3.00	0.99865
0.01	0.50399	0.51	0.69497	1.01	0.84375	1.51	0.93448	2.01	0.97778	2.51	0.99396	3.01	0.99869
0.02	0.50798	0.52	0.69847	1.02	0.84614	1.52	0.93574	2.02	0.97831	2.52	0.99413	3.02	0.99874
0.03	0.51197	0.53	0.70194	1.03	0.84850	1.53	0.93699	2.03	0.97882	2.53	0.99430	3.03	0.99878
0.04	0.51595	0.54	0.70540	1.04	0.85083	1.54	0.93822	2.04	0.97932	2.54	0.99446	3.04	0.99882
0.05	0.51994	0.55	0.70884	1.05	0.85314	1.55	0.93943	2.05	0.97982	2.55	0.99461	3.05	0.99886
0.06	0.52392	0.56	0.71226	1.06	0.85543	1.56	0.94062	2.06	0.98030	2.56	0.99477	3.06	0.99889
0.07	0.52790	0.57	0.71566	1.07	0.85769	1.57	0.94179	2.07	0.98077	2.57	0.99492	3.07	0.99893
0.08	0.53188	0.58	0.71904	1.08	0.85993	1.58	0.94295	2.08	0.98124	2.58	0.99506	3.08	0.99897
0.09	0.53586	0.59	0.72240	1.09	0.86214	1.59	0.94408	2.09	0.98169	2.59	0.99520	3.09	0.99900
0.10	0.53983	0.60	0.72575	1.10	0.86433	1.60	0.94520	2.10	0.98214	2.60	0.99534	3.10	0.99903
0.11	0.54380	0.61	0.72907	1.11	0.86650	1.61	0.94630	2.11	0.98257	2.61	0.99547	3.11	0.99906
0.12	0.54776	0.62	0.73237	1.12	0.86864	1.62	0.94738	2.12	0.98300	2.62	0.99560	3.12	0.99910
0.13	0.55172	0.63	0.73565	1.13	0.87076	1.63	0.94845	2.13	0.98341	2.63	0.99573	3.13	0.99913
0.14	0.55567	0.64	0.73891	1.14	0.87286	1.64	0.94950	2.14	0.98382	2.64	0.99585	3.14	0.99916
0.15	0.55962	0.65	0.74215	1.15	0.87493	1.65	0.95053	2.15	0.98422	2.65	0.99598	3.15	0.99918
0.16	0.56356	0.66	0.74537	1.16	0.87698	1.66	0.95154	2.16	0.98461	2.66	0.99609	3.16	0.99921
0.17	0.56749	0.67	0.74857	1.17	0.87900	1.67	0.95254	2.17	0.98500	2.67	0.99621	3.17	0.99924
0.18	0.57142	0.68	0.75175	1.18	0.88100	1.68	0.95352	2.18	0.98537	2.68	0.99632	3.18	0.99926
0.19	0.57535	0.69	0.75490	1.19	0.88298	1.69	0.95449	2.19	0.98574	2.69	0.99643	3.19	0.99929
0.20	0.57926	0.70	0.75804	1.20	0.88493	1.70	0.95543	2.20	0.98610	2.70	0.99653	3.20	0.99931
0.21	0.58317	0.71	0.76115	1.21	0.88686	1.71	0.95637	2.21	0.98645	2.71	0.99664	3.21	0.99934
0.22	0.58706	0.72	0.76424	1.22	0.88877	1.72	0.95728	2.22	0.98679	2.72	0.99674	3.22	0.99936
0.23	0.59095	0.73	0.76730	1.23	0.89065	1.73	0.95818	2.23	0.98713	2.73	0.99683	3.23	0.99938
0.24	0.59483	0.74	0.77035	1.24	0.89251	1.74	0.95907	2.24	0.98745	2.74	0.99693	3.24	0.99940
0.25	0.59871	0.75	0.77337	1.25	0.89435	1.75	0.95994	2.25	0.98778	2.75	0.99702	3.25	0.99942
0.26	0.60257	0.76	0.77637	1.26	0.89617	1.76	0.96080	2.26	0.98809	2.76	0.99711	3.26	0.99944
0.27	0.60642	0.77	0.77935	1.27	0.89796	1.77	0.96164	2.27	0.98840	2.77	0.99720	3.27	0.99946
0.28	0.61026	0.78	0.78230	1.28	0.89973	1.78	0.96246	2.28	0.98870	2.78	0.99728	3.28	0.99948
0.29	0.61409	0.79	0.78524	1.29	0.90147	1.79	0.96327	2.29	0.98899	2.79	0.99736	3.29	0.99950
0.30	0.61791	0.80	0.78814	1.30	0.90320	1.80	0.96407	2.30	0.98928	2.80	0.99744	3.30	0.99952
0.31	0.62172	0.81	0.79103	1.31	0.90490	1.81	0.96485	2.31	0.98956	2.81	0.99752	3.31	0.99953
0.32	0.62552	0.82	0.79389	1.32	0.90658	1.82	0.96562	2.32	0.98983	2.82	0.99760	3.32	0.99955
0.33	0.62930	0.83	0.79673	1.33	0.90824	1.83	0.96638	2.33	0.99010	2.83	0.99767	3.33	0.99957
0.34	0.63307	0.84	0.79955	1.34	0.90988	1.84	0.96712	2.34	0.99036	2.84	0.99774	3.34	0.99958
0.35	0.63683	0.85	0.80234	1.35	0.91149	1.85	0.96784	2.35	0.99061	2.85	0.99781	3.35	0.99960
0.36	0.64058	0.86	0.80511	1.36	0.91309	1.86	0.96856	2.36	0.99086	2.86	0.99788	3.36	0.99961
0.37	0.64431	0.87	0.80785	1.37	0.91466	1.87	0.96926	2.37	0.99111	2.87	0.99795	3.37	0.99962
0.38	0.64803	0.88	0.81057	1.38	0.91621	1.88	0.96995	2.38	0.99134	2.88	0.99801	3.38	0.99964
0.39	0.65173	0.89	0.81327	1.39	0.91774	1.89	0.97062	2.39	0.99158	2.89	0.99807	3.39	0.99965
0.40	0.65542	0.90	0.81594	1.40	0.91924	1.90	0.97128	2.40	0.99180	2.90	0.99813	3.40	0.99966
0.41	0.65910	0.91	0.81859	1.41	0.92073	1.91	0.97193	2.41	0.99202	2.91	0.99819	3.41	0.99968
0.42	0.66276	0.92	0.82121	1.42	0.92220	1.92	0.97257	2.42	0.99224	2.92	0.99825	3.42	0.99969
0.43	0.66640	0.93	0.82381	1.43	0.92364	1.93	0.97320	2.43	0.99245	2.93	0.99831	3.43	0.99970
0.44	0.67003	0.94	0.82639	1.44	0.92507	1.94	0.97381	2.44	0.99266	2.94	0.99836	3.44	0.99971
0.45	0.67364	0.95	0.82894	1.45	0.92647	1.95	0.97441	2.45	0.99286	2.95	0.99841	3.45	0.99972
0.46	0.67724	0.96	0.83147	1.46	0.92785	1.96	0.97500	2.46	0.99305	2.96	0.99846	3.46	0.99973
0.47	0.68082	0.97	0.83398	1.47	0.92922	1.97	0.97558	2.47	0.99324	2.97	0.99851	3.47	0.99974
0.48	0.68439	0.98	0.83646	1.48	0.93056	1.98	0.97615	2.48	0.99343	2.98	0.99856	3.48	0.99975
0.49	0.68793	0.99	0.83891	1.49	0.93189	1.99	0.97670	2.49	0.99361	2.99	0.99861	3.49	0.99976

Finally, we can calculate the probability that the undrained strength is less than a design value of 250 psf at a depth of 50 ft. Let $Y = 50X$. Then, Y has a normal distribution with a mean of 50(8.63) = 432 psf and a standard deviation of 50(2.11) = 106 psf. The probability that Y is less than 250 psf is calculated as follows

$$\mathrm{P}\left[Y \leq 250 \text{ psf}\right] = \Phi\left(\frac{250 - 432}{106}\right) = \Phi(-1.72) = 1 - \Phi(1.72) = 1 - 0.957 = 0.043$$

The *lognormal distribution* is related to the normal distribution as follows: if the logarithm of a variable has a normal distribution, then the variable has a lognormal distribution. The lognormal distribution is commonly used for three reasons. First, it results if you multiply many individual random variables together. Hence, any process that is the product of individual random variables will tend to be described by a lognormal distribution. Second, the lognormal distribution models variables that cannot be less than zero. Since many engineering properties, such as strength, are non-negative, the lognormal distribution is a reasonable model. Finally, the lognormal distribution is convenient for modeling quantities that vary over several orders of magnitude, such as hydraulic conductivity.

An example of a lognormal distribution for the hydraulic conductivity data set is shown on Fig. 2.20. Note that this distribution is symmetrical when plotted on a logarithmic scale, but positively skewed on an arithmetic scale.

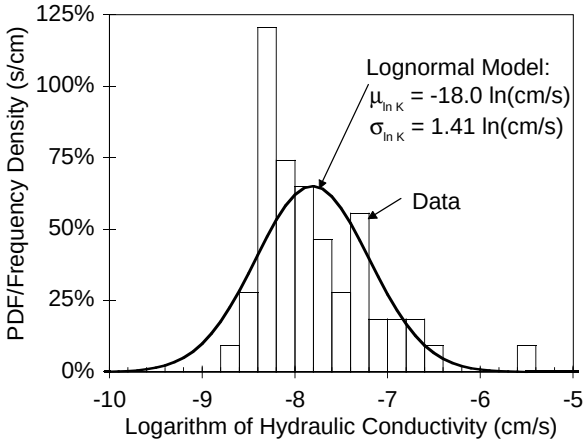

Figure 2.20 Probability density function for hydraulic conductivity

Since the lognormal distribution is related to the normal distribution, the CDF for the lognormal distribution can be calculated using the standard normal function. The relationship between the two is as follows

$$\mathrm{P}\left[X \leq x\right] = F_X(x) = \Phi\left(\frac{\ln(x) - \mu_{\ln X}}{\sigma_{\ln X}}\right)$$

where X has a lognormal distribution with parameters $\mu_{\ln X}$ and $\sigma_{\ln X}$ (Table 2.6), which are just the mean and standard deviation of $\ln(X)$. For example, the probability that the hydraulic conductivity (Fig. 2.20) is greater than 1×10^{-7} cm/s is calculated as follows

$$\mathrm{P}\left[X > 1 \times 10^{-7} \text{ cm/s}\right] = 1 - \Phi\left(\frac{\ln(1 \times 10^{-7}) - (-18.0)}{1.41}\right) = 1 - \Phi(1.33) = 1 - 0.908 = 0.092$$

2.5 Reliability-Based Design

Reliability-based design approaches are becoming common in civil engineering. For example, U.S. codes for concrete and steel design are reliability-based. In addition, a reliability-based approach was adopted by the European Community in the new Eurocode standards. These approaches are referred to by the names Load and Resistance Factor Design (LRFD) in the U.S. and Limit State Design (LSD) in Europe.

The objective of a reliability-based design approach is to assure satisfactory system performance within the constraint of economy. Most designs are developed without the benefit of complete information and under conditions of uncertainty. What maximum load will a structure experience over its lifetime? How will the strength of steel change as a function of time due to corrosion? Because of these uncertainties, there always exists a chance or risk of failure. In most cases, it is not practical or economical to eliminate this risk. All design approaches implicitly balance costs and benefits; a reliability-based approach attempts to achieve this balance in a more systematic and rational manner.

2.5.1 Traditional Design Approach

Conceptually, most problems can be described in terms of a load, S, and a resistance, R. The load represents the load applied to the system (e.g., an axial load on a column, the volume of water entering a treatment facility, etc.), while the resistance represents the capacity of the system (e.g., the axial capacity of column, the capacity of a treatment plant, etc.). Traditional design approaches are deterministic. We account for uncertainties in the load and resistance by requiring a resistance that is greater than the estimated load

$$R_{reqd} \geq F_S S$$

where F_S is a factor of safety. The factor of safety typically ranges between 1.0 and 3.0; however values as large as 10 or 100 may be used in some instances.

For example, consider an offshore pile that is subjected to a load of 4,000 kips during a storm, S = 4, 000 kips. Using a factor of safety of 1.5, we determine that the required pile capacity should exceed 1.5(4,000), or $R_{reqd} \geq 6,000$ kips.

2.5.2 Reliability-Based Design Approach

With a reliability-based approach, we attempt to account explicitly for uncertainties in the load and resistance. For example, assume that the load is modeled with a normal distribution with a mean of 4,000 kips and a c.o.v. of 0.20. Also, assume that the resistance is normally distributed with a mean value that is 1.5 times the mean load, μ_R = 1.5μ_S = 6, 000 kips, and a c.o.v. of 15 percent. We can now calculate the probability that the load exceeds the resistance as follows

$$\text{P}[S > R] = \text{P}[R \leq S] = \text{P}[R - S \leq 0] = \text{P}[X \leq 0]$$

Recall that one objective in developing theoretical random variable models was to provide a mathematical framework for combining random variables. It can be shown that a linear combination of normal random variables, such as $X = R - S$, where R and S have normal distributions, will also have a normal distribution. Further, the mean and standard deviation for X are given as follows

$$\mu_X = \mu_R - \mu_S = 6,000 - 4,000 = 2,000 \quad \text{kips}$$

$$\sigma_X = \sqrt{\sigma_R^2 + \sigma_S^2} = \sqrt{(0.2 \times 4,000)^2 + (0.15 \times 6,000)^2} = 1,200 \quad \text{kips}$$

assuming that R and S are statistically independent. The probability that the load exceeds the resistance is then calculated as follows

$$\mathrm{P}[X \leq 0] = \Phi\left(\frac{0 - 2,000}{1,200}\right) = \Phi(-1.67) = 0.047$$

Therefore, the probability of failure for this column is 0.047, and its *reliability* is 0.953 or 95.3 percent. The factor 1.67 in the above equation is known as the *reliability index*, β. As β increases, the probability of failure decreases. Hence, β is similar in behaviour to the factor of safety.

What if there is more uncertainty in the resistance, and its c.o.v. increases from 15 to 20 percent? Using the same factor of safety (i.e., F_S = 1.5), we will obtain a different probability of failure. The mean value of X remains the same, but σ_X increases from 1,200k to 1,440k. The probability of failure increases from 0.047 to 0.082, and the reliability decreases from 95.3 percent to 91.8 percent. Therefore, a consistent factor of safety of 1.5 does not necessarily produce a consistent level of reliability.

By explicitly accounting for uncertainties, we can attempt to achieve a consistent level of reliability using the reliability-based design approach. We can establish the required mean resistance, μ_R, to achieve a specified reliability (i.e., a target probability of failure). For example, what should μ_R be to obtain a reliability of 99 percent? We can answer this question as follows

$$\begin{aligned} \Phi - \beta &\leq 0.01 \\ \beta &\geq 2.33 \\ \therefore \quad \mu_X &\geq 2.33\sigma_X \end{aligned}$$

By substituting the equations for μ_X and σ_X from above, we obtain

$$\mu_R - 4,000 \geq 2.33\sqrt{800^2 + (0.15\mu_R)^2}$$

Solving for μ_R, we find that the probability of failure will be less than or equal to 0.01 if $\mu_R \geq 7,110$ kips. Therefore, we will achieve our target level of reliability if we multiply the mean load by a "safety factor" of $7,110/4,000$, or 1.78.

In summary, a reliability-based design approach consists of the following steps:

1) Select a target probability of failure, p_F. This failure probability is established considering costs, consequences of failure, engineering judgment, politics and experience. Historical failure probabilities for civil engineering facilities are between 10^{-3} to 10^{-4}; therefore, target failure probabilities for new designs are typically within this range.
2) Calculate the required reliability index, β, to achieve the target failure probability

   $$\beta = -\Phi^{-1}(p_F)$$

   If S and R are statistically independent normal variates, then

   $$\beta = \frac{\mu_R - \mu_S}{\sqrt{\sigma_R^2 + \sigma_S^2}}$$

3) Find the mean resistance required to achieve the target β.

2.5.3 From Theory to Practice

Practice is not yet ready (or willing) to implement a fully probabilistic design approach. Design codes are being developed using probabilistic analyses; however, the codes themselves are still deterministic. The following general equation is used to determine the required mean resistance

$$\phi\mu_R \geq \gamma\mu_S$$

where the load and resistance factors, γ (load factor) and ϕ (resistance factor), are specified for different design cases. In our example, we assumed that ϕ was equal to 1.0, and found that γ was 2.21 to achieve a target failure probability of 0.01. The load and resistance factors are intended to account for uncertainties in R and S, and they are developed from probabilistic analyses of typical design cases. However, the uncertainties and target failure probabilities used in the probabilistic analyses are transparent to the code user; only the load and resistance factors themselves are specified.

2.5.4 Advantages and Limitations of a Reliability-Based Design Approach

There are several advantages in using a reliability-based approach versus the traditional approach:

1) A factor of safety does not provide information on the level of safety in the design. The same factor of safety may produce two designs that have different reliabilities. A reliability-based approach allows us to quantify the reliability, and load and resistance factors are developed to achieve consistent levels of reliability among different designs.
2) Factors of safety are based on experience with similar designs. What if we don't have experience (e.g., a new construction material or a new environment)? What if our experience is not positive? A reliability-based approach provides the ability to develop new designs that achieve a specified reliability.
3) Since a factor of safety has no real meaning in terms of reliability, it is difficult to select an optimum factor of safety. By quantifying reliability, we can perform cost-benefit analyses to balance construction costs against the risk of failure.

However, reliability-based approaches in their current form (e.g., LRFD) do have limitations. The code user does not have control over the target failure probability, and cannot directly incorporate the uncertainties associated with their specific design. Further, even a purely probabilistic approach cannot prevent poor engineering; it can only help to make good engineering better.

Chapter 3

Correlation, Multiple RV's, and System Reliability

by Wilson Hon C. Tang

3.1 Correlation in Geotechnical Engineering

Empirical relations are often used in geotechnical engineering to correlate soil properties. For example, the compression index C_c with the void ratio e or liquid limit L_L, relative density D_r with SPT, and strength ratio $S_u/s'p$ with Plasticity Index I_p.

The purpose is to estimate soil parameters needed for analysis and design by using some indirect index properties that are relatively cheaper and easier to obtain. If indeed an excellent relation existed between the properties, this would provide a cost effective way for obtaining the required soil parameters. Oftentimes, the empirical relations could be far from perfect and hence the additional implicit uncertainties associated with this approach need to be assessed.

Fig. 3.1 shows two hypothetical empirical relations that have been established from test data. Clearly one would have more confidence in using relationship A. But an engineer may like to know how reliable it is in using relationship B. Would the reliability improve if one increased the number of indirect tests used, and by how much? Should the engineer use only direct tests? Could one supplement the information from limited number of direct tests with less costly indirect tests? To address these questions, the probabilistic implication of using an empirical relation is presented as follows.

Consider the simple case where the empirical relation is approximately linear and the scatter of the data is approximately constant about the prediction curve. A linear regression with constant variance can be performed (e.g. see Ang and Tang, 1975) to obtain an estimate of the mean value of Y as a function of x, i.e.E $\left[Y \mid x\right] = a + bx$, and also an estimate for the variance, i.e. Var $\left[Y \mid x\right]$. The former denotes the predicted value of Y for a given value of x whereas the latter denotes a measure of the error associated with using the empirical relation for prediction; in fact, the square root of Var $\left[Y \mid x\right]$ is referred to as the calibration error, i.e. σ_C. If the empirical relation has been established by using only a limited set of data, then additional estimation error will arise due to the lack of sufficient data for establishing the empirical relation. However this error will be generally small relative to the calibration error and it will be neglected in the subsequent examples.

In the following example, we try to compare the predicted value of a soil parameter and its prediction error based on several sources of information namely:

1) n direct tests
2) m indirect tests
3) subjective judgment

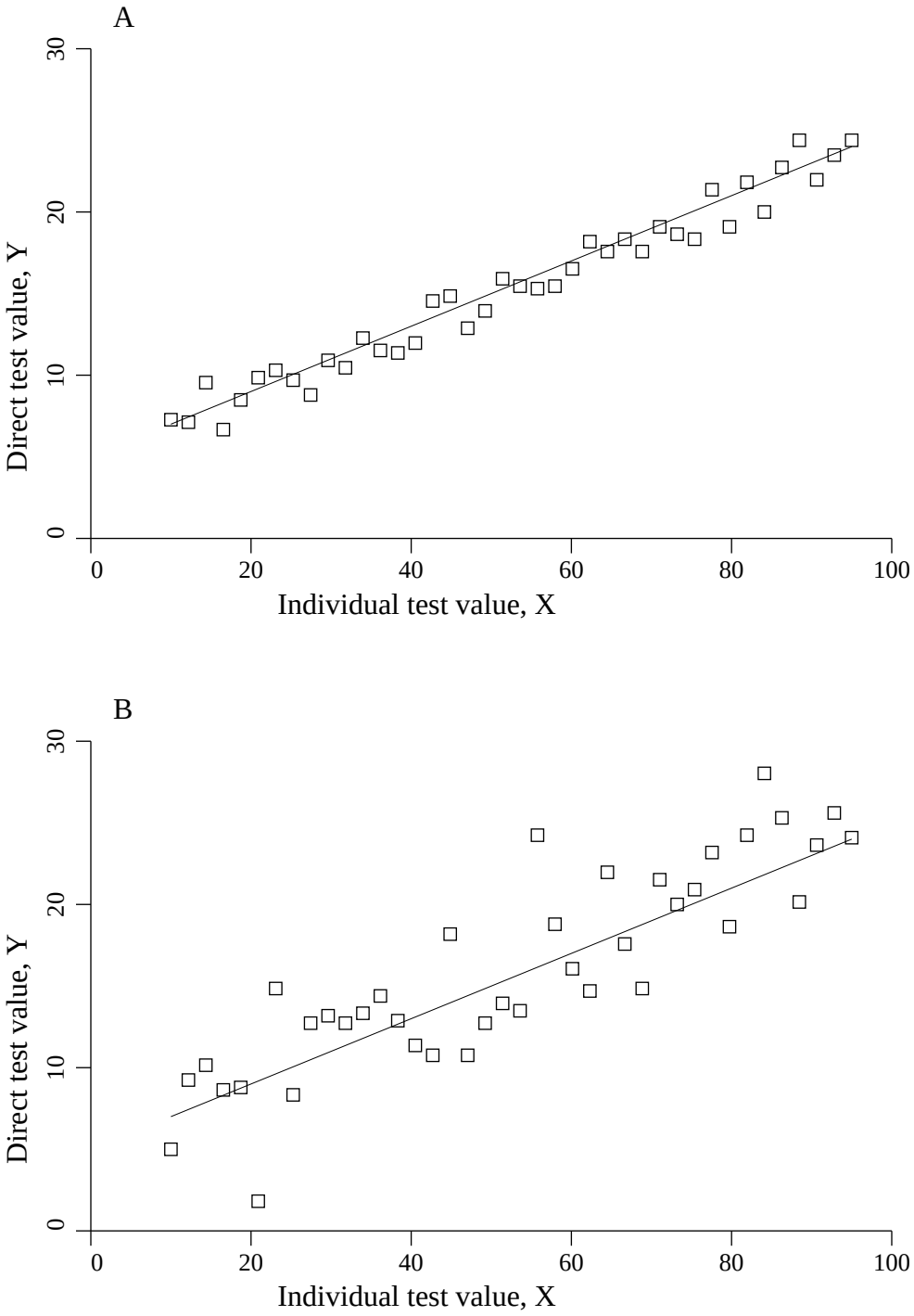

Figure 3.1 Example empirical relationships

For simplicity, the tests are assumed to be statistically independent. For the direct tests, the prediction error is proportional to the scatter of the data but inversely proportional to the number of tests n. For the indirect tests, the calibration error σ_c has to be added (in a root mean square sense) to the scatter of the data. Lastly, based on subjective judgement, the uncertainty of the soil parameter is described by a distribution for which the corresponding mean and standard deviation can be inferred as μ' and σ' respectively. Bayesian probability procedure is used for combining the estimates.

Assuming soil samples are statistically independent, the error associated with an estimate of the mean can be calculated as follows;

1) from direct tests;

$$\hat{\mu}_X = \frac{1}{n}\sum_{i=1}^{n} x_i \qquad \text{(estimator)}$$

$$\hat{\sigma}_{\hat{\mu}_X} = \frac{\hat{\sigma}_X}{\sqrt{n}} \qquad \text{(estimator error)}$$

where $\hat{\sigma}_X$ is the estimated standard deviation of X.

2) from indirect tests;

$$\hat{\mu}_X = \frac{1}{m}\sum_{i=1}^{m} x_{ci}$$

$$\hat{\sigma}_{\hat{\mu}_X} = \sqrt{\frac{\hat{\sigma}_X^2 + \sigma_c^2}{m}}$$

where σ_c is the standard deviation of the random calibration error.

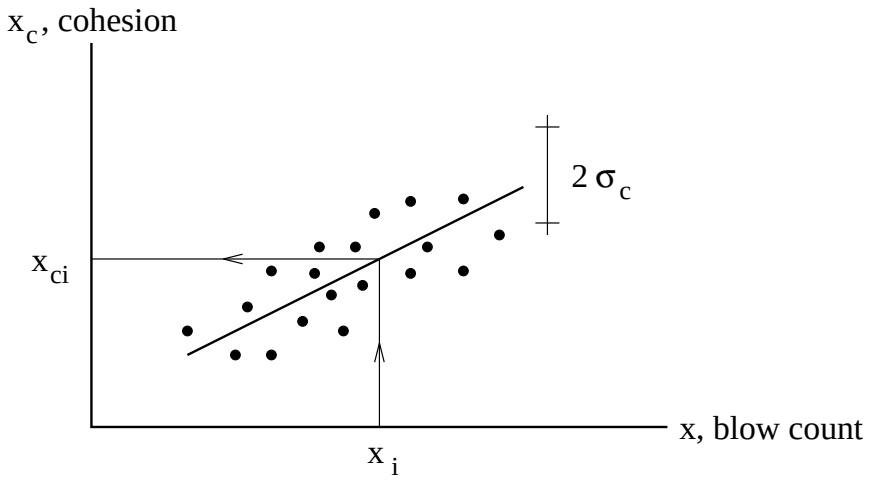

Figure 3.2

3) from subjective judgement

$$\hat{\mu}_X = \mu'$$

$$\hat{\sigma}_{\hat{\mu}_X} = \sigma'$$

An example to follow describes how 7 triaxial tests and 9 blow count values can be combined with judgmental information to yield the overall estimate of the mean cohesion of residual clay for Hong Kong and a measure of its overall error. The empirical relation used is

$$c' = 38N \qquad \text{(in psf)}$$

where N is the blow count (in blows per ft) with a calibration error of 750 psf based on the data reported by Lumb (1968) for residual soil in Hong Kong.

Example 1: Estimation of Mean Cohesion of Residual Clay

Assume $\hat{\sigma}_X = 215$. Sources of information;

i) experience: 2100 ± 500 psf with 95% probability

$$\hat{\mu}_{X_1} = 2100$$
$$\hat{\sigma}_{\hat{\mu}_{X_1}} = 255$$

ii) 7 triaxial tests: $\{2150, 1890, 1950, 1650, 2340, 1980, 2040\}$ psf

$$\hat{\mu}_{X_2} = \frac{1}{7}\sum_{i=1}^{7} x_i = 2000$$
$$\hat{\sigma}_{\hat{\mu}_{X_2}} = \frac{215}{\sqrt{7}} = 81.3$$

iii) 9 blow count values: $\{28, 45, 35, 52, 67, 71, 48, 50, 58\}$ blows per foot

$$\hat{\mu}_{X_3} = \frac{1}{9}\sum_{i=1}^{9} 38N_i = 1917$$
$$\hat{\sigma}_{\hat{\mu}_{X_3}} = \sqrt{\frac{215^2 + 750^2}{9}} = 260$$

Combining (i) and (ii) gives

$$\hat{\mu}_X = \frac{2100 \times 81.3^2 + 2000 \times 255^2}{81.3^2 + 255^2} = 2009$$
$$\hat{\sigma}_{\hat{\mu}_X} = \frac{81.3 \times 255}{\sqrt{81.3^2 + 255^2}} = 77.5$$

Combining further with (iii) gives

$$\hat{\mu}_X = \frac{2009 \times 260^2 + 1917 \times 77.5^2}{260^2 + 77.5^2} = 2002$$
$$\hat{\sigma}_{\hat{\mu}_X} = \frac{260 \times 77.5}{\sqrt{260^2 + 77.5^2}} = 74.3$$

The coefficient of variation of the final mean estimate is $\hat{\sigma}_{\hat{\mu}_X}/\hat{\mu}_X = 74.3/2002 = 3.7\%$.

Observations:

1) The prediction error using indirect tests could be smaller than that using direct tests provided that more indirect tests are used and the calibration error is relatively small.

2) In combining estimates from two sources of information, the formula for calculating the weighted mean is inversely proportional to the error of the respective estimates. Also the error of the combined estimate is always smaller than the error of the individual estimate.

Further reference:

1. LUMB, P., "Statistical Aspects of Field Measurements," Proceedings, Fourth Australian Road Research Conference, 1968, p.1761.

2. TANG, W., "A Bayesian Evaluation of Information for Foundation Engineering Design", in Statistics and Probability in Civil Engineering, Proceedings of the First ICASP, Hong Kong University Press, 1971, pp.174-185.

3.2 Performance Involving Multiple Random Variables

The following examples are used to demonstrate reliability problems that involves more than one random variable. In this case, the degree of correlation between random variables will be important factor affecting the reliability.

Example 2: Differential settlement between footings

Consider two adjacent footings as shown in Fig. 3.3. Suppose the settlement of each footing follows a normal distribution with a mean of 2 inches and a standard deviation of 0.5 inches. Assume that a differential settlement exceeding say 1 inch is considered to be unacceptable. Determine the probability of unacceptable differential settlement among this pair of footings.

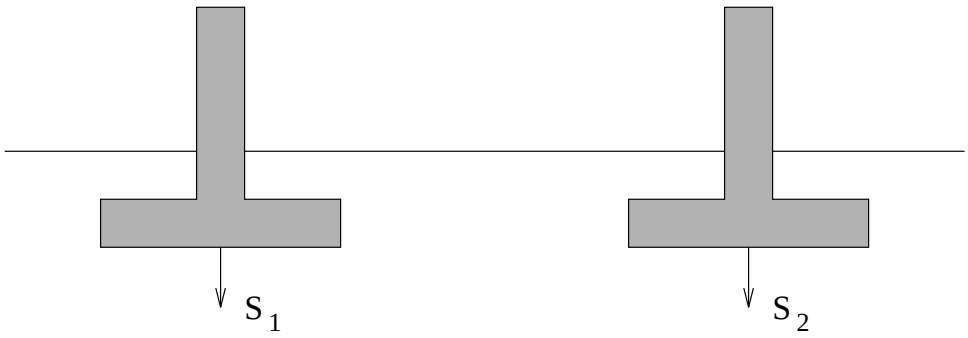

Figure 3.3

Case 1: The settlements are statistically independent

Let

$$D = S_1 - S_2$$

where S_1 and S_2 denote the settlement of footings 1 and 2. It could be shown that D also follows a normal distribution with mean and standard deviation as follows:

$$\mu_D = \mu_{S_1} - \mu_{S_2} = 2 - 2 = 0$$

$$\sigma_D = \sqrt{\sigma_{S_1}^2 + \sigma_{S_2}^2} = \sqrt{0.5^2 + 0.5^2} = 0.707$$

Hence, the probability of unacceptable differential settlement is

$$\begin{aligned} \mathrm{P}\left[|D| > 1\right] &= \mathrm{P}\left[D > 1\right] + \mathrm{P}\left[D < -1\right] = 2\mathrm{P}\left[D > 1\right] \\ &= 2\left[1 - \Phi\left(\frac{1-0}{0.707}\right)\right] \\ &= 0.157 \end{aligned}$$

Case 2: The settlements are correlated

Generally, the load and soil properties affecting the settlements between adjacent footings are similar. Suppose the correlation coefficient, ρ, is 0.8, then D is also normal with mean value 0 but its standard deviation becomes

$$\begin{aligned} \sigma_D &= \sqrt{\sigma_{S_1}^2 + \sigma_{S_2}^2 - 2\rho\sigma_{S_1}\sigma_{S_2}} \\ &= \sqrt{0.5^2 + 0.5^2 - 2(0.8)(0.5)(0.5)} \\ &= 0.316 \end{aligned}$$

and the probability of unacceptable differential settlement becomes

$$\begin{aligned} \mathrm{P}\left[|D| > 1\right] &= \mathrm{P}\left[D > 1\right] + \mathrm{P}\left[D < -1\right] = 2\mathrm{P}\left[D > 1\right] \\ &= 2\left[1 - \Phi\left(\frac{1-0}{0.316}\right)\right] \\ &= 0.00156 \end{aligned}$$

On the other hand, if indeed the settlements of the two footings are the same, i.e. perfectly correlated with $\rho = 1$, then

$$\sigma_D = \sqrt{0.5^2 + 0.5^2 - 2(1)(0.5)(0.5)} = 0$$

and hence $\mathrm{P}\left[|D| > 1\right]$ will equal to zero.

Fig. 3.4 shows how the probability of unacceptable differential settlement decreases with increasing correlation. In other words, the effect of correlation is to improve the performance reliability; neglecting this correlation effect could be very conservative.

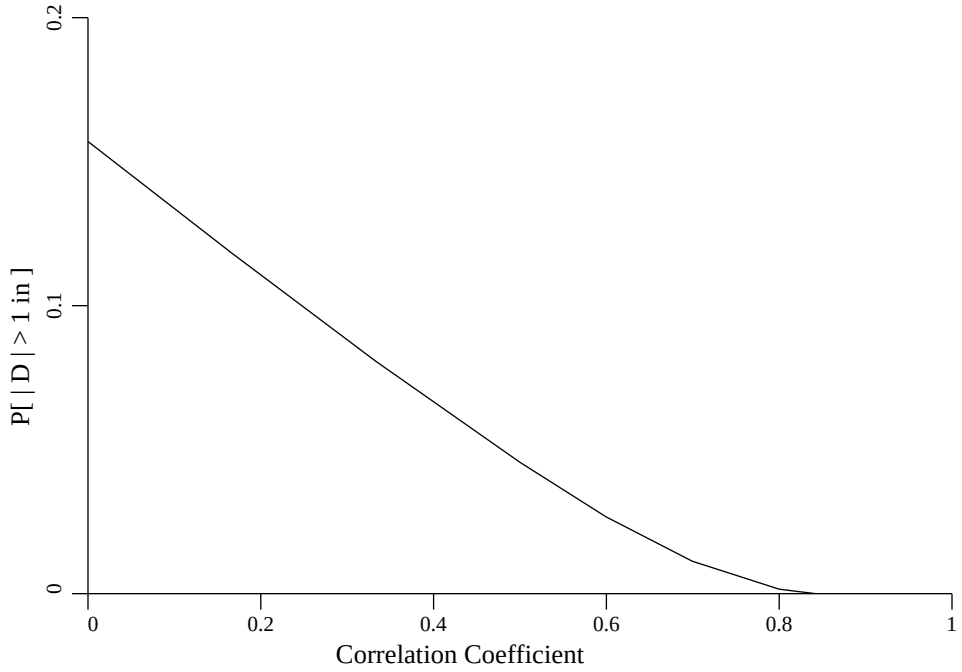

Figure 3.4 Probability of unacceptable differential settlement

Extension to multiple footings

Consider a grid of footings as shown in Fig. 3.5. Determining the probability of excessive settlement or differential settlement by following an analytical approach like that above will be very cumbersome. A practical procedure is through the Monte Carlo Simulation method. The method calls for the simulation of possible scenarios on the settlement values of each footing according to the probability distributions of the random variables involved, and then infer the probability of various events from the observed outcomes of all simulation runs. In the example as shown, three different models are studied where soft pocket can be present (in models 2 and 3) in an otherwise stiff medium. The soft pocket is considered an anomaly A whose occurrence between footings can be correlated (as in model 3). The probability of various settlement performance indicators (e.g., maximum settlement > allowable settlement, or maximum differential settlement between adjacent footings > allowable differential settlement) are presented in Fig. 3.5 for the three models. Generally, potential presence of anomalies worsen the performance (i.e. by increasing the probability of unsatisfactory performance); however, correlation between anomaly presence under adjacent footings improve the performance. Through the Monte Carlo Simulations procedure, the fraction of footings that have excessive settlement can be also easily estimated as shown.

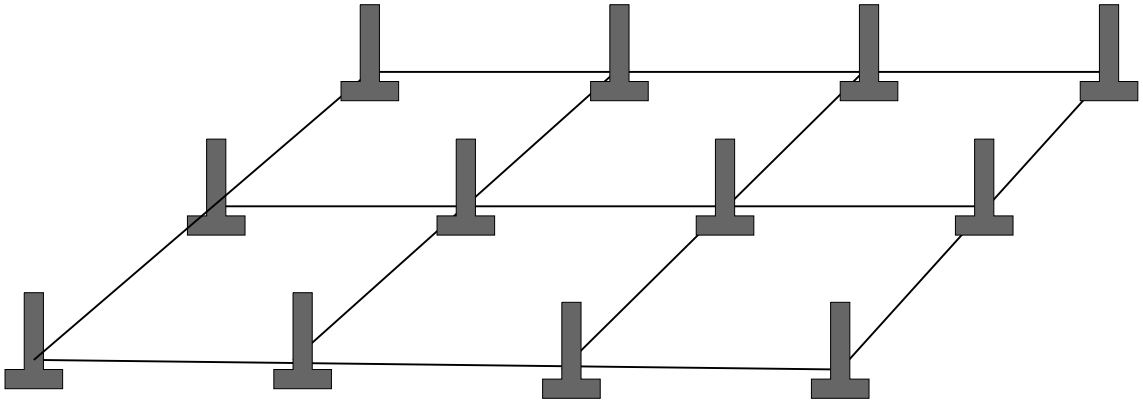

Figure 3.5 Grid of footings each settling by S_i

Model 1: S = N(1, 0.3) inches
correlation coefficient = 0.6

Model 2: Probability of soft pocket = 0.01
s.i. between footings
S_A = N(2, 0.6) inches

Model 3: Probability of A to A = 0.02

Allowable max. S is 2 inches
Allowable max. differential settlement is 1.5 inches

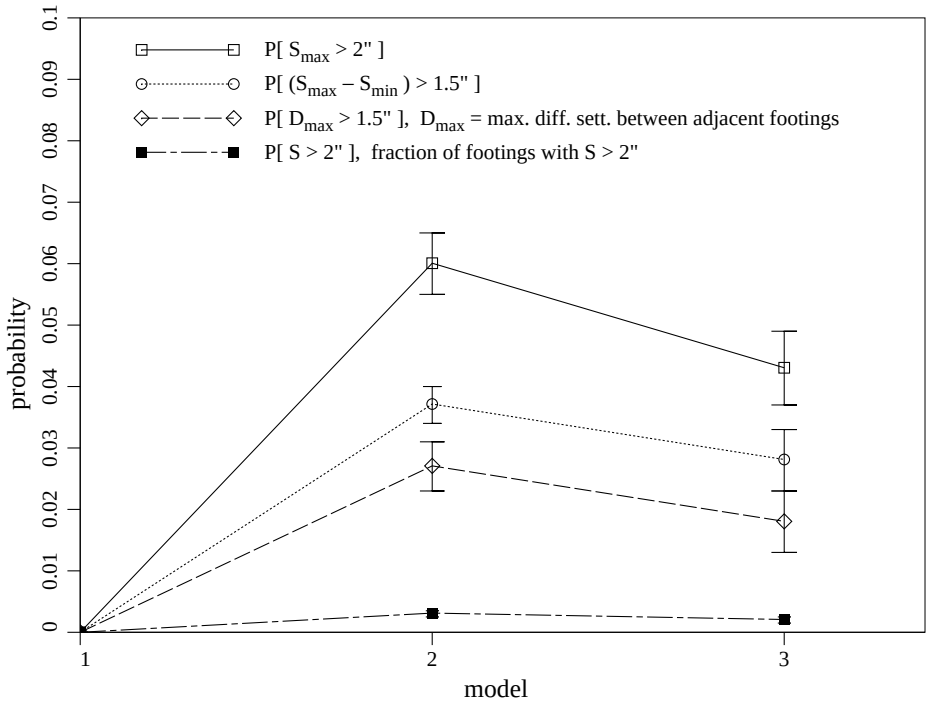

Figure 3.6 Estimated probabilities of unsatisfactory settlement performance – Models 1, 2, and 3 (50 runs with 200 samples per run)

Example 3: Consolidation settlement

In this example, a first order uncertainty analysis will be applied to the settlement problem. Note that relative contribution to the overall uncertainty depends both on sensitivity factors and the uncertainty of individual variables.

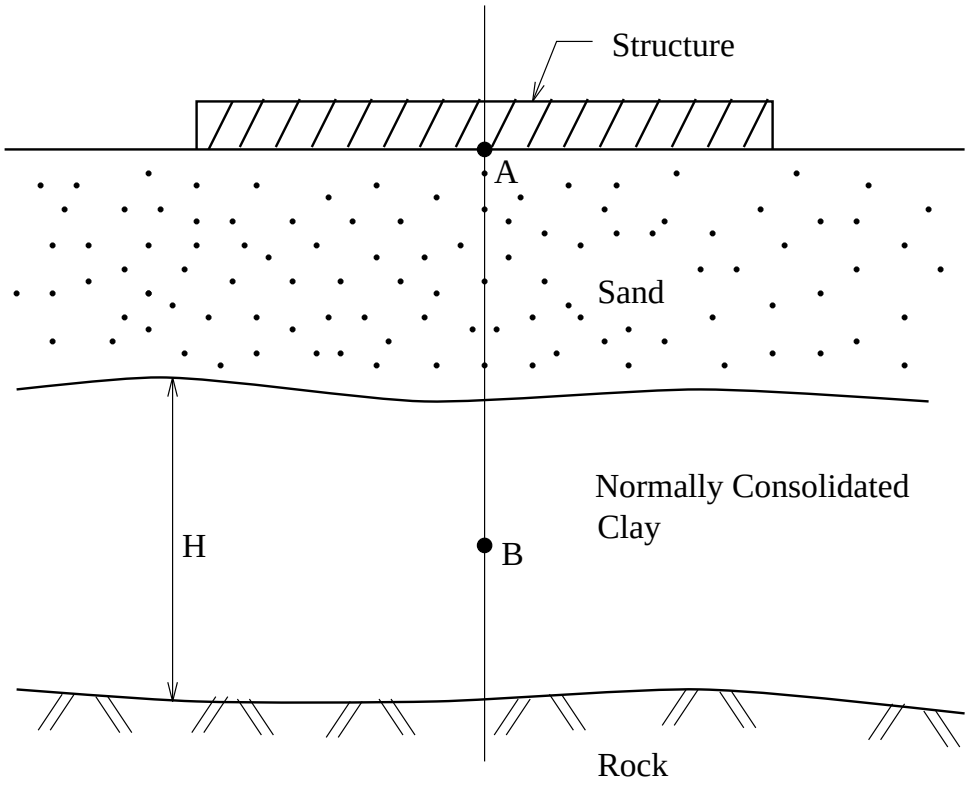

Figure 3.7 Settlement in consolidated clay

The actual settlement is expressed as

$$S = N\left(\frac{C_c}{1+e_o}\right) H \log_{10}\left(\frac{p_o+\Delta p}{p_o}\right)$$

where N is the model error, C_c is the compression index, p_o is the effective pressure at B, and Δp is the increase in pressure at B.

Given the statistics (where δ is the coefficient of variation)

Variable	Mean	SD	δ
N	1.0	0.100	0.1
C_c	0.396	0.099	0.25
e_o	1.19	0.179	0.15
H	168 inches	8.40	0.05
p_o	3.72 ksf	0.186	0.05
Δp	0.50 ksf	0.100	0.20

First order analysis of uncertainties:

If $Y = g(X_1, X_2, \ldots, X_m)$ then first order estimates of the mean, μ_Y, and coefficient of variation, δ_Y, of Y are

$$\mu_Y = g(\mu_{X_1}, \mu_{X_2}, \ldots, \mu_{X_m})$$
$$\delta_Y^2 = \sum_{j=1}^{m} \left(\frac{\partial g}{\partial X_j} \frac{\mu_{X_j}}{\mu_Y} \right)_{\mu}^2 \delta_j^2 = \sum_{j=1}^{m} S_j^2 \delta_j^2$$

In this case μ_S = 1.66.

Defining $S_j = (\partial S/\partial X_j)(\mu_{X_j}/\mu_S)$, the components contributing to the uncertainty in S can be found as follows;

X_j	μ_{X_j}	δ_j	S_j	$S_j^2\,\delta_j^2$	%
N	1.0	0.10	1.0	0.01	8.4
C_c	0.396	0.25	1.0	0.0625	52.4
e_o	1.19	0.15	-0.55	0.0068	5.7
H	168	0.05	1.0	0.0025	2.1
p_o	3.72	0.05	-0.94	0.0022	1.8
Δp	0.50	0.20	0.94	0.0353	29.6

Giving δ_S = 0.345.

3.3 Multiple Failure Modes - System Reliability

Example 4: Retaining wall

Three failure modes can be identified in Fig. 3.8, namely (i) overturning of the wall, (ii) horizontal sliding of the wall and (iii) bearing capacity failure of the foundation. The system probability of failure will be the probability of at least one of these modes will occur. Because of the correlation between the failure modes, the system failure probability can only be practically determined in terms of bounds. First order reliability method (FORM) was used first in determining the failure probability of individual mode.

Note that in the conventional approach, one can only determine the factor of safety for each mode; however, in the probabilistic approach, one can combine the individual failure mode probability to estimate the total failure probability for the system.

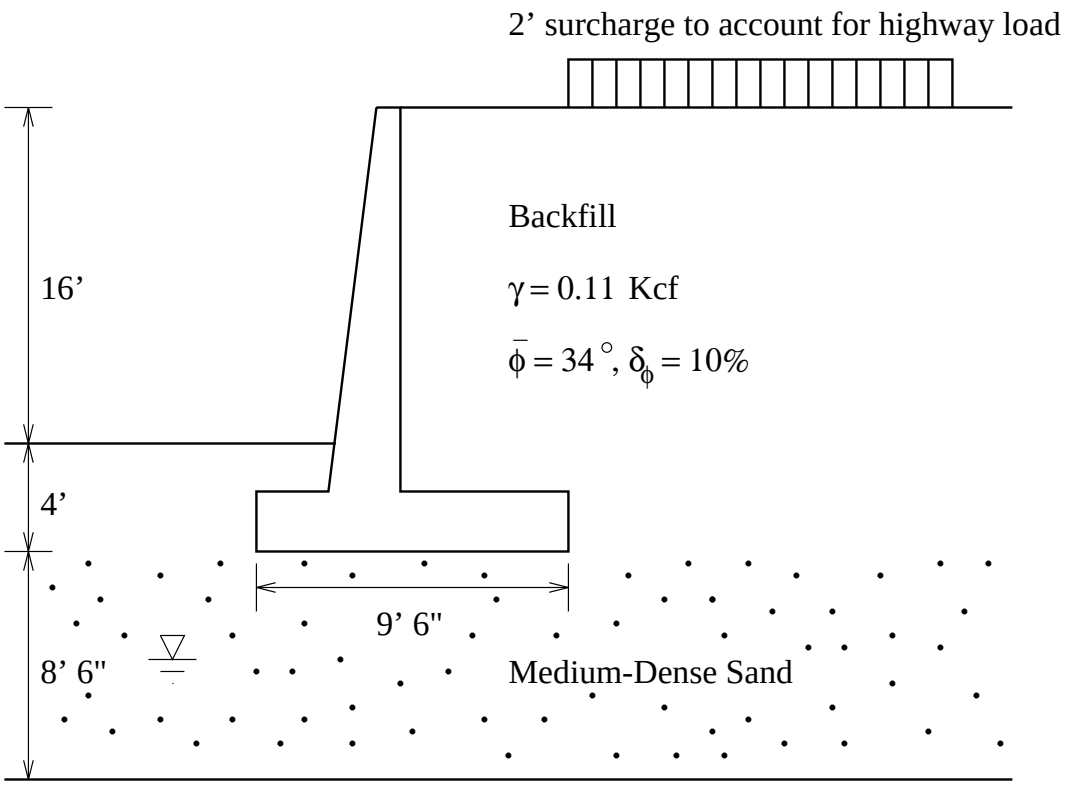

Figure 3.8 Retaining wall reliability

Potential Failure Modes:

1) Overturning of wall

$$g_1(\underset{\sim}{X}) = 112.5 - 195.1 \tan^2\left(45 - \tfrac{\phi}{2}\right)$$

2) Horizontal sliding of the wall

$$g_2(\underset{\sim}{X}) = 20.14 \tan\delta - 26.6 \tan^2\left(45 - \tfrac{\phi}{2}\right)$$

3) Bearing capacity failure of wall foundations
   – assume negligible contribution in this example

For the overturning mode,

$$p_{F_1} = 0.3 \times 10^{-7}$$

For the horizontal sliding mode,

$$p_{F_2} = 0.01044$$

Hence the first-order bounds on the failure probability are

$$0.01044 \leq p_F \leq 0.01044 + 0.3 \times 10^{-7}$$

indicating that the failure probability is about 0.01044. The first order bound is sufficient in this case because there is a dominant failure mode, namely the horizontal sliding.

Example 5: Slope failure

For a given slope, there could be thousands of potential slip surfaces. The slopes can fail through sliding along each of those slip surfaces, although with varying likelihood. Hence the probability

of slope failure would be equal to the probability that at least one of these slip surfaces will have resistance less than the driving load caused by the weight of the soil. Fortunately in this case, the soil resistance between individual slip surfaces are highly correlated. Hence the system failure probability could be close to the slip surface with the highest probability of failure. For example, Oka & Wu (1990) show that for a cut slope in Chicago, the probability of failure considering all slip surfaces is less than twice the failure probability of the most critical slip surface.

Note that in the non-probabilistic approach, we consider only the slip surface with the lowest factor of safety. The questions of: "Is that really the most critical slip surface considering various uncertainties?" and "How would all those other potential slip surfaces affect the safety level of the slope?" are not addressed.

Chapter 4

Data Analysis/Geostatistics

by Gordon A. Fenton

4.1 Random Field Models

Consider a clay barrier of extent 40×40 metres. If permeability tests were carried out at sufficiently close spacing, the permeability K might appear as shown in Fig. 4.1, which plots log-permeability against spatial position. Clearly this permeability field, $K(\underset{\sim}{x})$, appears quite random. In the following, vectors will be denoted by underscoring the symbol with a tilde character, so that $\underset{\sim}{x}$ is a vector describing a spatial position with coordinates (x_1, x_2, x_3) in three-dimensional space. Similarly, matrices will be denoted by underscoring with two tildes, for example $\underset{\approx}{A}$.

It seems reasonable to make the following observations about the field displayed in Fig. 4.1;

- points which are very close together tend to have similar permeabilities, that is the permeabilities are *highly correlated*.
- points which are far apart may have quite different permeabilities. In this case the permeabilities are *poorly correlated*.

In general, correlation between points tends to decrease with distance.

To produce a plot like that shown in Fig. 4.1, a significant amount of information must be gathered from the field, which is an expensive undertaking. On the other hand, if the information is not gathered then the permeability at most points is *uncertain* and this uncertainty must enter into any design decisions. As engineers, the task is to minimize sampling costs while still being able to make informed decisions. For this, random fields are ideally suited as models of the spatially distributed uncertainty and they can be used to produce probability statements regarding the design criteria.

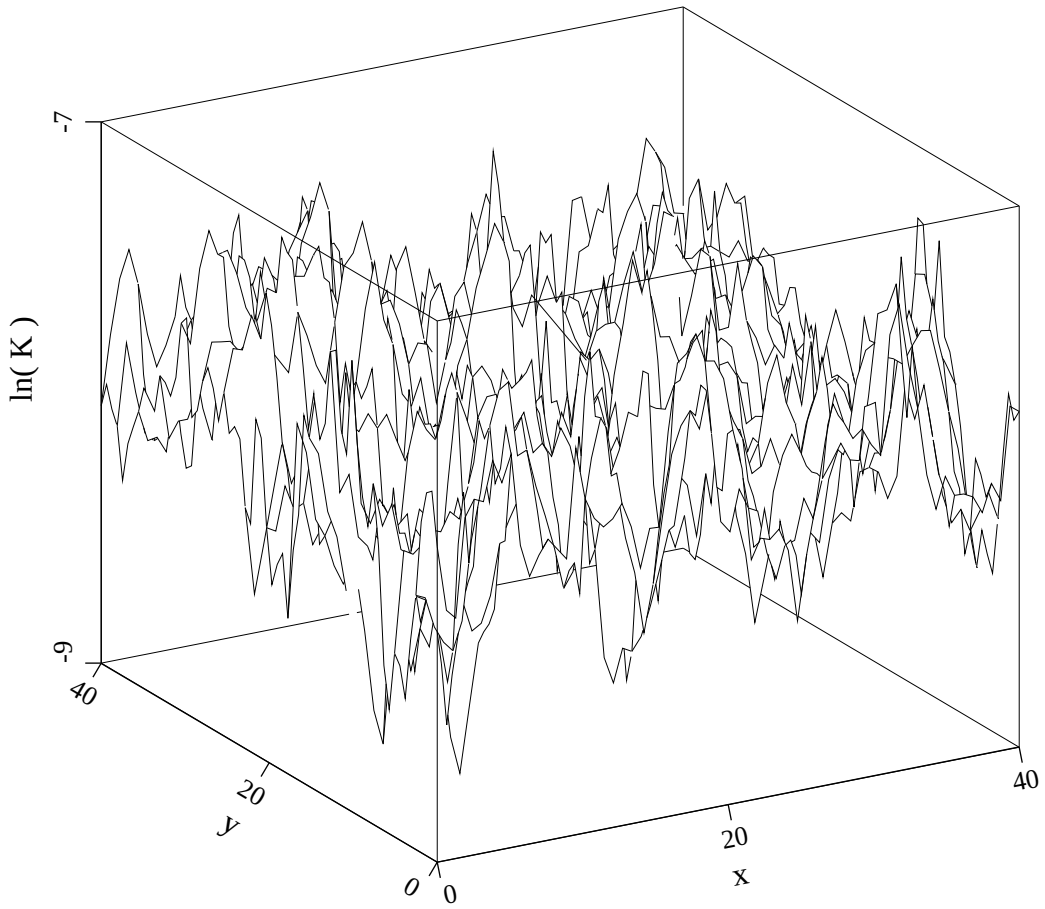

Figure 4.1 Permeability field measured over a 40×40 metre square.

One of the major features of a random field representation of a soil is the concept of statistical dependence between field values at different points. In general a random field, $X(\underset{\sim}{x})$, is characterized by;

1) its mean, $\mu(\underset{\sim}{x})$. This may be spatially constant, or may vary as a function of $\underset{\sim}{x}$, the latter a feature of *non-stationary*, also called *non-homogeneous*, random fields,
2) its variance, $\sigma^2(\underset{\sim}{x})$, which represents the degree of scatter in the field about its mean,
3) its correlation structure, $\rho(\underset{\sim}{x}, \underset{\sim}{x}')$, which gives the correlation coefficient between $X(\underset{\sim}{x})$ and $X(\underset{\sim}{x}')$ for any two points $\underset{\sim}{x}$ and $\underset{\sim}{x}'$,
4) its higher order moments: in practice, these may be difficult to estimate accurately,

.

.

.

5) its complete multivariate joint probability density function (PDF). This is the complete probabilistic description of all the points in the field from which probability calculations can be made.

Specifically, a random field is a set of random variables, X_1, X_2, ..., each associated with the value of the soil property of interest at the points $\underset{\sim}{x}_1, \underset{\sim}{x}_2, \ldots$ in the field.

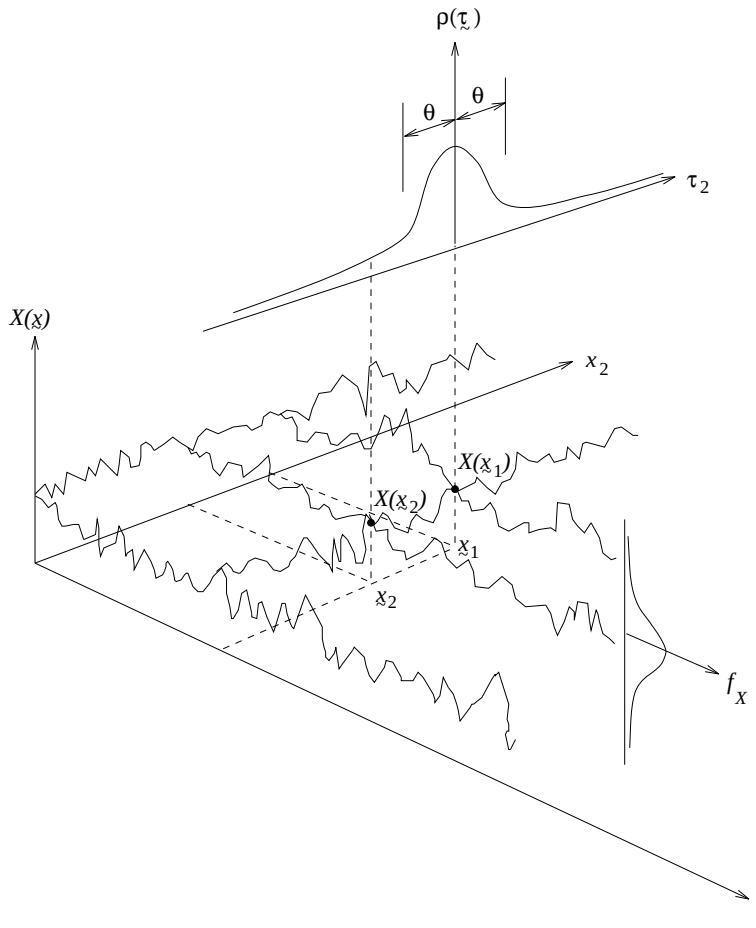

Figure 4.2 2-D random field showing correlation structure and marginal distribution.

Due to difficulties in estimating higher order moments, random field representations are often restricted to information about the mean, variance and correlation structure. This usually leads to the adoption of relatively simple joint pdf's as models for the field, for example multivariate normal or lognormal distributions. The correlation structure is often assumed to be a simple function of distance between points, governed by a single parameter. A commonly used model is one in which the correlation decays exponentially with distance, τ;

$$\rho(\tau) = \exp\left\{-\frac{2|\tau|}{\theta}\right\}$$

where the parameter θ is call the *scale of fluctuation*. Loosely speaking θ is the distance beyond which the field is effectively uncorrelated (i.e. for the above model, if the distance between two points is $\tau > \theta$, then the correlation coefficient between these two points is less than 0.14). Another way of looking at it is that any two points closer together than θ tend to be strongly correlated. As a result, fields having small scales of fluctuation tend to vary erratically over shorter distances – they appear very 'rough'. Fields having large scales of fluctuation, according to the above model, tend to be more slowly varying and smoother. From the point of view of data gathering, the latter type of field often presents problems. What may appear to be a trend in the data may in fact just be a slow variation that sooner or later reverses direction.

How a random field model is used depends on the questions being asked and the type of data available. In particular, the issue of whether or not data is available at the site being investigated

has a significant impact on how the random field model is defined and used. Some possible scenarios are as follows;

1) data is gathered at the site in question over its entire domain
   - here a random field is being modeled whose values are known at the data site locations and no attempt will be made to extrapolate the field beyond the range of the data.
   - a representative random field model can always be estimated – estimates for μ_X, σ_X^2 and correlation structure are "local" and can be considered to be reasonably accurate for the purposes of modeling the site.
   - best estimates of the random field between data sites should be obtained using Best Linear Unbiased Estimation or *Kriging*.
   - probability estimates should be obtained using the conditioned random field. One possible approach is to use conditional simulation (all realizations pass through the known data but are random between the data sites).
2) data is gathered at a similar site or over a limited portion of the site to be modeled
   - in this case, there is much greater uncertainty in applying the statistics obtained from one site to that of another or in extending the results to a larger domain. Typically some assumptions need to be made about the 'representativeness' of the sample. This situation typically arises in the preliminary phases of a design problem, before the site has been cleared, for example.
   - if the statistics can be considered representative, probability estimates can be made either analytically or through Monte Carlo simulations. Kriging is not an option since data is not available over the domain in question.
   - the treatment of trends in the data needs to be more carefully considered. If the trend seems to have some physical basis (such as an increase in cone tip resistance with depth), then it may be reasonable to assume that the same trend exists at the site in question. However, if the trend has no particular physical basis, then it is entirely possible that quite a different trend will be seen at the site in question. The random field model should be able to accommodate this uncertainty.

4.2 Data Analysis

4.2.1 Estimating the Mean

The task of data analysis and geostatistics is to deduce from a set of data the appropriate parameters of a random field model of the soil property(s) in question. This generally means that values for the mean, variance and correlation structure are to be found. Unfortunately, the fact that the soil property in question exhibits spatial correlation complicates the estimation process. To illustrate this, consider the usual estimator of the mean;

$$\hat{\mu}_X = \frac{1}{n}\sum_{i=1}^{n} X_i \tag{4.1}$$

If the field can be considered stationary, so that each X_i has the same mean, then $\mathrm{E}[\hat{\mu}_X] = \mu_X$ and this estimator is considered *unbiased* (it is 'aimed' at the quantity to be estimated). It should be

recognized that if a different set of observations of X are used in the above, the estimated mean will also likely be different, that is $\hat{\mu}_X$ is itself a random variable. If the X_i's are *independent* then the variance of $\hat{\mu}_X$ decreases as n increases. Specifically,

$$\text{Var}\,[\hat{\mu}_X] = \sigma_X^2/n$$

which goes to zero as the number of independent observations, n, goes to infinity.

However, consider what happens when the X_i's are completely correlated, as in $X_1 = X_2 = \cdots = X_n$;

$$\hat{\mu}_X = \frac{1}{n}\sum_{i=1}^{n} X_i = X_1$$

and $\text{Var}\,[\hat{\mu}_X] = \sigma_X^2$, that is there is no reduction in the variability of the estimator $\hat{\mu}_X$ as n increases. In general the true variance of the estimator $\hat{\mu}_X$ will lie somewhere between σ_X^2 and σ_X^2/n. In detail

$$\text{Var}\,[\hat{\mu}_X] = \frac{1}{n^2}\sum_{i=1}^{n}\sum_{j=1}^{n}\text{Cov}\left[X_i, X_j\right] = \left[\frac{1}{n^2}\sum_{i=1}^{n}\sum_{j=1}^{n}\rho_{ij}\right]\sigma_X^2 \simeq \gamma(T)\sigma_X^2$$

where ρ_{ij} is the correlation coefficient between X_i and X_j and $\gamma(T)$ is call the *variance function*. The variance function lies between 0 and 1 and gives the amount of variance reduction that takes place when X is averaged over the sampling domain $T = n\Delta x$. For highly correlated fields, the variance function tends to remain close to 1, while for poorly correlated fields, the variance function tends towards $\Delta x/T = 1/n$. Fig. 4.3 shows examples of a process $X(t)$ superimposed by its average over a width $T = 0.2$ for poorly and highly correlated processes. When the process is poorly correlated, the variability of the average tends to be much smaller than that of the original $X(t)$, while if the process is highly correlated, the average tends to follow $X(t)$ closely with little variance reduction.

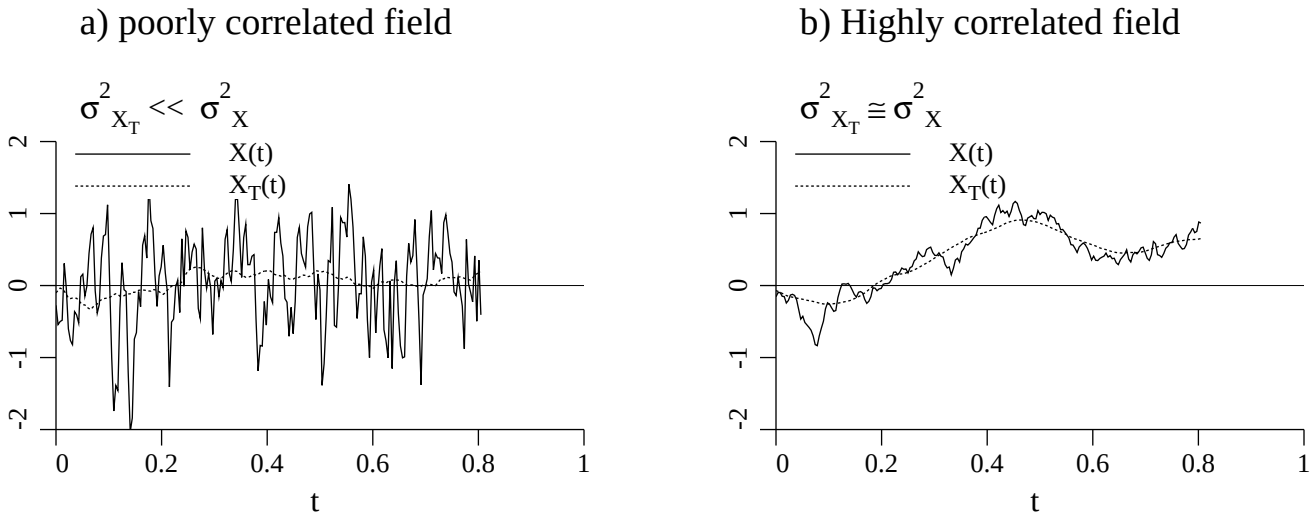

Figure 4.3 Effect of averaging on variance.

The implications of this discussion are as follows: while the mean is typically estimated using Eq. (4.1), it is important to remember that, in the case of random fields with significant spatial correlation, this estimator may itself be highly variable and increasing the number of samples

within a fixed domain may not decrease its variability (it would be better to increase the sampling domain size). See, for example Fig. 4.4.

On the other hand, the fact that the mean estimator may remain highly variable is really only important when the estimator is going to be used to model a random soil property at another site. If the data is being gathered at the site in question, then increasing the number of samples *does* reduce the uncertainty at the site, even if the true mean of the soil property in general remains questionable.

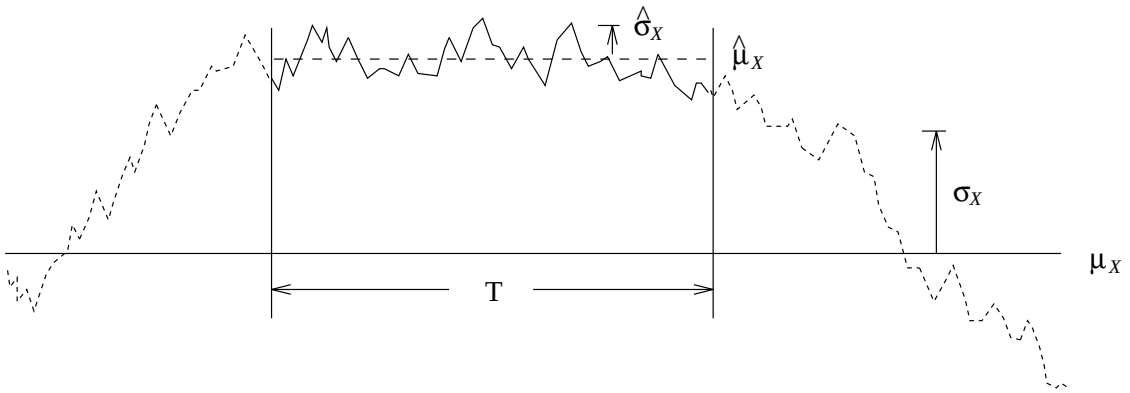

Figure 4.4 Local estimates of mean and variance over sampling domain T.

4.2.2 Estimating the Variance

Now consider a typical estimator of the variance;

$$\hat{\sigma}_X^2 = \frac{1}{n}\sum_{i=1}^{n}(X_i - \hat{\mu}_X)^2 \tag{4.2}$$

It can be shown that this is a biased estimator with expectation

$$\mathrm{E}\left[\hat{\sigma}_X^2\right] = \sigma_X^2\Big(1 - \gamma(T)\Big) \tag{4.3}$$

In the presence of correlation, $\hat{\sigma}_X^2 < \sigma_X^2$ since $\gamma(T)$ lies between 0 and 1. In fact $\hat{\sigma}_X^2 \to 0$ as the field becomes increasingly correlated (since $\gamma(T) \to 1$ in this case). This situation is illustrated in Fig. 4.4 where a slowly varying (highly correlated) soil property is sampled over a relatively short distance T. In this case, the estimated variance is much smaller than the true variance and the estimated mean is considerably different than the true mean. In the case where the X_i's are independent, $\gamma(T)$ tends towards $1/n$ so that Eq. (4.2) is seen to be still biased. Sometimes the unbiased estimator

$$\hat{\sigma}_X^2 = \frac{1}{n-1}\sum_{i=1}^{n}(X_i - \hat{\mu}_X)^2 \tag{4.4}$$

is preferred.

Again, it can be seen that the estimate given by Eq. (4.2) tends to become quite uncertain as the field becomes increasingly correlated. However, this is again only important if a good estimate of the true variance is being sought – if T denotes the site in question then the data will accurately reflect that site (but cannot be used to extrapolate).

4.2.3 Trend Analysis

In the preceding sections, a stationary random field was implicitly assumed, having spatially constant mean and variance. In many cases this is not so, at least not apparently so, over the sampling domain. Often distinct trends in the mean can be seen, and sometimes the variance also clearly changes with position. We reiterate that if such trends are not physically based, i.e. if there is no reason to suspect that identical trends would be repeated at another site, then their direct estimation depends on whether the data is being used to characterize this site or another. If the data is collected at the site to be estimated, then the direct estimation of the trends is worthwhile, otherwise probably not. If unexplainable trends are encountered during an exploration and the results are to be used to characterize another site, then probably a larger sampling domain needs to be considered.

Assume that the data is collected at the site to be characterized. In such a case, the task is to obtain estimates of $\mu_x(\underset{\sim}{x})$ and $\sigma_x^2(\underset{\sim}{x})$, both as functions of position. Trends in the variance typically require significant amounts of data to estimate accurately. The sampling domain is subdivided into smaller regions within each of which the variance is assumed spatially constant. This allows a 'block-wise' estimation of the variance which may then be used to estimate a trend. Thus the estimation of a non-stationary variance is simply a re-iteration of the stationary variance estimation procedure discussed earlier. Since often there is insufficient data to allow such a sophisticated analysis, the variance is usually assumed globally stationary.

Trends in the mean, in the case of stationary variance, can be obtained by least-squares regression techniques. Here it is assumed that the mean can be described by a function of the form

$$\hat{\mu}_x(\underset{\sim}{x}) = \sum_{k=1}^{M} a_k g_k(\underset{\sim}{x}) \tag{4.5}$$

where a_k are the unknown coefficients to be solved for, and $g_k(\underset{\sim}{x})$ are pre-specified functions of spatial position, $\underset{\sim}{x}$. In that complicated function are often unjustifiable, usually the mean trend is taken to be linear so that, in one dimension, $g_1(x) = 1$, $g_2(x) = x$ and $M = 2$. In two dimensions, the corresponding mean function would be bilinear, with $g_1(\underset{\sim}{x}) = 1$, $g_2(\underset{\sim}{x}) = x_1$, $g_3(\underset{\sim}{x}) = x_2$ and $g_4(\underset{\sim}{x}) = x_1 x_2$. The coefficients a_k may be obtained by solving the so-called *normal* equations;

$$\underset{\approx}{G}^T \underset{\approx}{G} \underset{\sim}{a} = \underset{\approx}{G}^T \underset{\sim}{y} \tag{4.6}$$

where $\underset{\sim}{y}$ is the vector of observations (the measured values of the soil property in question), $\underset{\sim}{a}$ is the vector of unknown coefficients in Eq. (4.5) and $\underset{\approx}{G}$ is a matrix made up of the specified functions $g_k(\underset{\sim}{x}_i)$ evaluated at each of the observation locations, $\underset{\sim}{x}_i$;

$$\underset{\approx}{G} = \begin{bmatrix} g_1(\underset{\sim}{x}_1) & g_2(\underset{\sim}{x}_1) & \cdot & \cdot & \cdot & g_M(\underset{\sim}{x}_1) \\ g_1(\underset{\sim}{x}_2) & g_2(\underset{\sim}{x}_2) & \cdot & \cdot & \cdot & g_M(\underset{\sim}{x}_2) \\ \cdot & \cdot & \cdot & & & \cdot \\ \cdot & \cdot & & \cdot & & \cdot \\ \cdot & \cdot & & & \cdot & \cdot \\ g_1(\underset{\sim}{x}_n) & g_2(\underset{\sim}{x}_n) & \cdot & \cdot & \cdot & g_M(\underset{\sim}{x}_n) \end{bmatrix}$$

Although the matrix $\underset{\approx}{G}$ is of size $n \times M$, the normal equations boil down to just M equations in the M unknown coefficients of $\underset{\sim}{a}$.

With this estimate of the mean, the process, $X(\underset{\sim}{x})$, can be converted into a mean stationary process $X'(\underset{\sim}{x}) = X(\underset{\sim}{x}) - \hat{\mu}_X(\underset{\sim}{x})$. The deviation or residual process X' is now approximately mean zero. If a plot of $X'(\underset{\sim}{x})$ over space seems to indicate a non-stationary variance, then the variance $\sigma_X^2(\underset{\sim}{x})$ can be estimated by subdividing the sampling domain into small regions as discussed above. Otherwise an unbiased estimate of the stationary variance is

$$\hat{\sigma}_X^2 = \frac{1}{n-M}\sum_{i=1}^{n}\Big(X_i - \hat{\mu}_X(\underset{\sim}{x}_i)\Big)^2$$

where M is the number of terms in Eq. (4.5).

If a non-stationary variance is detected and estimated, an approximately stationary field in both mean and variance can be produced through the transformation

$$X'(\underset{\sim}{x}) = \frac{X(\underset{\sim}{x}) - \hat{\mu}_X(\underset{\sim}{x})}{\hat{\sigma}_X(\underset{\sim}{x})}$$

In addition, such a transformation implies that X' has zero mean and unit variance (at least in approximation).

4.2.4 Estimating the Correlation Structure

An estimator of the correlation structure of a one-dimensional random field will be developed here. The extension to the multi-dimensional case is only slightly more complicated.

Consider the sequence of random variables $\{X_1, X_2, \ldots, X_n\}$ sampled from $X(x)$ at a sequence of locations separated by distance Δx. For the following estimator, it is essential that the data be equispaced. An unbiased estimator for the covariance, $B(j\Delta x)$ between any two random variables along x separated by the distance $j\Delta x$, for $j = 0, 1, \ldots, n - M - 1$ is given by

$$\hat{B}(j\Delta x) = \frac{1}{n-M-j}\sum_{i=1}^{n-j}\Big(X_i - \hat{\mu}_X(x_i)\Big)\Big(X_{i+j} - \hat{\mu}_X(x_{i+j})\Big)$$

where M is the number of unknowns used to estimate $\mu_X(x)$. The correlation coefficient is then estimated as

$$\hat{\rho}_X(j\Delta x) = \frac{\hat{B}(j\Delta x)}{\hat{\sigma}_X^2}$$

where $\hat{\sigma}_X^2 = \hat{B}(0)$ is the estimated variance.

In two dimensions, the estimator for the covariance at lag $\underset{\sim}{\tau} = \{j\Delta x_1, k\Delta x_2\}$ involves a sum over all data pairs separated by the lag $\underset{\sim}{\tau}$. Similarly in higher dimensions. The normalizing factor $1/(n - M - j)$ becomes $1/(N_{\underset{\sim}{\tau}} - M)$ where $N_{\underset{\sim}{\tau}}$ is the total number of data pairs separated by $\underset{\sim}{\tau}$ in the data set.

4.2.5 Example: Statistical Analysis of Permeability Data

Consider a set of permeability measurements made by infiltrometer on 2 ft. by 2 ft. cells extracted from a rectangular test pad of poorly compacted clay, as shown in Table 4.1. The test pad is of dimension 16 ft. by 16 ft. and the (x_1, x_2) coordinates shown on the table correspond to the center of each 2 ft. square cell. All values are in units of 10^{-7} cm/sec.

Table 4.1 Permeability data over a 16 foot square clay test pad.

x_2	x_1 (ft.)							
(ft.)	1.0	3.0	5.0	7.0	9.0	11.0	13.0	15.0
1.0	53.69	61.94	82.38	65.49	49.71	17.85	42.83	14.71
3.0	98.42	46.87	109.41	99.40	7.01	16.71	20.70	1.88
5.0	41.81	6.32	20.75	31.51	6.11	26.88	33.71	13.48
7.0	149.19	11.47	0.63	14.88	8.84	73.17	40.83	29.96
9.0	140.93	30.31	1.04	0.92	2.81	34.85	3.31	0.24
11.0	105.74	1.27	10.58	0.21	0.04	0.57	2.92	7.09
13.0	99.05	12.11	0.12	0.97	5.09	6.90	0.65	1.29
15.0	164.42	7.38	13.35	10.88	8.53	2.22	3.26	0.73

A quick review of the data reveals first that it is highly variable with $K_{max}/K_{min} > 4000$ and second that it tends from very high values at the left edge (x_1 = 1) to small values as x_1 increases. There also appears to be a similar, but somewhat less pronounced trend in the x_2 direction, at least for larger values of x_1.

The high variability is typical of permeability data, since a boulder will have permeability approaching zero, while an airspace will have permeability approaching infinity – soils typically contain both at some scale. Since permeability is bounded below by zero, a natural distribution to use in a random model of permeability is the lognormal – this has been found by many researchers to be a reasonable distribution for permeability. If K is lognormally distributed, then $\ln K$ will be normally distributed. In fact the parameters of the lognormal distribution are just the mean and variance of $\ln K$ (see Table 2.6). Adopting the lognormal hypothesis, it is appropriate before proceeding to convert the data listed in Table 4.1 into $\ln K$ data, as shown in Table 4.2.

Two cases will be considered in this example;

1) the data is to be used to characterize other 'similar' clay deposits. This is the more likely scenario for this particular sampling program.

2) the site to be characterized is the 16 foot square test area (which may be somewhat hypothetical since it has been largely removed for laboratory testing).

Table 4.2 Log-Permeability data over a 16 foot square clay test pad.

x_2	x_1 (ft.)							
(ft.)	1.0	3.0	5.0	7.0	9.0	11.0	13.0	15.0
1.0	-12.13	-11.99	-11.71	-11.94	-12.21	-13.24	-12.36	-13.43
3.0	-11.53	-12.27	-11.42	-11.52	-14.17	-13.30	-13.09	-15.49
5.0	-12.38	-14.27	-13.09	-12.67	-14.31	-12.83	-12.60	-13.52
7.0	-11.11	-13.68	-16.58	-13.42	-13.94	-11.83	-12.41	-12.72
9.0	-11.17	-12.71	-16.08	-16.20	-15.08	-12.57	-14.92	-17.55
11.0	-11.46	-15.88	-13.76	-17.68	-19.34	-16.68	-15.05	-14.16
13.0	-11.52	-13.62	-18.24	-16.15	-14.49	-14.19	-16.55	-15.86
15.0	-11.02	-14.12	-13.53	-13.73	-13.97	-15.32	-14.94	-16.43

Starting with case (1), any apparent trends in the data are treated as simply part of a longer scale fluctuation – the field is assumed to be stationary in mean and variance. Using Eqs. (4.1) and (4.4) the mean and variance are estimated as

$$\hat{\mu}_{\ln K} = -13.86$$
$$\hat{\sigma}^2_{\ln K} = 3.72$$

To estimate the correlation structure, a number of assumptions can be made;

a) assume that the clay bed is isotropic, which appears physically reasonable. Hence an isotropic correlation structure would be adopted which can be estimated by averaging over the lag τ in any direction. For example, when τ = 2 ft. the correlation can be estimated by averaging over all samples separated by 2 ft. in any direction.

b) assume that the principle axes of anisotropy are aligned with the x_1 and x_2 coordinate axes and that the correlation function is *separable*. Now $\hat{\rho}_{\ln K}(\tau_1, \tau_2) = \hat{\rho}_{\ln K}(\tau_1)\hat{\rho}_{\ln K}(\tau_2)$ is obtained by averaging in the two coordinate directions separately and lag vectors not aligned with the coordinates need not be considered. Because of the reduced number of samples contributing to each estimate, the estimates themselves will be more variable.

c) assume that the correlation structure is more generally anisotropic. Lags in any direction must be considered separately and certain directions and lags will have very few data pairs from which to derive an estimate. This typically requires a large amount of data.

Assumption (a) is preferred, but (b) will also be examined to judge the applicability of the first assumption. In assumption (b), the directional estimators are given by

$$\hat{\rho}_{\ln K}(j\Delta\tau_1) = \frac{1}{\hat{\sigma}^2_{\ln K}(n_2(n_1 - j) - 1)} \sum_{k=1}^{n_2} \sum_{i=1}^{n_1 - j} (X'_{ik})(X'_{i+j,k}), \qquad j = 0, 1, \ldots, n_1 - 1$$

$$\hat{\rho}_{\ln K}(j\Delta\tau_2) = \frac{1}{\hat{\sigma}^2_{\ln K}(n_1(n_2 - j) - 1)} \sum_{k=1}^{n_1} \sum_{i=1}^{n_2 - j} (X'_{ki})(X'_{k,i+j}), \qquad j = 0, 1, \ldots, n_2 - 1$$

where $X'_{ik} = \ln K_{ik} - \hat{\mu}_{\ln K}$ is the deviation in $\ln K$ about the mean, n_1 and n_2 are the number of samples in the x_1 and x_2 directions respectively, and where $\Delta\tau_1 = \Delta\tau_2 = 2$ ft. in this example.

The subscripts on X' or $\ln K$ index first the x_1 direction and second the x_2 direction. The isotropic correlation estimator of assumption (a) is obtained using

$$\hat{\rho}_{\ln K}(j\Delta\tau) = \frac{1}{\hat{\sigma}^2_{\ln K}(n_2(n_1 - j) + n_1(n_2 - j) - 1)} \left\{ \sum_{k=1}^{n_2} \sum_{i=1}^{n_1 - j} (X'_{ik})(X'_{i+j,k}) + \sum_{k=1}^{n_1} \sum_{i=1}^{n_2 - j} (X'_{ki})(X'_{k,i+j}) \right\},$$
$$j = 0, 1, \ldots, \max(n_1, n_2) - 1$$

in which if $n_1 \neq n_2$, then the $(n_i - j)$ appearing in the denominator must be treated specially. Specifically for any $j > n_i$, the $(n_i - j)$ term is set to zero.

Fig. 4.5 shows the estimated directional and isotropic correlation functions for the $\ln K$ data. Note that at higher lags, the curves become quite erratic. This is typical since they are based on fewer sample pairs as the lag increases. Also shown on the plot is a fitted exponentially decaying correlation function. The scale of fluctuation, θ, is estimated to be about 5 ft. in this case by simply passing the curve through the estimated correlation at lag τ = 2 ft. Note that the estimated scale is quite sensitive to the mean. For example, if the mean is known to be -12.0 rather than -13.86, then the estimated scale using this data jumps to 15 ft. In effect, the estimated scale is quite uncertain; it is best used to characterize the site at which the data was taken. Unfortunately, significantly better scale estimators have yet to be developed.

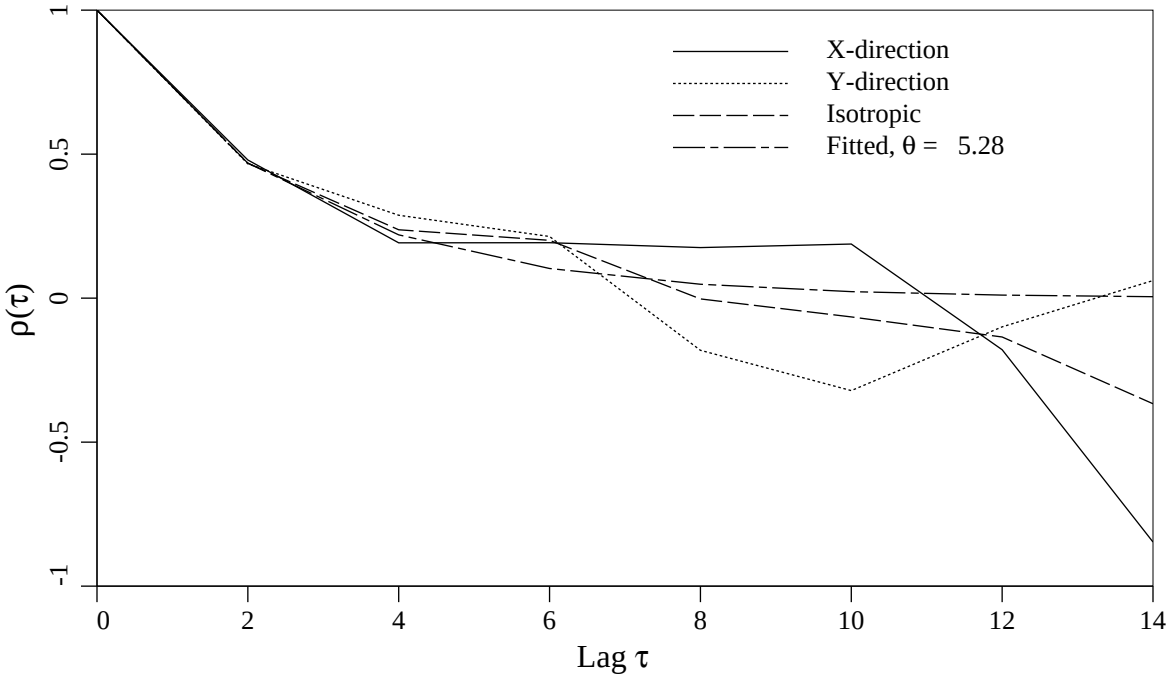

Figure 4.5 Estimated and fitted correlation function for $\ln K$ data.

For case (2), where the data is being used to characterize the site from which it was sampled, the task is to estimate the trend in the mean. This can be done in a series of steps starting with simple functions for the mean (i.e. constant) and progressing to more complicated functions (i.e. bilinear, biquadratic, etc.) monitoring the residual variance for each assumed form. The form which accounts for a significant portion of the variance without being overly complex is selected.

Performing a least squares regression with a bilinear mean function on the data in Table 4.2 gives

$$\hat{\mu}_{\ln K}(\underset{\sim}{x}) = -11.88 - 0.058x_1 - 0.102x_2 - 0.011x_1x_2$$

with corresponding residual variance of 2.58 (was 3.72 for the constant mean case). If a biquadratic mean function is considered, the regression yields,

$$\hat{\mu}_{\ln K}(\underline{x}) = -12.51 + 0.643x_1 + 0.167x_2 - 0.285x_1x_2 - 0.0501x_1^2 - 0.00604x_2^2 + 0.0194x_1^2x_2 + 0.0131x_1x_2^2 - 0.000965x_1^2x_2^2$$

with a residual variance of 2.18. Since there is not much of a reduction in variance using the more complicated biquadratic function, the bilinear form is selected. For simplicity, only two functional forms were compared here. In general one might want to consider all the possible combinations of monomials to select the best form.

Adopting the bilinear mean function, the residuals $\ln K' = \ln K - \hat{\mu}_{\ln K}$ are shown in Table 4.3.

Table 4.3 Log-Permeability residuals.

x_2	x_1 (ft.)							
(ft.)	1.0	3.0	5.0	7.0	9.0	11.0	13.0	15.0
1.0	-0.077	0.203	0.623	0.533	0.403	-0.487	0.533	-0.397
3.0	0.749	0.192	1.225	1.308	-1.159	-0.106	0.288	-1.929
5.0	0.124	-1.539	-0.133	0.513	-0.900	0.806	1.262	0.569
7.0	1.620	-0.681	-3.311	0.118	-0.132	2.247	1.937	1.896
9.0	1.785	0.558	-2.499	-2.307	-0.874	1.949	-0.088	-2.406
11.0	1.721	-2.343	0.133	-3.432	-4.736	-1.720	0.266	1.512
13.0	1.886	0.185	-4.036	-1.547	0.513	1.212	-0.749	0.340
15.0	2.612	-0.046	0.986	1.229	1.431	0.523	1.346	0.298

Fig. 4.6 illustrates the estimated correlation structure of the residuals. Notice that the fitted scale of fluctuation has decreased to about 3 ft. This is typical since subtracting the mean tends to reduce the correlation between residuals. The estimated mean, variance and correlation function (in particular the scale of fluctuation) can now be used confidently to represent the random field of log-permeabilities at the site.

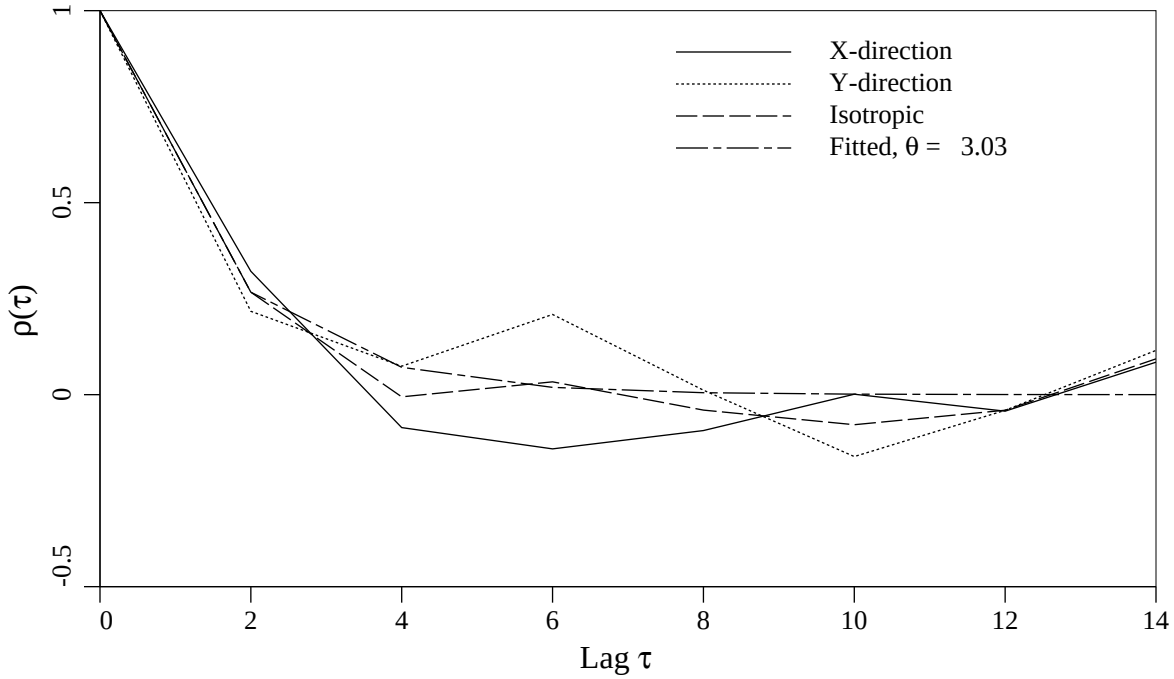

Figure 4.6 Estimated and fitted correlation function for $\ln K - \hat{\mu}_{\ln K}$ data.

4.3 Best Linear Unbiased Estimation

The purpose of Best Linear Unbiased Estimation (BLUE), also known as Kriging, is to provide a best estimate of the soil properties between known data. The basic idea is to estimate $X(\underset{\sim}{x})$ at any point using a weighted linear combination of the values of X at each observation point. Suppose that $X_1, X_2, \ldots, X_n$ are observations of the random field, $X(\underset{\sim}{x})$, at the points $\underset{\sim}{x}_1, \underset{\sim}{x}_2, \ldots, \underset{\sim}{x}_n$. Then the BLUE of $X(\underset{\sim}{x})$ at $\underset{\sim}{x}$ is given by

$$\hat{X}(\underset{\sim}{x}) = \sum_{i=1}^{n} \beta_i X_i \tag{4.7}$$

where the n unknown weights β_i are to be determined. In the regression analysis performed previously the goal was to find a global trend for the mean. Here, the goal is to find the best estimate at a particular point. It seems reasonable that if the point $\underset{\sim}{x}$ is particularly close to one of the observations, say X_k, then the weight, β_k, associated with X_k would be high. However, if $X(\underset{\sim}{x})$ and X_k are in different (independent) soil layers, for example, then perhaps β_k should be small. Rather than using distance to determine the weights in Eq. (4.7), it is better to use covariance (or correlation) between the two points since this reflects not only distance but also the effects of differing geologic units, etc.

If the mean can be expressed as in the regression analysis, Eq. (4.5)

$$\hat{\mu}_X(\underset{\sim}{x}) = \sum_{k=1}^{M} a_k g_k(\underset{\sim}{x}) \tag{4.8}$$

then the unknown weights can be obtained from the matrix equation

$$\underset{\approx}{K}\underset{\sim}{\beta} = \underset{\sim}{M} \tag{4.9}$$

where $\underset{\approx}{K}$ and $\underset{\sim}{M}$ depend on the covariance structure,

$$\underset{\approx}{K} = \begin{bmatrix} C_{11} & C_{12} & \cdots & C_{1n} & g_1(\underset{\sim}{x}_1) & g_2(\underset{\sim}{x}_1) & \cdots & g_M(\underset{\sim}{x}_1) \\ C_{21} & C_{22} & \cdots & C_{2n} & g_1(\underset{\sim}{x}_2) & g_2(\underset{\sim}{x}_2) & \cdots & g_M(\underset{\sim}{x}_2) \\ \vdots & \vdots & & \vdots & \vdots & \vdots & & \vdots \\ C_{n1} & C_{n2} & \cdots & C_{nn} & g_1(\underset{\sim}{x}_n) & g_2(\underset{\sim}{x}_n) & \cdots & g_M(\underset{\sim}{x}_n) \\ g_1(\underset{\sim}{x}_1) & g_1(\underset{\sim}{x}_2) & \cdots & g_1(\underset{\sim}{x}_n) & 0 & 0 & \cdots & 0 \\ g_2(\underset{\sim}{x}_1) & g_2(\underset{\sim}{x}_2) & \cdots & g_2(\underset{\sim}{x}_n) & 0 & 0 & \cdots & 0 \\ \vdots & \vdots & & \vdots & \vdots & \vdots & & \vdots \\ g_M(\underset{\sim}{x}_1) & g_M(\underset{\sim}{x}_2) & \cdots & g_M(\underset{\sim}{x}_n) & 0 & 0 & \cdots & 0 \end{bmatrix}$$

in which C_{ij} is the covariance between X_i and X_j and

$$\underset{\sim}{\beta} = \begin{Bmatrix} \beta_1 \\ \beta_2 \\ \vdots \\ \beta_n \\ -\eta_1 \\ -\eta_2 \\ \vdots \\ -\eta_M \end{Bmatrix} \qquad \underset{\sim}{M} = \begin{Bmatrix} C_{1x} \\ C_{2x} \\ \vdots \\ C_{nx} \\ g_1(\underset{\sim}{x}) \\ g_2(\underset{\sim}{x}) \\ \vdots \\ g_M(\underset{\sim}{x}) \end{Bmatrix}$$

The quantities η_i are a set of Lagrangian parameters used to solve the variance minimization problem subject to non-bias conditions. Beyond allowing for a solution to the above system of equations, they will be ignored in this simple treatment. The covariance C_{ix} appearing in the RHS vector $\underset{\sim}{M}$ is the covariance between the i^{th} observation point and the point $\underset{\sim}{x}$ at which the best estimate is to be calculated.

Note that the matrix $\underset{\approx}{K}$ is purely a function of the observation point locations and covariances – thus it can be inverted once and then Eqs. (4.9) and (4.7) used repeatedly at different spatial points to build up the field of best estimates (for each spatial point, the RHS vector $\underset{\sim}{M}$ changes, as does the vector of weights, $\underset{\sim}{\beta}$).

The Kriging method depends upon two things; 1) knowledge of how the mean varies functionally with position, i.e. $g_1, g_2, \ldots$ need to be specified, and 2) knowledge of the covariance structure of the field. Usually, assuming a mean which is either constant (M = 1, $g_1(\underset{\sim}{x})$ = 1, $a_1 = \hat{\mu}_x$) or linearly varying is sufficient. The correct order can be determined by

1) plotting the results and visually checking the mean trend, or by
2) performing a regression analysis, or by
3) performing a more complex structural analysis – see *Mining Geostatistics* by Journel and Huijbregts (Academic Press, 1978) for details on this approach.

The covariance structure can be estimated by the methods discussed in the previous section, if sufficient data is available, and used directly in Eq. (4.9) to define $\underset{\approx}{\underset{\approx}{K}}$ and $\underset{\sim}{M}$ (with, perhaps some interpolation for covariances not directly estimated). In the absence of sufficient data, a simple functional form for the covariance function is often assumed. A typical model is one in which the covariance decays exponentially with separation distance $\tau_{ij} = |\underset{\sim}{x}_1 - \underset{\sim}{x}_2|$;

$$C_{ij} = \sigma_X^2 \exp\left\{-\frac{2|\tau_{ij}|}{\theta}\right\}$$

As mentioned previously, the parameter θ is called the *scale of fluctuation*. Such a model now requires only the estimation of two parameters, σ_X^2 and θ, but assumes that the field is *isotropic* and *statistically homogeneous*. Non-isotropic models are readily available and often appropriate for soils which display layering.

4.3.1 Estimator Error

Associated with any estimate of a random process derived from a finite number of observations is an estimator error. This error can be used to assess the accuracy of the estimate. Defining the error as the difference between the estimate, $\hat{X}(\underset{\sim}{x})$, and its true (but unknown and random) value, $X(\underset{\sim}{x})$, the estimator mean and corresponding error variance are given by

$$\mu_{\hat{x}}(\underset{\sim}{x}) = \mathrm{E}\left[\hat{X}(\underset{\sim}{x})\right] = \mathrm{E}\left[X(\underset{\sim}{x})\right] = \mu_X(\underset{\sim}{x})$$

$$\hat{\sigma}_E^2 = \mathrm{E}\left[\left(\hat{X}(\underset{\sim}{x}) - X(\underset{\sim}{x})\right)^2\right] = \sigma_X^2 + \underset{\sim}{\beta}_n^T(\underset{\approx}{\underset{\approx}{K}}_{n\times n}\underset{\sim}{\beta}_n - 2\underset{\sim}{M}_n)$$

where $\underset{\sim}{\beta}_n$ and $\underset{\sim}{M}_n$ are the first n elements of $\underset{\sim}{\beta}$ and $\underset{\sim}{M}$ defined in the previous section, and $\underset{\approx}{\underset{\approx}{K}}_{n\times n}$ is the $n \times n$ upper left submatrix of $\underset{\approx}{\underset{\approx}{K}}$ containing the covariances, also defined in the previous section. Note that $\hat{X}(\underset{\sim}{x})$ can also be viewed as the conditional mean of $X(\underset{\sim}{x})$ at the point $\underset{\sim}{x}$. The conditional variance at the point $\underset{\sim}{x}$ would then be $\hat{\sigma}_E^2$.

4.3.2 Example: Foundation Consolidation Settlement

In the spirit of Example 3 discussed in Section 3.2 of these notes (see Fig. 3.7), consider the estimation of consolidation settlement under a footing at a certain location given that soil samples/tests have been obtained at 4 neighboring locations. Fig. 4.7 shows a plan view of the footing and sample locations. The samples and local stratigraphy are used to estimate the soil parameters C_c, e_o, H, and p_o appearing in the consolidation settlement equation

$$S = N\left(\frac{C_c}{1+e_o}\right) H \log_{10}\left(\frac{p_o + \Delta p}{p_o}\right)$$

at each of the sample locations. Each of these 4 parameters are then treated as spatially varying and random between observation points. It is assumed that the estimation error in obtaining the parameters from the samples is negligible compared to field variability, and so this source of uncertainty will be ignored. The model error parameter, N, is assumed an ordinary random variable (not a random field) with mean 1.0 and standard deviation 0.1. The increase in pressure at mid-depth of the clay layer, Δp depends on the load applied to the footing. As in Section 3.2, we will again assume that $\mathrm{E}[\Delta p] = 0.5$ ksf with standard deviation 0.1.

The task now is to estimate the mean and standard deviation of C_c, e_o, H, and p_o at the footing location using the neighboring observations. Table 4.4 lists the soil settlement properties obtained at each of the 4 sample points.

Table 4.4 Derived soil sample settlement properties.

Sample Point	C_c	e_o	H (inches)	p_o (ksf)
1	0.473	1.42	165	3.90
2	0.328	1.08	159	3.78
3	0.489	1.02	179	3.46
4	0.295	1.24	169	3.74
μ	0.396	1.19	168	3.72
σ^2	0.009801	0.03204	70.56	0.03460

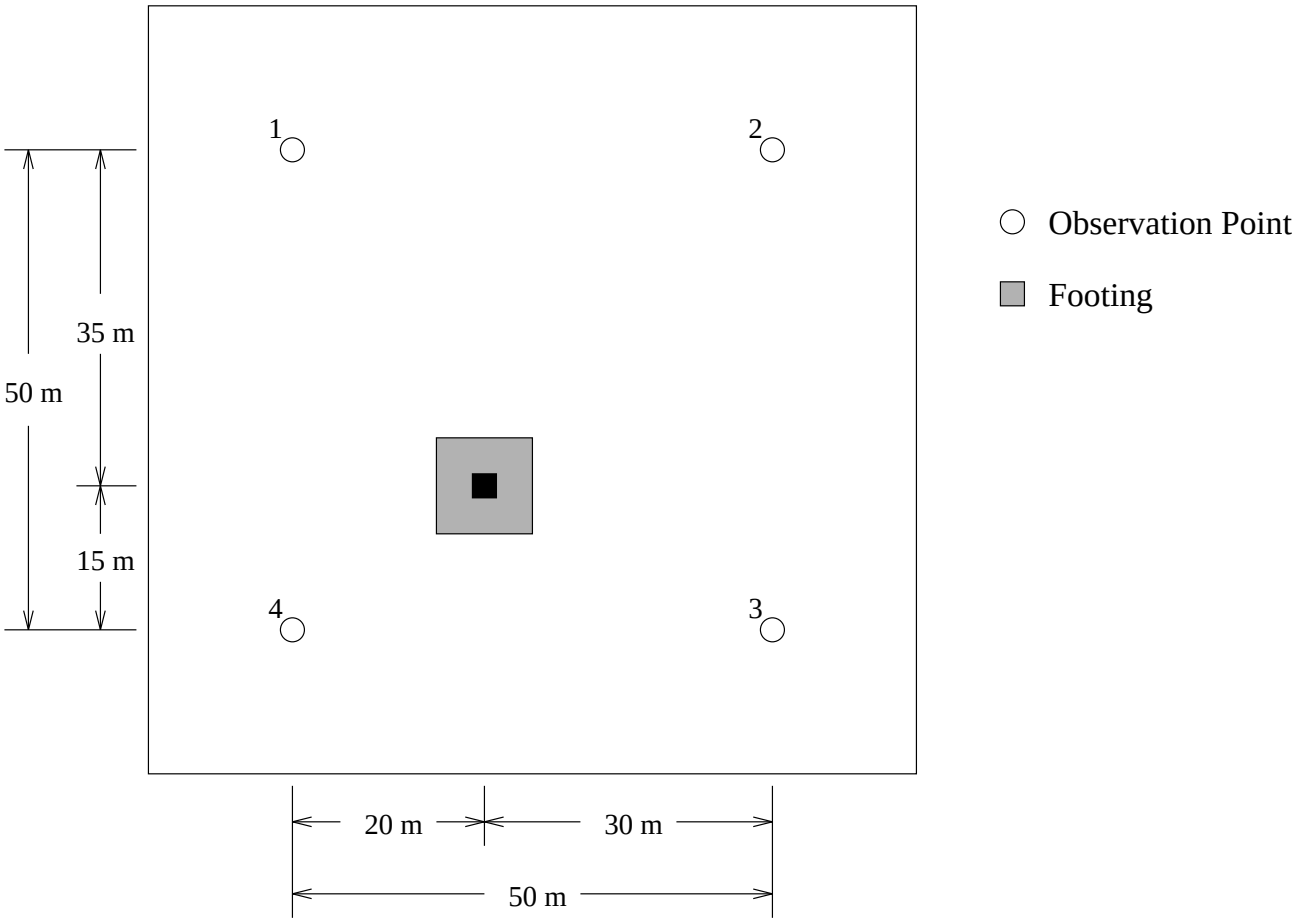

Figure 4.7 Consolidation settlement plan view with sample points.

In Table 4.4, we have assumed that all 4 random fields are stationary, with spatially constant mean and variance, the limited data not clearly indicating otherwise. In order to obtain a Best Linear Unbiased Estimate at the footing location, we need to establish a covariance structure for the field.

Obviously 4 sample points is far too few to yield even a rough approximation of the covariance between samples, especially in two dimensions. Let us assume that experience with similar sites and similar materials leads us to estimate a scale of fluctuation of about 60 m using an exponentially decaying correlation function, that is we assume that the correlation structure is reasonably well approximated by

$$\rho(\underset{\sim}{x}_i, \underset{\sim}{x}_j) = \exp\left\{-\frac{2}{60}|\underset{\sim}{x}_i - \underset{\sim}{x}_j|\right\}$$

In so doing, we are assuming that the clay layer is horizontally isotropic, also a reasonable assumption. This yields the following correlation matrix between sample points;

$$\underset{\approx}{\rho} = \begin{bmatrix} 1.000 & 0.189 & 0.095 & 0.189 \\ 0.189 & 1.000 & 0.189 & 0.095 \\ 0.095 & 0.189 & 1.000 & 0.189 \\ 0.189 & 0.095 & 0.189 & 1.000 \end{bmatrix}$$

Furthermore, it is reasonable to assume that the same scale of fluctuation applies to all 4 soil properties. Thus, the covariance matrix associated with the property C_c between sample points is just $\sigma^2_{C_c}\underset{\approx}{\rho}$ = 0.009801$\underset{\approx}{\rho}$. Similarly, the covariance matrix associated with e_o is its variance ($\sigma^2_{e_o}$ = 0.03204) times the correlation matrix, etc.

In the following, we will obtain BLUE estimates from each of the 4 random fields ($C_c(\underset{\sim}{x})$, $e_o(\underset{\sim}{x})$ independently. Note that this does not imply that the estimates will be independent, since if the sample properties are themselves correlated, which they most likely are, then the estimates will also be correlated. It is believed that this is a reasonably good approximation given the level of available data. If more complicated cross-correlation structures are known to exist, and have been estimated, the method of *co-Kriging* can be applied – this essentially amounts to the use of a much larger covariance (Kriging) matrix and the consideration of all four fields simultaneously. Co-Kriging also has the advantage of also ensuring that the error variance is properly minimized. However, co-Kriging is not implemented here, since the separate Kriging preserves reasonably well any existing point-wise cross-correlation between the fields and since little is known about the actual cross-correlation structure.

The Kriging matrix associated with the clay layer thickness H is then

$$\underset{\approx}{K}_H = \begin{bmatrix} 70.56 & 13.33 & 6.682 & 13.33 & 1 \\ 13.33 & 70.56 & 13.33 & 6.682 & 1 \\ 6.682 & 13.33 & 70.56 & 13.33 & 1 \\ 13.33 & 6.682 & 13.33 & 70.56 & 1 \\ 1 & 1 & 1 & 1 & 0 \end{bmatrix}$$

where, since we assumed stationarity, M = 1 and $g_1(\underset{\sim}{x})$ = 1 in Eq. (4.8). Placing the coordinate axis origin at sample location 4 gives the footing coordinates $\underset{\sim}{x}$ = (20, 15). Thus, the right hand side vector $\underset{\sim}{M}$ is

$$\underset{\sim}{M}_H = \begin{Bmatrix} \sigma^2_H\rho(\underset{\sim}{x}_1, \underset{\sim}{x}) \\ \sigma^2_H\rho(\underset{\sim}{x}_2, \underset{\sim}{x}) \\ \sigma^2_H\rho(\underset{\sim}{x}_3, \underset{\sim}{x}) \\ \sigma^2_H\rho(\underset{\sim}{x}_4, \underset{\sim}{x}) \\ 1 \end{Bmatrix} = \begin{Bmatrix} (70.56)(0.2609) \\ (70.56)(0.2151) \\ (70.56)(0.3269) \\ (70.56)(0.4346) \\ 1 \end{Bmatrix} = \begin{Bmatrix} 18.41 \\ 15.18 \\ 23.07 \\ 30.67 \\ 1 \end{Bmatrix}$$

Solving the matrix equation $\underset{\approx}{K}_H \underset{\sim}{\beta}_H = \underset{\sim}{M}_H$ gives the following four weights (ignoring the Lagrange parameter);

$$\underset{\sim}{\beta}_H = \left\{ \begin{array}{c} 0.192 \\ 0.150 \\ 0.265 \\ 0.393 \end{array} \right\}$$

in which we can see that the samples which are closest to the footing are most heavily weighted (more specifically, the samples which are most highly correlated with the footing location are the most heavily weighted), as would be expected.

Since the underlying correlation matrix is identical for all 4 soil properties, the weights will be identical for all 4 properties, thus the best estimates at the footing are

$$\begin{aligned}
\hat{C}_c &= (0.192)(0.473) + (0.150)(0.328) + (0.265)(0.489) + (0.393)(0.295) = 0.386 \\
\hat{e}_o &= (0.192)(1.42) + (0.150)(1.08) + (0.265)(1.02) + (0.393)(1.24) = 1.19 \\
\hat{H} &= (0.192)(165) + (0.150)(159) + (0.265)(179) + (0.393)(169) = 169 \\
\hat{p}_o &= (0.192)(3.90) + (0.150)(3.78) + (0.265)(3.46) + (0.393)(3.74) = 3.70
\end{aligned}$$

The estimation errors are given by the equation

$$\hat{\sigma}_E^2 = \sigma_X^2 + \underset{\sim}{\beta}_n^T (\underset{\approx}{K}_{n \times n} \underset{\sim}{\beta}_n - 2\underset{\sim}{M}_n)$$

Since the $n \times n$ submatrix of $\underset{\approx}{K}$ is just the correlation matrix times the appropriate variance, and similarly $\underset{\sim}{M}_n$ is the correlation vector (between samples and footing) times the appropriate variance, the error can be rewritten

$$\hat{\sigma}_E^2 = \sigma_X^2 \left(1 + \underset{\sim}{\beta}_n^T (\underset{\approx}{\rho} \underset{\sim}{\beta}_n - 2\underset{\sim}{\rho}_x) \right)$$

where $\underset{\sim}{\rho}_x$ is the vector of correlation coefficients between the samples and the footing (see the calculation of $\underset{\sim}{M}_H$ above). For the Kriging weights and given correlation structure, this yields

$$\hat{\sigma}_E^2 = \sigma_X^2 (0.719)$$

which gives the following individual estimation errors;

$$\begin{aligned}
\hat{\sigma}_{C_c}^2 &= (0.009801)(0.719) = 0.00705 \quad \rightarrow \quad \hat{\sigma}_{C_c} = 0.0839 \\
\hat{\sigma}_{e_o}^2 &= (0.03204)(0.719) = 0.0230 \quad \rightarrow \quad \hat{\sigma}_{e_o} = 0.152 \\
\hat{\sigma}_H^2 &= (70.56)(0.719) = 50.7 \quad \rightarrow \quad \hat{\sigma}_H = 7.12 \\
\hat{\sigma}_{p_o}^2 &= (0.03460)(0.719) = 0.0249 \quad \rightarrow \quad \hat{\sigma}_{p_o} = 0.158
\end{aligned}$$

In summary, then, the variables entering the consolidation settlement formula have the following statistics based on the preceding Kriged estimates;

Variable	Mean	SD	δ
N	1.0	0.1	0.1
C_c	0.386	0.0839	0.217
e_o	1.19	0.152	0.128
H	169	7.12	0.042
p_o	3.70 ksf	0.158	0.043
Δp	0.50 ksf	0.100	0.20

The most significant difference between these results and those shown in Section 3.2, Example 3, are the reduced standard deviations. This is as expected since incorporation of observations tends to reduce uncertainty. Now, a first order analysis of the settlement gives

$$\mu_S = (1.0)\left(\frac{0.386}{1+1.19}\right)(169)\log_{10}\left(\frac{3.7+0.5}{3.7}\right) = 1.64$$

To estimate the settlement coefficient of variation, a first order analysis is again used as in Section 3.2;

$$\delta_S^2 = \sum_{j=1}^{m}\left(\frac{\partial S}{\partial X_j}\frac{\mu_{X_j}}{\mu_S}\right)_\mu^2 \delta_j^2 = \sum_{j=1}^{m} S_j^2\delta_j^2$$

where the subscript μ on the derivative implies that it is evaluated at the mean of all random variables. The variable X_j is replaced by each of N, C_c, etc., in turn. Evaluation of the derivatives at the mean leads to the following table;

X_j	μ_{X_j}	δ_j	S_j	$S_j^2\,\delta_j^2$
N	1.0	0.100	1.0	0.01
C_c	0.386	0.217	1.0	0.0471
e_o	1.19	0.128	-0.54	0.0048
H	169	0.042	1.0	0.0018
p_o	3.70	0.043	-0.94	0.0016
Δp	0.50	0.200	0.94	0.0353

so that

$$\delta_S^2 = \sum_{j=1}^{m} S_j^2\delta_j^2 = 0.10057$$

giving a coefficient of variation for the settlement at the footing of 0.317. This is roughly a 10% decrease from the result obtain without the benefit of any neighboring observations. Although this does not seem significant in light of the increased complexity of the above calculations, it needs to be remembered that the contribution to overall uncertainty coming from N and Δp amounts to over 40%. Thus, the coefficient of variation δ_S will decrease towards it's minimum (barring improved information about N and/or Δp) of 0.212 as more observations are used and/or observations are taken closer to the footing. For example, if a fifth sample were taken midway between the other 4 samples (at the center of Fig. 4.7), then the variance of each estimator decreases by a factor of 0.46 from the point variance (rather than the factor of 0.719 found above) and the settlement

c.o.v. becomes 0.285. Note that the reduction in variance can be found prior to actually performing the sampling since the estimator variance depends only on the covariance structure and the assumed functional form for the mean. Thus, the Kriging technique can also be used to plan an optimal sampling scheme – sample points are selected so as to minimize the estimator error.

4.4 Probabilities

Once the random field model has been defined for a site, there are ways of analytically obtaining probabilities associated with design criteria, such as the probability of failure. For example, by assuming a normal or lognormal distribution for the footing settlement in the previous section, one can easily estimate the probability that the footing will exceed a certain settlement given it's mean and standard deviation. Assuming the footing settlement to be normally distributed with mean 1.64 inches and a c.o.v. of 0.317 (standard deviation = (0.317)(1.64) = 0.52) then the probability that the settlement will exceed 2.5 inches is

$$\mathrm{P}\left[S > 2.5\right] = 1 - \Phi\left(\frac{2.5 - 1.64}{0.52}\right) = 1 - \Phi(1.65) = 0.05$$

4.4.1 Random Field Simulation

Sometimes the system being designed is too complicated to allow the calculation of probabilities analytically. Fortunately there is a simple, albeit computer intensive, solution; simulate realizations of the random field and analyze each to produce realizations of the response. From a set of response realizations, one can build up a picture of the response distribution from which probability estimates can be derived. This is called *Monte Carlo Simulation* (MCS). With computers becoming faster and faster, MCS is becoming increasingly attractive.

Assume that the mean and covariance structure for the random field to be modeled has been established. Since the mean and covariance completely specifies a jointly normal distribution, the following discussion will cover only the generation of normally distributed random fields. Non-normal random fields can often be obtained through a suitable transformation of a normally distributed field. For example, a lognormally distributed random field can be obtained from

$$X(\underset{\sim}{x}) = \exp\left\{\mu_{\ln X}(\underset{\sim}{x}) + \sigma_{\ln X}(\underset{\sim}{x}) \cdot G(\underset{\sim}{x})\right\}$$

where $\mu_{\ln X}$ and $\sigma_{\ln X}$ are the mean and standard deviation of the normally distributed $\ln X$, possibly both functions of $\underset{\sim}{x}$, and $G(\underset{\sim}{x})$ is a normally distributed random field with zero mean, unit variance, and correlation function $\rho_{\ln X}$.

The simulation of a normally distributed random field starts with the generation of a sequence of *independent* standard normally distributed random variables (zero mean, unit variance). Given two random variables *uniformly* distributed between 0 and 1, denoted U_i and U_{i+1}, two independent *standard normal* variates can be produced according to

$$Z_i = \sqrt{-2\ln(1-U_i)}\cos(2\pi U_{i+1})$$
$$Z_{i+1} = \sqrt{-2\ln(1-U_i)}\sin(2\pi U_{i+1})$$

The choice of whether to use $(1 - U_i)$ or simply U_i inside the logarithm is arbitrary. However, if the pseudo-random number generator on your computer has the possibility of returning $U_i = 0$, the logarithm function may fail unless $(1 - U_i)$ is used. Usually uniform random number generators on the interval $(0, 1)$ exclude one or the other bound. See *Numerical Recipes in C* (or Fortran) by Press *et al.*, Cambridge University Press, New York, 1992 for some good uniform random number generators. These are highly recommended since random number generators supplied with some standard libraries are suspect.

Once a sequence of independent standard normally distributed random variables are available, there are quite a number of different algorithms all designed to produce a random field. Only the simplest will be considered here. The random field to be simulated is represented by a n points, $\underset{\sim}{x}_1, \underset{\sim}{x}_2, \ldots, \underset{\sim}{x}_n$ and realizations of $X_1, X_2, \ldots, X_n$ are desired at each point, with the correct mean and covariance structure on average. If $\underset{\approx}{\rho}$ is the correlation matrix associated with these points, having components

$$\rho_{ij} = \frac{\text{Cov}\left[X_i, X_j\right]}{\sigma_X(\underset{\sim}{x}_i)\sigma_X(\underset{\sim}{x}_j)}$$

then $\underset{\approx}{\rho}$ can be decomposed into the product of a lower triangular matrix and its transpose,

$$\underset{\approx}{L}\underset{\approx}{L}^T = \underset{\approx}{\rho}$$

This is sometimes called Cholesky decomposition and standard algorithms for its computation exist (see again *Numerical Recipes*). It will only fail in the event that one or more of the X_i's are perfectly correlated. For example, if X_i is perfectly correlated with X_j, then the Cholesky decomposition of ρ will fail. The solution is to take $X_j(\underset{\sim}{x}_j) = X_i(\underset{\sim}{x}_i) + \mu_X(\underset{\sim}{x}_j) - \mu_X(\underset{\sim}{x}_i)$, and eliminate X_j from the correlation matrix. This simplifies to just taking $X_j = X_i$ in the event that the mean is stationary. If more than one pair of variates are perfectly correlated, one in each pair must be eliminated from direct consideration in a similar fashion.

Another difficulty with the Cholesky decomposition approach is that it becomes unwieldy and prone to numerical round-off errors (often leading to failure) when the number of points in the field becomes large. Often $n = 500$ or so is a practical limit, reducing if the field is highly correlated. In 2-D situations, this limits the field to about 25 by 25 points and about 8 by 8 by 8 in 3-D. For larger problems, more efficient algorithms are available. See Fenton (1994) for some of the more common algorithms.

Given the matrix $\underset{\approx}{L}$, a properly correlated (on average) standard normal random field can be obtained by linearly combining the independent standard normal variates as follows

$$G_i = \sum_{j=1}^{i} L_{ij} Z_j, \qquad i = 1, 2, \ldots, n$$

Finally, the known mean and variance can be reintroduced to yield realizations for X_i which, on average, will show the correct target statistics;

$$X_i = \mu_X(\underset{\sim}{x}_i) + \sigma_X(\underset{\sim}{x}_i)G_i$$

Once a realization of the random field X has been generated, it can be used as input to a deterministic analysis. For example, X could be the compression index field C_c which, coupled with random field realizations for e_o, H, and p_o, could be used to compute settlements under an array of footings. From this computation, the maximum settlement and differential settlement can be readily extracted. Repeating over an ensemble of realizations would allow the construction of a histogram of, say, maximum differential settlements from which probability statements could be made.

4.4.2 Conditional Simulation

The preceding section discusses the simulation of so-call *unconditioned* random fields. In the event that data is available at the site being simulated, *conditional* simulation should be employed to ensure that the random field realizations match the data at the data locations exactly. An unconditional simulation ignors this additional information and will lead to higher variability in the response quantities.

Suppose that the random field $X(\underset{\sim}{x})$ has been measured at the points $\underset{\sim}{x}_1, \underset{\sim}{x}_2, \ldots, \underset{\sim}{x}_p$ and is to be simulated at the points $\underset{\sim}{x}_{p+1}, \underset{\sim}{x}_{p+2}, \ldots, \underset{\sim}{x}_n$. That is, we want to produce realizations of $X(\underset{\sim}{x})$ which exactly match the data at p points and are random at the remaining $n-p$ points. Then the simulation of the conditioned random field involves the following steps;

1) from the known data, compute best linear unbiased estimates of the field at the unknown points $\underset{\sim}{x}_{p+1}, \ldots, \underset{\sim}{x}_n$. Call this field $X_k(\underset{\sim}{x})$. At the known points, X_k is equal to the data. **Note:** since this is a simulation, the field mean must be prespecified. This means that the BLUE system of equations becomes

$$\underset{\approx}{K}_{n\times n}\underset{\sim}{\beta}_n = \underset{\sim}{M}_n$$

that is, the Kriging matrix and RHS vectors involve only the covariances, and the estimator becomes

$$\hat{X}_k(\underset{\sim}{x}) = \mu_X(\underset{\sim}{x}) + \sum_{i=1}^{n} \beta_i(X_i - \mu_X(\underset{\sim}{x}_i))$$

2) generate an unconditioned realization of the random field using the specified mean, variance, and correlation structure according to the method presented in the previous subsection. Call this field $X_u(\underset{\sim}{x})$,

3) compute best linear unbiased estimates of the field at the unknown points using $X_u(\underset{\sim}{x}_1), X_u(\underset{\sim}{x}_2), \ldots, X_u(\underset{\sim}{x}_p)$ as the known data. That is, produce a BLUE field from the unconditioned simulation. Call this field $X_s(\underset{\sim}{x})$. Again, this estimation uses only the covariances, as in step(1).

4) combine the three fields to produce the conditioned realization, X_c as follows,

$$X_c(\underset{\sim}{x}) = X_k(\underset{\sim}{x}) + [X_u(\underset{\sim}{x}) - X_s(\underset{\sim}{x})]$$

Notice that at the known points, $X_s = X_u$, so that the conditioned field exactly matches the data. Between the known points, the term $[X_u(\underset{\sim}{x}) - X_s(\underset{\sim}{x})]$ represents a random deviation which is added to the BLUE estimate X_k such that the mean of X_c is X_k with increasing variance away from the known points.

4.5 Summary

The use of random field models is not without its difficulties. This was particularly evident in the estimation discussion since random field parameters must often be derived from a single realization (the site being explored). The interpretation of trends in the data as true trends in the mean or simply as large scale fluctuations is a question which currently can only be answered by engineering judgement. The science of estimation in the presence of correlation between samples is not at all well developed.

As a result, the statistical parameters used to model a random field are generally uncertain and statements regarding probabilities are equally uncertain. That is, because of the uncertainty in

estimates of mean properties, statements regarding the probability of failure of a slope, for example, cannot be regarded as absolute. However, they often yield reasonable approximations based on a very rational approach to the problem. In addition, probabilities can be used effectively in a relative sense; the probability of failure of design A is less than that of design B. Since relative probabilities are less sensitive to changes in the underlying random field parameters they can be more confidently used in making design choices.

Appendix A Basic Concepts of Probability and Reliability

From *Probabilistic Methods in Geotechnical Engineering*
National Research Council Report, 1995

A.1 Background

An evaluation of the usefulness and role of reliability in geotechnical engineering cannot be made without a clear understanding of the probability and risk assessment principles and methods that are used. Accordingly, a brief overview of some basic concepts is presented in this appendix. Although a text on basic probability and reliability concepts specifically written for geotechnical engineers is current not available (with the possible exception of Harr, 1977), several texts (Benjamin and Cornell, 1970; Ang and Tang, 1975, 1984; Harr, 1987) that pertain to civil engineering as a whole can be referred to for a comprehensive and detailed treatise of the subject.

A.2 Description of Uncertainties and Probability Assessment

Geotechnical engineers are very familiar with uncertainties. The uncertainty may be in the form of a lack of information about the subsurface soil profile or a large scatter in the soil test results, or it may be associated with a substantial deviation of the measured field performance from its predicted value. When measurements on a given random variable are available, a histogram is often used to portray the uncertainties associated with the variable. The graph is a plot of the number of observed values for respective intervals of values of the variable. An example of such a plot is Fig. A.1, which shows a histogram of the undrained shear strength measured from laboratory testing of a set of soil samples collected from a site. This plot shows that the measured soil strengths for this soil range from 0.8 to 1.6 ksf. The measured strengths are roughly symmetrical about the central value of 1.2 ksf. Fig. A.2 shows a histogram of the ratio, N, of the measured-versus-predicted pile capacity from a set of pile load tests.[1] The actual capacity of a test pile ranges from as low as 40 percent of the value predicted to as great as twice that predicted value. The shape of the histogram is skewed toward higher values of the ratio N, which implies that exceptionally large ratios may be observed. Besides drawing the histogram, statistical measures can be calculated from a given set of observed data to gain a better understanding of the distribution of the variable.

A common statistic, the *sample mean*, is mathematically defined as the average of the observed values. It is a measure of the central tendency of the random variable. For the above case of pile capacity, if the prediction model does not contain any systematic bias, the mean value of the observed ratios will be approximately 1.0. Any deviation of the computed mean of N from 1.0 indicates that bias may be present in the model, which could mean either consistent over prediction or underprediction by the model. The *sample variance*, which is defined as the average of the squared deviation from the sample mean for all observed values, describes the amount of dispersion of the variable from the central value. Because the variance has a dimension that is a

[1] The pile tests were all in clay, and their capacities were predicted according to the procedures in the 16th edition of Recommended Practice 2A of the American Petroleum Institute (1986). To assure consistency, the soil strength for all the test piles are based on unconfined compressive strengths on pushed samples or equivalent.

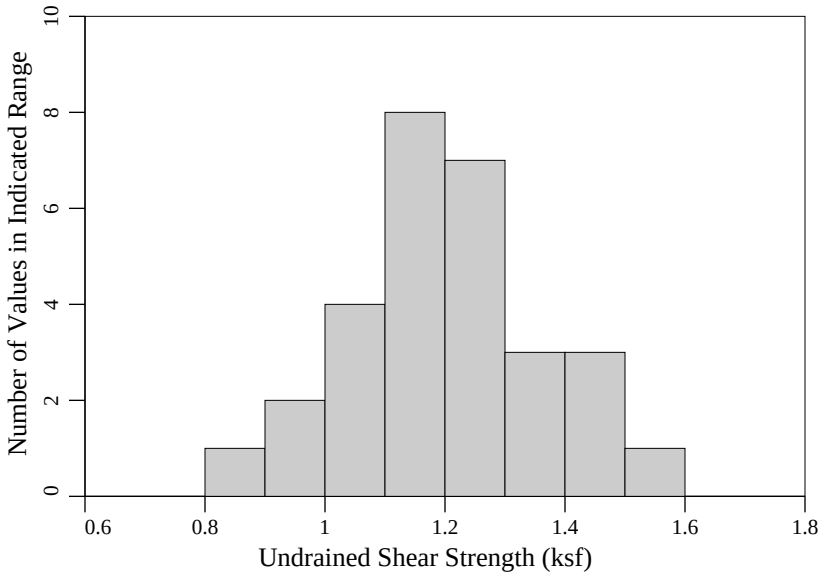

Figure A.1 An example histogram of soil strength data.

square of the dimension of the mean, the *sample standard deviation*, which is the square root of the variance, may be used to measure the average dispersion of the variable from its mean value. An even more convenient measure of the dispersion is given by the coefficient of variation (c.o.v.), which is the ratio of standard deviation to the mean and is a dimensionless quantity. Typical c.o.v. values for shear strength of soil are 20 to 40 percent, whereas the value for the soil density is smaller, around 5 percent.

In the above examples, the values observed represent only one set of observations. Another set of observations would not likely give exactly the same individual values. Thus, the histogram, as well as the sample statistics defined above, is subject to variation between sets of observations. This is particularly true of the number of observations in each set is small. In fact, the measured data, such as those cited above, only serve to provide some information on the nature of the uncertainties associated with the variable under consideration. Besides the directly measured data at a given site, an engineer often has a strong feeling about which values a geotechnical variable will likely have on the basis of judgement and prior experience. Indeed, this subjective information is most useful in augmenting a small data base or (in the absence of measured data) in determining a probability model for the geotechnical variable.

A *probability density function* (PDF) may be introduced to model the relative likelihood of a random variable. The PDF describes the relative likelihood that the variable will have a certain value within the range of potential values. In a case where the engineer believes that a given set of measured data does not represent a set of realistic sample values of the engineering variable and no other information is available, a PDF can be fitted over the frequency diagram, which is a modified histogram whose ordinate has been scales, so that the area under the histogram is unity. For instance, a *normal distribution* is a common probability distribution model used to fit a symmetrical bell-shaped histogram. If the engineer adopts a normal distribution to model the undrained shear strength in Fig. A.1, the parameters of the normal distribution, namely μ and σ, can be estimated by the sample mean and sample standard deviation, respectively.

In most situations, however, the choice of the PDF will be based on engineering judgement instead of a histogram, because either the sample size of the observations is small, or the engineer believes

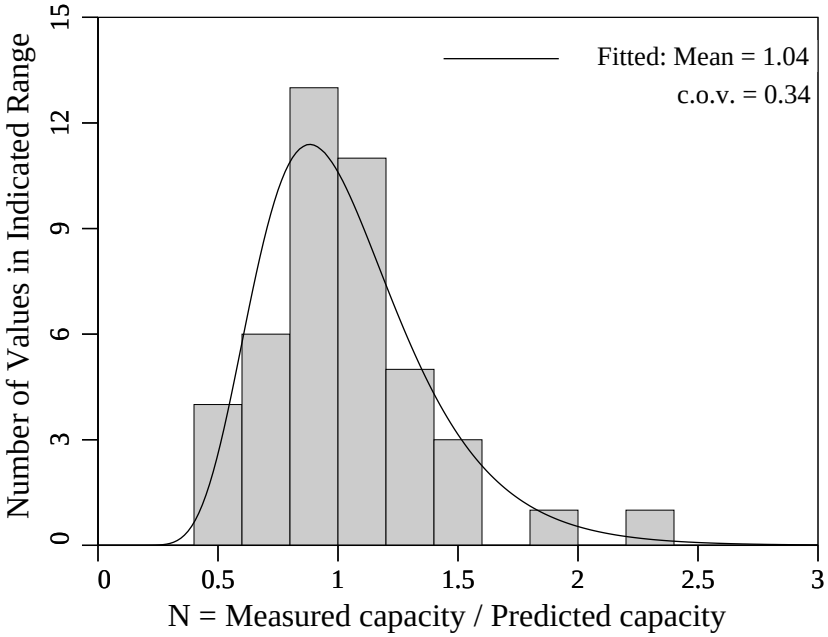

Figure A.2 Histogram of pile-test data. (The pile tests are all in clay, and their axial capacities are predicted according to the 16th edition of American Petroleum Institute, Recommended Practice 2A, 1986. Source: Tang, 1988).

that the values measured are not representative of the values of the pertinent variable, as is discussed further in the next section. In a broad sense, the PDF may be used to express the overall feeling of the engineer on the basis of all the evidence that is available. The evidence may include results of various types of tests, geological history, geotechnical performance in similar soils, and the engineer's intuition. The *mean value* of the PDF represents the engineer's best estimate of the random variable without the addition of conservative assumptions, and the *standard deviation*, or c.o.v., of the PDF represents the engineer's assessment of the uncertainty. A convenient probability distribution type (e.g. normal or logonormal) may be selected, and calibrated with those mean values and standard deviations that are consistent with the engineer's judgement, to yield the judgmentally based PDF of the variable. If an engineer is only confident with the maximum and minimum values of a variable, a uniform distribution over the range may be used as a conservative PDF, whereas a triangular distribution can model approximately the engineer's perception of the relative likelihood over the given range of values. The PDF associated with an engineer's belief can change with time, especially when there is new evidence that is contrary to the engineer's previous opinion. The subject of updating probability with additional information will be discussed in a later section.

Once the PDF of a random variable is established, it can be used to calculate the probability of an event associated with a range of values of the variable. For instance, suppose that the undrained shear strength of the soil at a site is modeled by a normal distribution with parameters μ and σ equal to 1.2 and 0.17 ksf, respectively. The probability that the undrained shear strength, for example, for the next test specimen from the site, will be less than 1.03 ksf is given by

$$\int_{-\infty}^{1.03} f_X(x)\,dx = \Phi\left(\frac{1.03-1.2}{0.17}\right) = \Phi(-1.0) = 1-\Phi(1.0) = 1-0.841 = 0.159 \qquad (A.1)$$

where $f_X(x)$ is the PDF of the random undrained shear strength, and $\Phi(x)$ is the probability of a standard normal variate (i.e., with mean 0 and standard deviation 1.0) less than x. Some

typical values of the function are presented in Table 2.7; for negative values of x, the function $\Phi(x) = 1 - \Phi(-x)$.

The advantage of the probability model is that with appropriate judgement of the engineer the PDF extends beyond the information portrayed by the observed data. The PDF incorporates the engineer's judgement on the applicability of the data for the specific site, as well as any other pertinent factors. Caution has to be exercised, however, to ensure the appropriateness of the PDF in representing the engineer's state of belief. Judgement of the engineer should also play a significant role in the appropriate use of the probability estimated from the chosen PDF.

An engineer may also estimate the likelihood of a given event directly, that is without going through the PDF, based on judgmental information. Vick (1992) suggested a workable procedure for encoding probabilities from engineers. As described in the approach adopted here to model uncertainties, a judgmental probability or probability distribution should be more valuable than one estimated strictly from observed data. It quantifies the engineer's opinion based on his or her experience and interpretation of the available information. By using these judgmental probabilities, engineers can be assured that judgment, the most important element in a reliability evaluation of geotechnical performance will not be ignored but instead will be enhanced.

A.3 From Soil Specimen to In Situ Property

The random variable in the first example (see Fig. A.1) is the undrained shear strength of soil. However, the measured data represent only the undrained shear strengths of discrete soil specimens, which are determined using a given test procedure. This is not necessarily the strength that governs the performance at the site. In fact, the pertinent soil property controlling the performance of a foundation system often involves a much larger volume of soil. for instance, the average shear strength along a potential slip surface will control the failure of a slope, and the average compressibility of a volume of soil beneath a footing will control the settlement of the footing. In these two cases, the soil properties from each of the many points that constitute the domain of influence will contribute to the performance. Hence a domain-average property is needed instead of the property of discrete soil specimens. Sometimes, extreme low or high values of the soil property within a small local region may also govern system performance. Examples include the initiation of progressive failure in a slope by a local zone of weal material and piping failure in an earth dam that is induced by a small zone of highly permeable material. Even in these cases, the local zone involved is often much larger than the size of a typical soil specimen. In any event, the pertinent soil property is the average soil property over an appropriate spatial domain, large or small; this soil property is referred to as the "spatial average property". To evaluate correctly the site performance, the probabilistic description (e.g. mean value and c.o.v.) of the spatial average property must be determined.

Two factors are involved here. First, there is a size effect. The law of averaging would imply that the average soil property over a given volume or area will exhibit a smaller scatter than the properties at individual locations. Hence, in many circumstances there is a reduction in variability that depends on the size of the domain to be averaged, although in some circumstances, increasing the size of this domain may actually increase the variability. In addition, the correlational structure of the soil property will also affect the amount of reduction in variability. To study the effect of correlation, observe first that soil samples collected adjacent to each other are likely to have properties that are similar to each other compared with the relationships between those collected at large distances apart. Also, soil specimens tested by the same device will likely show less scatter in the measured values than if they were tested by different devices in separate laboratories. The

degree of correlation as a function of separation distance between soil samples depends on the specific soil type and deposit characteristics and on the property considered. Nevertheless, the more erratic the variation (i.e., less correlated) of the soil property with distance and the larger the soil domain considered, the larger the reduction in the variability of the average property will be. this phenomenon is a result of the increasing likelihood that unusually high property values at some points will be balanced by low values at other points; therefore, the average property is less likely to take on exceptionally high or low values.

Second, the in situ soil property at incipient failure is not necessarily duplicated by the sampling and testing procedure performed on the soil specimen. Some of the causes of variance are sample disturbance, different stress conditions, and macrofeatures that may not be well represented by a small specimen. Each of these causes can yield test results that are consistently lower or higher than the in situ value; for example, a fissured clay might have a lower in situ strength than that measured in small samples. Hence, a bias may exist that needs to be corrected and incorporated into the overall uncertainty evaluation.

To account for the effect of the two factors described in the last paragraph, Tang (1984) proposed the following expressions for relating the mean and c.o.v. of the average soil property in situ to those of the tested soil specimens:

$$\bar{A} = \bar{N}\bar{x} \tag{A.2}$$

$$\text{c.o.v.} = \delta = \sqrt{\Delta^2 + \Delta_o^2 + \gamma(D)\delta_t^2} \tag{A.3}$$

where the mean soil property estimated from laboratory or field tests, $\bar{x}$, is modified by the mean bias, N, of the respective test to yield the mean average soil property, A. For the first c.o.v. on the right side of Eq. (A.3), Δ denotes the uncertainty in the bias caused by the discrepancy between specimen and in situ property. The value of N and Δ can be assessed subjectively by the engineer after the factors causing the discrepancy are identified and evaluated. The second c.o.v. Δ_o, denotes the uncertainty contribution from taking a limited number of samples, which can be expressed as a function of the sample size. The third term is the product of the square of δ_t; the c.o.v. of property values from tests on specimens; and $\gamma(D)$, a variance reduction factor depending on the size of the averaging domain D and the spatial correlation characteristics of the soil properties (Vanmarcke, 1984). Uncertainty contributed by the first two components is often termed "systematic" in contrast to the last component, which is termed "random". Systematic uncertainties impose the same effect (or discrepancy) on each soil element throughout the spatial domain considered and hence are not subject to the averaging effect, unlike the spatial variability in the last term. It should be emphasized that the c.o.v. values reported in the literature are often estimated from measured test values for small soil specimens, which generally are not representative of the in situ soil properties governing geotechnical performance. Therefore, these c.o.v. values are essentially those denoted by δ_t in Eq. (A.3). They generally cannot be used directly in reliability analysis; they need to be modified by factors to account for the spatial averaging reduction and the hidden systematic bias and error associated with the given type of test procedure for determining that property. As shown in Fig. A.3 for a case where the test strength has a conservative bias, the probabilities calculated for an event, for example, undrained shear strength less than 1.0 ksf, can be substantially different using the probability distribution based on the test specimen statistics (curve B) rather than using that based on the average strength along a slip surface (curve A).

The discussion in this section considers a soil medium consisting of a single material type. In problems such as instability of rock slopes that is induced by the most unfavourably oriented joint, specific localized properties will affect the performance instead of the average property. In this case, undesirable extreme conditions are more likely to occur as the volume of the soil or rock increases. Another case is the phenomenon of progressive failure initiated at some local weak

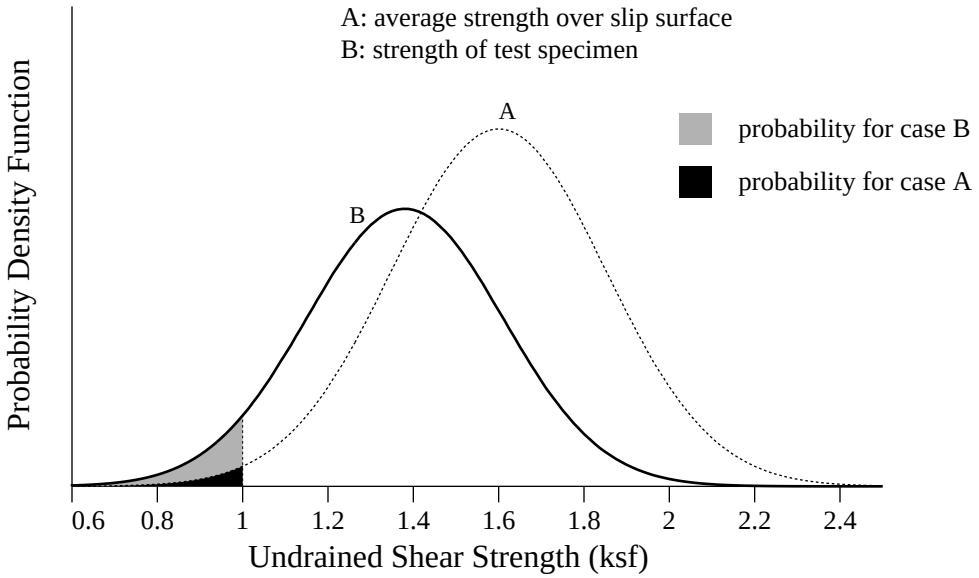

Figure A.3 Discrepancy between distribution of in situ property and those of specimen property.

zone. The larger the domain of soil considered, the more adverse it will become. If the soil stratum consists of other materials whose properties are drastically different from those of the main soil material, it will require a different model and analysis procedure.

Example

The average density of a 10-m-thick soil layer is estimated based on the following information:

1) Nine soil samples taken at widely scattered locations have been tested for their densities, which yielded a mean of 1,800 kg/m^3 and a standard deviation of 200 kg/m^3. Assume random test error is negligible compared with spatial variability.
2) Assume prefect correlation among soil densities in the horizontal plane and an exponential correlation model with parameter 0.3 m in the vertical direction.
3) From long experience, the densities measured at this laboratory exhibit some discrepancy from those in situ. this discrepancy could range between 0.9 and 1.06; that is, the true in situ density may be from 90 to 106 percent of the laboratory-measured values.

The c.o.v., δ_t, denoting the inherent spatial variability of density between specimens is 200/1,800 or 0.111. For the given exponential correlation model and the averaging domain of 10 m, the factor $\gamma(D)$ is estimated to be 0.058 (Tang, 1984). The error due to limited samples is given by $0.111/\sqrt{9}$ or 0.037 by assuming that the nine sample values are statistically independent. Lastly, the error due to systematic bias can be evaluated by assuming a uniform distribution between 0.9 and 1.06 for the correction factor N. which yields a mean value, $\bar{N}$, of 0.98 and a c.o.v., Δ, of 0.047. Incorporating all of these component statistics into Eq. (A.2) and Eq. (A.3), the mean and overall c.o.v. of the spatial average density are

$$\bar{A} = (0.98)(1800) = 1764 \quad \text{kg/m}^3 \tag{A.4}$$

$$\delta = \sqrt{0.047^2 + 0.037^2 + 0.058(0.111)^2} = 0.066 \tag{A.5}$$

A.4 From Field-Test to Field Performance

Geotechnical engineers often have collected data on field-test performance and compared these data with those predicted according to a geotechnical model. The field tests may involve actual full-size foundation systems or simply scaled-down field tests or even laboratory model tests. An example has been shown in Fig. A.2 for the case of axial pile capacity based on a large number of pile tests. In principle, the probability distribution of this ratio, especially that established on the basis of high-quality field tests, can be used to determine the uncertainty associated with a given performance prediction model, which in turn may be used to estimate the probability of failure of the given geotechnical system. However, the applicability of this procedure depends on the performance of the geotechnical system under consideration being representative of the population of the field-test systems used in assessing the model bias and c.o.v. If there is a discrepancy, additional factors are required to modify the predicted performance. The bias and c.o.v. associated with each of the factors can be estimated from reported research studies or can be based on judgement of the engineer. An example of the use of pile test data in Fig. A.2 for evaluating the in situ capacity of an offshore pile is given below.

Example

A large database from test piles was compiled by Olson and Dennis (1982) from which the discrepancies between the measured capacity and that predicted by a given pile-capacity prediction model were analyzed (Tang, 1988). Large scatter in the ratio of predicted-versus-measured capacity was observed, as shown in Fig. A.2 for piles in clay. To apply this result to the evaluation of the axial capacity of an offshore pile, corrections are needed to account for the effects of factors such as

1) loading rate, because the strain rate in most pile tests is a fraction of 1 mm/minute, whereas that during a severe storm could be much larger, on the order of 200 mm/second or 10,000 mm/minute;
2) pile compressibility, because offshore piles are generally much longer than short piles tested on land;
3) consolidation level, because the time at which the critical storm hits could be years after the installation of the piles, whereas test piles normally are tested within months of installation; so the soil surrounding the test piles may have been subject to a different degree of consolidation relative to the actual pile; and
4) the specific sampling/testing procedure used for soil strength determination at the given site, which may be in contrast to that used for determining the statistics of the model bias and c.o.v. The bias and c.o.v. associated with each of these factors have been assessed and then combines through a fist-order probability model to yield the overall bias and c.o.v. of the in situ pile capacity (Tang, 1989) as

$$\bar{Q} = \bar{N}_1 \bar{N}_2 \cdots \bar{N}_m Q_p \tag{A.6}$$

$$\delta_Q = \sqrt{\delta_1^2 + \delta_2^2 + \cdots + \delta_m^2} \tag{A.7}$$

where $\bar{N}_i$ and δ_i denote the respective bias (i.e., mean and c.o.v.) of the individual correction factor for the ith effect. The values of $\bar{N}_i$ and δ_i depend on the dimension of the pile, the sampling/testing procedure for soil strength determination, and the environmental conditions at the proposed site (Tang, 1988). For a 300-ft pile in a typical site at the Gulf of Mexico, with soil strengths determined by unconfined

compression tests on driven samples, the overall mean bias is estimated to be 2.15, and overall c.o.v. is about 0.432. This implies that the pile capacity is expected to be 2.15 times the predicted value. On the other hand, if unconfined, unconsolidated strength tests on pushed samples were used for determining the soil strengths, the corresponding overall bias and c.o.v. would be 0.865 and 0.197, respectively.

A.5 Factor of Safety

Satisfactory performance of a geotechnical system often depends on its capacity relative to the applied load. For a pile foundation system, a pile fails by plunging if the axial capacity of the pile provided by the surrounding soil is less than the axial load from the superstructure. Slope failure occurs if the total sliding resistance along a potential slip surface is less than the driving force caused by the soil weight and other loads. Hence, in the simplest case, a safety factor can be defined as the ratio of the available resistance, R, to the applied load, L, or

$$F = R/L \tag{A.8}$$

such that failure is given by the event $\{F < 1\}$. For the case where the applied load is known, or if an engineer would like to assess the safety subject to a prescribed design load, L is a constant and F can be alternatively defined as the factor by which the available resistance must be divided to cause failure. The definition of safety factor in Eq. (A.8) should not be confused with the traditional design safety factor, which is treated deterministically as the ratio of the nominal resistance to the nominal load. Further discussion of the traditional design safety factor is presented at the end of this subsection.

Since the available resistance and available load are each subject to uncertainties, they should be modeled as random variables; thus, F, in turn, will also be a random variable. The relationship between the probability of failure and the probability distributions of R and L is shown in Fig. A.4a. The resistance can take on any value covered by the extent of the PDF of R, that is, $f_R(r)$, whereas the load can take on any value covered by the extent of the PDF of L, that is, $f_L(\ell)$. The region under the overlapping portion of the two PDF curves denotes the zone where the resistance may be less than the load. Although the area of overlap is not the probability of failure, the relative size of the overlapping region may be used as a rough comparison of the relative likelihoods of failure. As the mean resistance increases (Fig. A.4b), likelihood of the failure decreases as expected. A decrease in the likelihood of failure can also be achieved by reducing the dispersion or uncertainty in the resistance (Fig. A.4c). Mathematically, the probability of failure is calculated from the convolution integral as follows

$$\text{P [failure]} = \int_0^\infty \left[\int_9^\ell f_R(r)\, dr \right] f_L(\ell)\, d\ell \tag{A.9}$$

where the probability of the resistance being less than a given load value ℓ, which is given by the bracket within the integral, is weighted by the PDF of the load over all possible values of ℓ. A reliability index, β, has been commonly used in the reliability literature to denote the reliability level without the explicit determination of the probability of failure. For the safety factor, F, as defined in Eq. (A.8), β is approximately the ratio of the natural logarithm of the mean F (which is approximately equal to the ratio of mean resistance over mean load) to the c.o.v. of F;[2] a large value

[2] This definition of β is not the standard definition of β associated with the first order reliability method, which is presented later in this section, but it serves to demonstrate the relationship between the mean safety factor, uncertainties of load and resistance, and the probability of failure without using a more elaborate formulation.

of β represents a higher reliability or smaller probability of failure. The reliability level associated with a reliability index β is approximately given by the function $\Phi(\beta)$, evaluated at β, from Table 2.7. The probability of failure is simply $1 - \Phi(\beta)$. As shown in Figs. A.5a through A.5c, the distribution of the safety factor corresponding to the cases of Figs. A.4a through A.4c may be used to determine the respective probabilities of failure, namely the probability that F is less than 1. The value of β is larger for cases b and c relative to that for case a. By reducing the uncertainty of the resistance, the spread of the safety factor distribution decreases as shown in Fig. A.5c, yielding a smaller probability of failure. Moreover, as the mean safety factor increases, the PDF shifts to the right (Fig. A.5b) and the probability of failure decreases.

The conventional factors of safety commonly used by engineers are based on nominal values of resistance and load. They are not mean safety factors. The conventional safety factor depends on the physical model, the method of calculation, and most importantly, on the choice of soil parameters. Usually there is a lack of consensus on these choices, and a large range of levels of conservatism on the choice of soil strength and methods of analysis is common. The uncertainty level associated with the resistance and load is not explicitly considered. Consequently, inconsistency is likely to exist among engineers and between applications for the same engineer. The same conventional safety factor can be associated with a large range of reliability level and thus is not a consistent measure of safety, as demonstrated in the following example. The use of a reliability index, β, such as that introduced earlier in this section, can provide significant improvement over the use of the traditional design safety factor in measuring the relative safety between the designs.

Example

In dam design, structural engineers designing concrete gravity dams use F = 3.0 for foundation design with respect to sliding failure, while geotechnical engineers designing earth dams use F = 1.5 for similar foundation design. Does this mean that concrete gravity dams are twice as safe as earth dams in regard to sliding? The answer is probably "no". The reasons are (1) geotechnical engineers tend to be more conservative in selecting soil strength parameters, and (2) the value of F is generally not directly related to the likelihood of failure. Reliability methods offer a tool to compare the relative safety between the two design methods. Consider a simple case in which a dam is 600 ft wide at the base with a height, h, in ft to be designed. The average undrained strength of the soil supporting the dam is 1,000 psf based on unconfined-compression tests on pushed samples. Suppose the dam is designed with respect to the sliding mode at the base to resist a lateral hydrostatic pressure of $0.5 \times 62.5 \times h^2$ psf.

For a concrete dam, the design height of the dam can be obtained by equating the ratio of nominal resistance to nominal load, that is, $(1000 \times 600)/(0.5 \times 62.5 \times h^2)$ to 3.0 yielding a height of 80 ft. Similarly, for an earth dam, if the geotechnical engineer adopted a conservative undrained soil strength equal to two-thirds of the average value measured, the design height can be obtained by equating the ratio $(0.67 \times 1000 \times 600)/(0.5 \times 62.5 \times h^2)$ to 1.5, yielding a height of 87 ft.

To evaluate the reliability of each of these two designs with respect to the sliding-failure mode, assume for simplicity that the in situ undrained soil strength is 0.9 of that measured and that its uncertainty is represented by a c.o.v. of 30 percent. The mean safety factor for the concrete dam is estimated by $(0.9 \times 1000 \times 600)/(0.5 \times 62.5 \times 80^2)$, that is, 2.7. Hence its reliability index is $(\ln 2.7)/(0.3) = 3.31$. Similarly, the reliability index for the earth dam is estimated as 2.75, which is substantially more than half of the value of β for the concrete dam. The probability of sliding failure for the concrete dam is 0.00047, compared with 0.00347 for the earth dam. In other words, for the values assumed in this

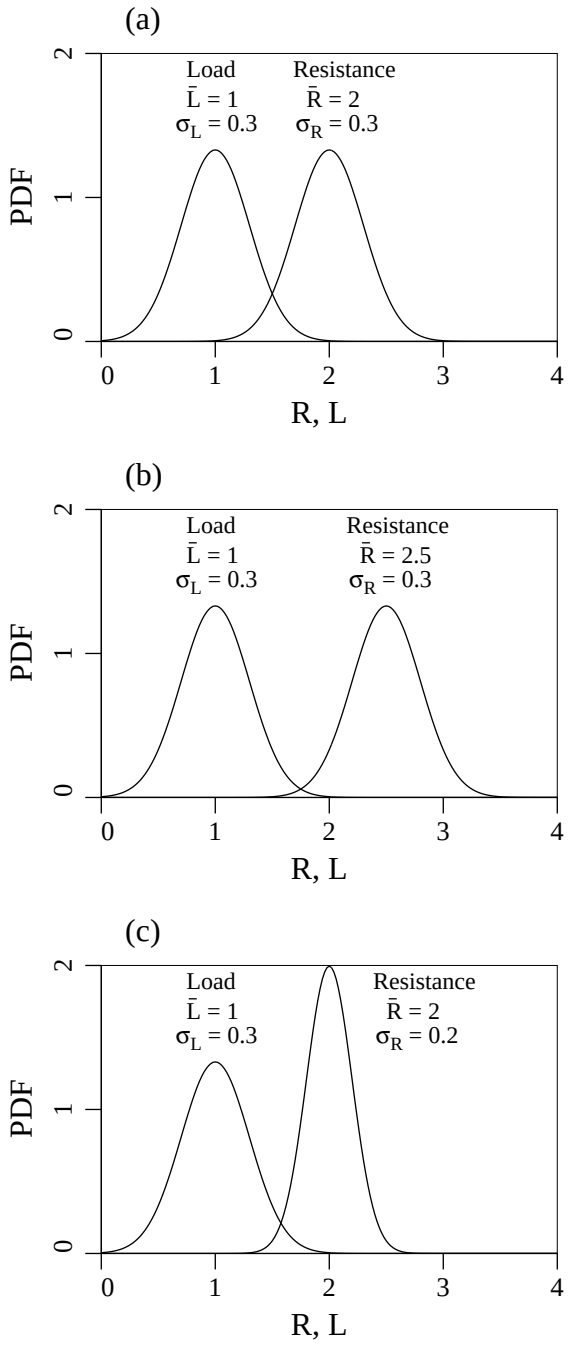

Figure A.4 PDF of load and resistance.

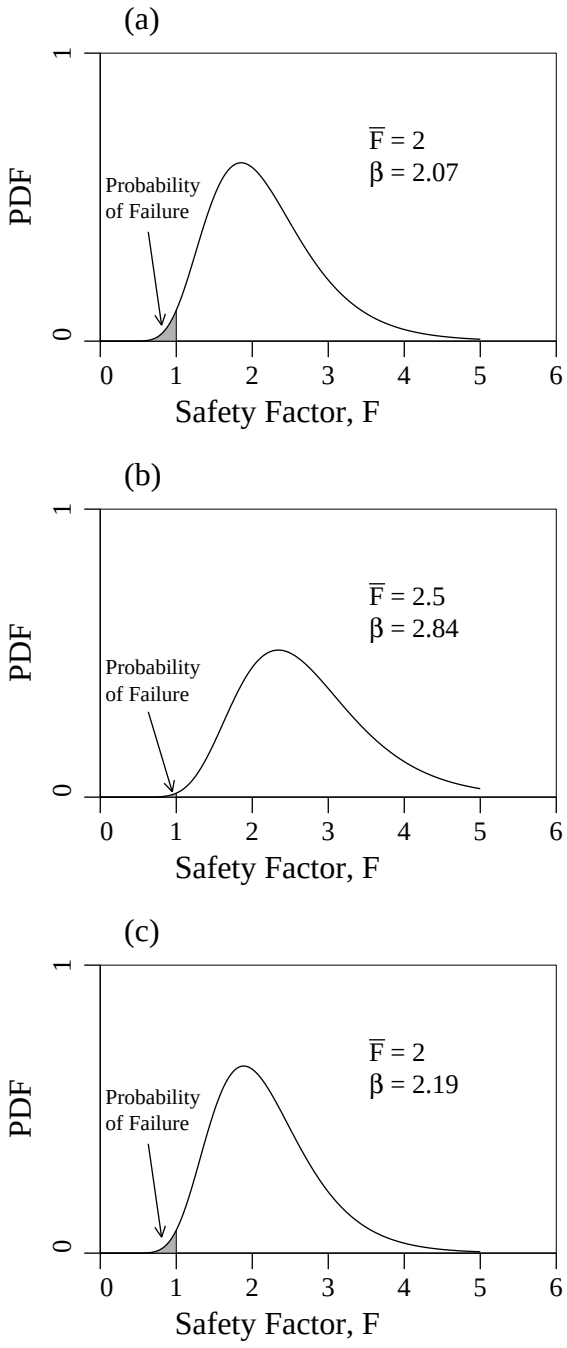

Figure A.5 PDF of safety factor.

example, the earth dam is about seven times more likely to slide than a concrete dam. On the other hand, if the geotechnical engineer had adopted a very conservative undrained soil strength equal to 40 percent of the average value measured, the design height of the earth dam would be 71 ft and the corresponding probability of sliding failure of the earth dam would be 0.00002. In spite of its smaller factor of safety, the earth dam would be only about one-twentieth as likely to fail as the concrete dam for this case.

The simple expression of R/L used in defining the factor of safety may not be obvious at times. for instance, in the stability analysis of a slope, the weight of the soil at the toe can act as counterweight to resist the driving moment caused by the main mass of the soil slope. This contribution can be either treated as additional resistance or reduced load. Depending on how this contribution is treated, it may introduce a discrepancy in the evaluation of the reliability index according to the approximate procedure presented earlier. To overcome this problem, a generalized safety factor, F, may be used to define the satisfactory performance of a geotechnical system. The safety factor can be represented by a general performance function

$$F = g(X_1, X_2, \ldots, X_m) \qquad (A.10)$$

where the X_i's are the component variables. In fact, this formulation is more general, because the resistance is usually a function of soil properties and geometric variables. Moreover, performance pertaining to settlement or leakage rate may be more conveniently expressed as a function of the loads, hydraulic head, soil, and other geometric variables instead of the ratio R/L.

In principle, for given PDF of each of the component variables in the performance function in Eq. (A.10), the probability that $\{F < 1\}$ can be calculated. However, the calculation can be mathematically cumbersome, involving many levels of analytical or numerical integration. Moreover, the engineer may be able to estimate perhaps only the mean value and the c.o.v. (but not the PDF) of most of the component variables due to a general lack of data. As a result, one may need to resort to approximate procedures for evaluating the probability of failure.

Consider the first case where the PDF of each component variable is satisfactorily prescribed by the engineer. The mathematical problem of performing the multiple integration can be avoided by using Monte Carlo simulation. By this procedure, values of the component variables are randomly generated according the their respective PDFs; these values are then used to calculate the value of the safety factor. By repeating this process many times, the probability of failure can be estimated by the proportion of times that the safety factor is less than one. The estimate is reasonably accurate only if the number of simulations is very large; also, the smaller the probability of failure, the larger the number of simulations that will be required. When the PDF of some (or even all) of the component variables are not prescribed but their mean values and c.o.v.'s are available, the first-order reliability method may be used to determine the reliability index and the corresponding probability of failure approximately. The method is based on the truncation of the Taylor series expansion of the safety factor beyond the first-order term. Therefore, the method will yield a good approximation if the function $g(\cdot)$ is nearly linear or if the uncertainties of the component variables are small, for example if the c.o.v. is less than 15 percent. Otherwise, the results may be inaccurate or difficult to obtain. The second-order reliability method has been successful in improving the accuracy of the results in some cases. Essentially, this method retains one more term in the Taylor series expansion; hence, it can approximate some nonlinear $g(\cdot)$ better. However, the method generally requires additional information about the component variables beyond their mean and c.o.v. values, for instance their probability distribution type. for more details of the first-order and second-order reliability method procedures, refer to Ang and Tang (1984) and Madsen et al. (1986).

A simpler use of the first-order method is to relate the c.o.v. of the safety factor to the c.o.v.'s of the component variables. For instance, the c.o.v. of the safety factor in Eq. (A.10) is approximately equal to

$$\delta_F = \sqrt{\sum_i S_i^2 \delta_i^2} \qquad (A.11)$$

where δ_i is the c.o.v. of each variable X_i, and S_i is the sensitivity factor denoting the percent change in safety factor for each percent of change in the value of X_i. The sensitivity factor may be determined analytically or numerically by taking the partial derivative of the function $g(\cdot)$ with respect to each variable. Both the sensitivity factor and the c.o.v. of the component variable are important in determining the contribution of a given variable to the c.o.v. of F. The benefit of an uncertainty analysis, such as that in Eq. (A.11), is that the relative contribution of uncertainties from each variable, including the model error, can be compared on a consistent basis. This information can help the allocation of future research efforts or additional site explorations, because one can identify the variables that have the most effect on (or contribution to) the overall c.o.v. of the safety factor. Reduction of the c.o.v. in these variables will likely yield the largest improvement in the reliability of the current system as well as similar systems in the future. Finally, for a geotechnical system whose performance involves complex numerical procedures in lieu of an analytical function, the point estimate method proposed by Rosenblueth (1975) can be used efficiently to obtain approximate estimates of the mean and c.o.v. of the safety factor.

A.6 Reliability-Based Design

The discussion thus far has focused on evaluating the reliability of a geotechnical system when the uncertainties of the pertinent variables are defined. In a design situation, one would be interested in choosing a design that will achieve a desired or prescribed level of safety. As shown earlier in Figs. A.4 and A.5, a geotechnical engineer can increase the reliability by increasing the mean resistance, by reducing the c.o.v. of the resistance, or by decreasing the loads. To obtain a higher ratio of mean resistance to the design load, one can deliberately adopt a low or conservative value as the design resistance to be checked against the designed load. This in turn will yield a mean resistance that has a high value relative to the design load. for instance, the design resistance may be a fraction of the mean resistance, which can be obtained by introducing a resistance factor ϕ (smaller than one) to be multiplied by the mean resistance. By applying the first-order reliability method, one can determine the appropriate value of the resistance factor from the following equation

$$\phi_i = 1 - \alpha_i^* \beta \delta_i \qquad (A.12)$$

which shows that the resistance factor ϕ_i depends on the uncertainty level of the ith variable (given by c.o.v. δ_i), the desired level of reliability (given by β), and a coefficient α_i^* that measures the sensitivity of the ith variable relative to the other component variables. With this approach, the more uncertain variables (i.e., those with large δ_i or the more important variables (i.e., those with large α_i^*) will have relatively smaller resistance factors ϕ_i.

Alternatively, the design resistance can be obtained by dividing the mean resistance by a factor γ (larger than one). The relationship between the two factors is simply $\gamma = 1/\phi$. Eurocode No. 7, Geotechnics, prefers to use γ as the resistance factor.

In determining the resistance factors for geotechnical design in the proposed design code based on Load and Resistance Factor Design procedures, a value of β should be used that is about the same as the average β associated with the current design. In other words, it is implicitly assumed that the average reliability level of the current designed is found to be acceptable and desirable.

A.7 Multiple Modes of Failure

Safety of a geotechnical system may involve its satisfactory performance with respect to several model of failure. For instance, a retaining wall could fail by overturning, sliding, or inadequate bearing capacity. Realistically, each of the failure modes could happen, reducing failure of the system. The probability of foundation failure will generally increase with the number of potential model. Pertinent questions include: "Which mode is critical, or most likely to occur?" and "How much additional risk is contributed by the noncritical failure modes?" Probabilistic analysis can provide answers to these questions by evaluating the probability of failure of each mode and can further calculate the probability that at least one mode will fail (i.e., system failure). For example, in the case of a foundation subject to two modes of failure, the probability of system failure is given by the probability of the union of the two failure events E_1 and E_2 namely

$$\mathrm{P}[E_1 \cup E_2] = \mathrm{P}[E_1] + \mathrm{P}[E_2] - \mathrm{P}[E_1 \cap E_2] \qquad (A.13)$$

which is the sum of the individual failure probabilities after subtracting the probability that both modes occur. The last term in Eq. (A.13) will be simply the product of $\mathrm{P}[E_1]$ and $\mathrm{P}[E_2]$ if the two failure modes are statistically independent or unrelated. It is recognized that the consequences, such as physical damages, of these failure modes are not necessarily the same. Hence, to assess the potential losses or damages in addition to the overall probability, one should assess the probability of individual failure modes, weigh each by the respective loss, and combine each contribution to determine the overall expected loss. On the other hand, the failure of a geotechnical system may sometimes require the failure of a number of component events together. For instance, in the example of dam design in karst terrain, the event of failure is the uncontrolled reservoir release, which requires the occurrence of the following five events: (1) existence of a foundation sinkhole; (2) collapse of sinkhole; (3) dike fill cracks; (4) piping, and (5) dike breaching. The probability of the failure event in this case is the product of the five component probabilities, which is much smaller than any of the individual component probabilities.

Consider next the case of a geotechnical system consisting of several components. for instance, the foundation of an offshore platform may consist of many similar piles. for a given direction of wave loading, the pile subjected to the largest load (defined as the critical pile) may not necessarily be the first to fail; in fact, each of the piles could be the first to fail. Again, one would be interested in how much additional risk is contributed by the noncritical piles toward initial failure of the pile system. Fortunately, the failure of the first pile in this case is not likely to lead to collapse of the platform system. It may require the failure of several more piles before the pile system fails completely. A pertinent question is "What is the additional reserve implicit in the pile system beyond the failure of the first pile?" Probabilistic methods can be used to evaluate the relative likelihood of various failure-path scenarios. Moreover, these methods can provide a measure of the redundancy accounting for the combined effect of the *expected* reserve capacity as well as the *uncertainties* in the system. For example, a redundancy factor can be defined as the ratio of probability of initial failure to the probability of complete system failure. In other words, if there is only a small likelihood of system failure given that a component has already failed, or if system failure is very unlikely compared with initial failure, the redundancy factor will assume a large value as expected.

The importance of system consideration in reliability evaluation cannot be understated. In the case of slopes, sliding can occur along one of the many slip surfaces. For a long tunnel system, collapse also can occur at any section. Because most of the reliability analysis is based on the critical slip surface or the critical cross section of the tunnel, procedures are needed to extrapolate these critical component probabilities to those of the entire geotechnical system. Probabilistic methods can provide the necessary analytical framework.

A.8 Updating of Information

Geotechnical engineers traditionally have used the observational method to help them deal with uncertainties in site conditions or performance behaviour. The engineer will begin with a few hypotheses about the site conditions, and field observations are then gathered to pinpoint the correct hypothesis. This procedure can be formalized by applying probability theory. Whenever there is additional information about the site, be it from a site exploration program for a new site, measurements from nondestructive diagnostic tests for an existing infrastructure, or observations during an early phase of construction, Bayesian probability procedures provide a logical basis for revising the engineer's judgement of the site characteristics. Conceptually, the updated probability of a given hypothesis, H_1, based on observation, E, is determined from Bayes' theorem as

$$\mathrm{P}''[H_1] = k\mathrm{L}[E \mid H_1]\mathrm{P}'[H_1] \qquad (A.14)$$

where $\mathrm{P}'[H_1]$ may represent the estimated probability of Hypothesis 1 prior to the observation; $\mathrm{L}[E \mid H_1]$, commonly referred to as the likelihood function, is the likelihood of Hypothesis 1 producing the observation, and k is a normalizing constant such that the sum of the updated probabilities of all potential hypotheses will be 1.0. Essentially, the likelihood function represents information from the observation; it is used to modify the prior judgemental probabilities to obtain the updated probabilities. Bayes' theorem thus furnishes a systematic means of quantifying relative likelihood of the respective conceptual models in light of the observations and the respective reliability associated with each observation scheme. These probability values can be used to discriminate between contending models; they also can be used to update the performance reliability of a proposed geotechnical system. More importantly, by explicitly considering the relative reliability of respective observation schemes and relative likelihood of the conceptual models before and after the observations, the usefulness of each observation scheme in improving the overall system performance can be compared beforehand. This will facilitate the selection of what to measure or observe. Waste-remediation decisions, which increasingly involve geotechnical engineers, can benefit greatly from the above-described probabilistic observational method; this is also true for many other geotechnical applications, ranging from dam safety to repair/maintenance decisions concerning deteriorating infrastructures.

Hachich and Vanmarcke (1983) demonstrated an application of Bayesian methods to update the relative likelihood of two hypotheses of the drainage conditions of a dam based on piezometer measurements. The method was used by Tang et al. (1994) to update the coefficient of compression of waste material based on a set of settlement plates installed at a landfill site. These authors also showed how the Bayesian updating procedure could be incorporated in a probabilistic observational method to facilitate decisions associated with a landfill cover design. The following simple example demonstrates the essence of the Bayesian updating procedure:

Example

> Leakage of contaminated material is suspected from a given landfill. Monitoring wells are proposed to verify if leakage has occurred. The locations to two wells are shown in Fig. A.6. For simplicity, suppose that if leakage has occurred, the engineer estimates that the probability that it will be observed by Well A is 80 percent, whereas well B is 90 percent likely to detect the leakage.
>
> Assuming that neither well will erroneously register any contamination if there is no leakage from the landfill. Before any of these wells is installed, the engineer believes that there is a 70 percent chance that the leakage has happened. Consider first the case that well A has been installed and no contaminants have been observed. Clearly, the engineer's

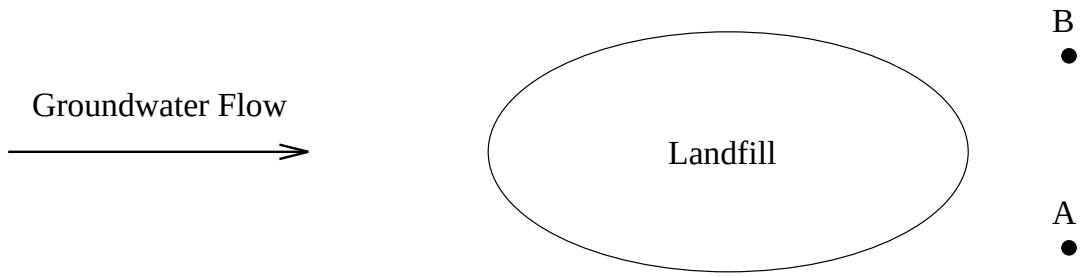

Figure A.6 Locations of monitoring wells for potential leakage of contaminants from a landfill.

belief that leakage has occurred will decrease. With this observation, Bayes' theorem yields

$$\mathrm{P}\left[L \mid \bar{A}\right] = \frac{\mathrm{P}\left[\bar{A} \mid L\right]\mathrm{P}[L]}{\mathrm{P}\left[\bar{A} \mid L\right]\mathrm{P}[L] + \mathrm{P}\left[\bar{A} \mid \bar{L}\right]\mathrm{P}\left[\bar{L}\right]} = \frac{0.2 \times 0.7}{0.2 \times 0.7 + 1 \times 0.3} = 0.318$$

where L denotes the event of leakage, $\bar{L}$ denotes the event of no leakage, A denotes the event of well A detecting contamination, $\bar{A}$ denotes the event of well A not detecting contamination, and $\mathrm{P}[L]$ is the engineer's estimate of leakage probability. In probability theory, $\mathrm{P}\left[L \mid \bar{A}\right]$ represents the *conditional probability*, namely the probability of leakage given that well A did not detect contaminants. Although the observation from well A seems to support the hypothesis that leakage has not occurred, the hypothesis cannot be fully substantiated because of the imperfect detectability of well A and also because of the engineer's prior judgment. By considering these factors, the engineer would now believe that there is only a 31.8 percent chance that leakage has occurred.

Suppose well B also has been installed, and it also fails to detect any contamination. By applying Bayes' theorem again, the probability of leakage based on the combined observations that both wells did not detect contamination is

$$\begin{aligned}\mathrm{P}\left[L \mid \bar{A} \cap \bar{B}\right] &= \frac{\mathrm{P}\left[\bar{A} \cap \bar{B} \mid L\right]\mathrm{P}[L]}{\mathrm{P}\left[\bar{A} \cap \bar{B} \mid L\right]\mathrm{P}[L] + \mathrm{P}\left[\bar{A} \cap \bar{B} \mid \bar{L}\right]\mathrm{P}\left[\bar{L}\right]} \\ &= \frac{0.2 \times 0.1 \times 0.7}{0.2 \times 0.1 \times 0.7 + 1 \times 1 \times 0.3} = 0.045 \qquad (A.15)\end{aligned}$$

In the above calculation, the detectabilities between the wells have been assumed independent for simplicity. Hence, $\mathrm{P}\left[\bar{A} \cap \bar{B} \mid L\right]$ is simply the product of $\mathrm{P}\left[\bar{A} \mid L\right]$ and $\mathrm{P}\left[\bar{B} \mid L\right]$. The results show that the observations from the two monitoring wells apparently imply that there is practically no likelihood of a leak. However, because of the imperfect reliability of the wells in diagnosing the leakage event, there is still a probability, though very small, that leakage has indeed happened.

A.9 Uncertainty in Mapping of Material Types

Uncertainty in mapping arises when it is necessary to infer the type of soil material that exists at unobserved points from data obtained at points of observation. An example is the inference of the soil profile from borehole information during the characterization phase of a site. The question is, "What is the probability of finding a specific material type at a point, given that the material has been found or not found at another point or points?" The probability can be evaluated with the application of Bayesian methods, given a geological model of the spatial distribution of the material type. Wu et al. (1989) presented contour maps showing the probability of encountering clay at a given point in a soil stratum based on borehole samples and cone penetration records collected at a North Sea site. In fact, Bayes' theorem has been used extensively in conjunction with site characterization (e.g., Baecher, 1972; Wu and Wong, 1981). For instance, the unexpected presence of geologic anomalies, such as pockets of weak material in as stiff soil stratum or sand lenses in an otherwise impermeable clay stratum, can cause geotechnical failures. Even if a given site exploration program has not encountered such geologic anomaly, the experience of the engineer with the geology of the region may suggest that it could still by present at the site. In this case, the engineer's judgment can be combined with the level of site exploration efforts spent (e.g., number of borings) by means of the Bayesian procedure to estimate the likelihood of anomaly presence and the probability distribution of its size and location (Halim and Tang, 1993). The effects of these potential geologic anomalies then can be incorporated in the reliability evaluation of the geotechnical system.

A.10 Decision Under Uncertainty

Very often, engineers- or more appropriately, their clients-have to decide between alternatives that comprise different levels of expenditure and different probabilities of success. To rank a set of design alternatives, the potential risk associated with a given alternative should be considered, as well as the capital cost of the alternative. A decision tree, such as that shown in Fig. A.7 for a landslide mitigation decision at a given site, can be used. The procedure identifies first the available alternatives of action and the possible outcomes, or sequences of outcome events associated with each alternative. Then the respective consequences or costs for each scenario or path can be assessed. The probability of each branch of outcome can be determined either from probabilistic models or by the engineer's judgement based on the available information. The probability of a path is simply the product of the respective probabilities. The expected cost of each alternative is the summation of the path probability multiplied by the path consequence over all outcome scenarios for that alternative. The alternative with the least expected cost is considered optimal if the commonly used expected value criteria is adopted for the decision. In this example, the optimal alternative for landslide mitigation at the site is to install a drainage system.

When the input probabilities and costs to the above decision analysis are only crude estimates, a sensitivity analysis should be performed to check if the optimal alternative will change within the estimated range of values for each probability or cost (see, e.g., Vick and Bromwell, 1989; Massmann et al., 1991).

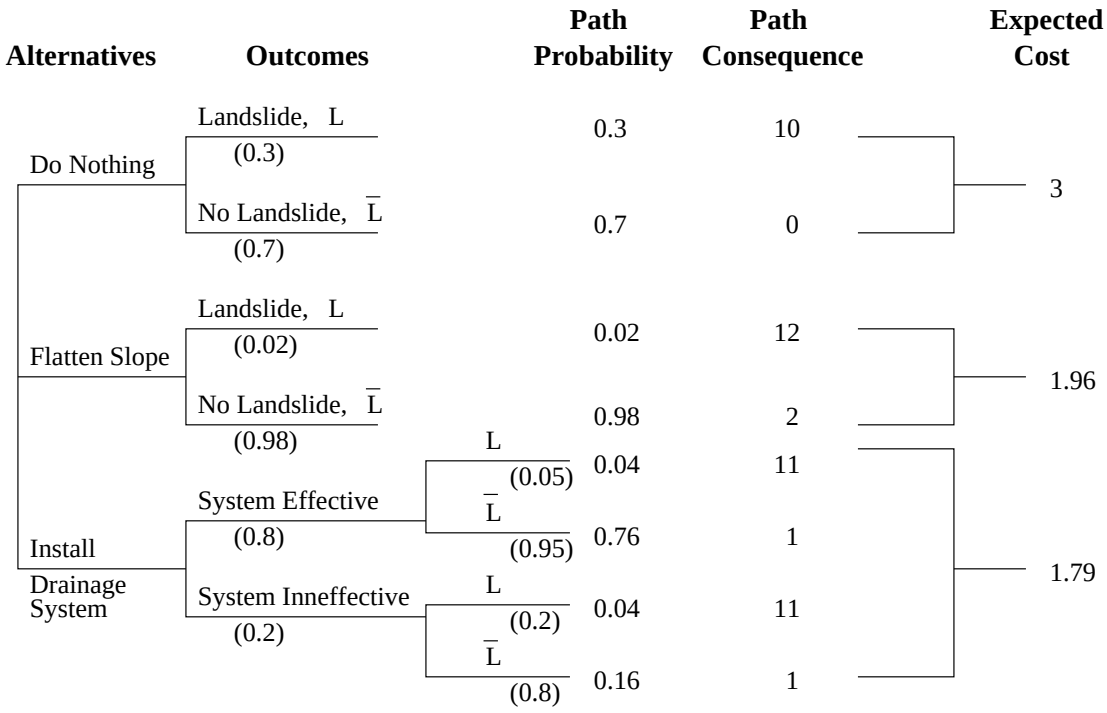

Figure A.7 Decision tree for landslide mitigation.

Appendix B A Selected Bibliography

B.1 Articles and Books

AMERICAN PETROLEUM INSTITUTE, 1986. Recommended practice for planning, design and constructing fixed offshore platforms. *API Recommended Practice 2A*, Sixteenth Edition. Washington, D.C.

ANG, H.A.-S., and TANG, W.H., 1975. *Probability Concepts in Engineering Planning and Design, Vol. 1: Basic Principles*, John Wiley & Sons, New York.

ANG, A.H.-S., and TANG, W.H., 1984. *Probability Concepts in Engineering Planning and Design, Vol. 11: Decision, Risk and Reliability*, John Wiley & Sons, New York: Currently distributed by BookMasters, Inc., Ohio.

BAECHER, G.B., 1972. *Site Exploration: A Probabilistic Approach*, PhD Thesis, Massachusetts Institute of Technology, Cambridge, Massachusetts.

BAECHER, G.B., 1979. Analyzing exploration strategies. Site Characterization and Exploration, C.H. Dowding, ed., New York: American Society of Civil Engineers.

BAECHER, G.B., 1986. Geotechnical error analysis. Pp. 23–31 in *Structure Foundations*, Transportation Research Record 1105. Transportation Research Board, National Research Council, Washington, D.C.

BENJAMIN, J.R., and CORNELL, C.A., 1970. *Probability, Statistics and Decision for Civil Engineers*, McGraw-Hill, New York.

BENSON, C.H., and CHARBENEAU, R.J., 1991. Reliability analysis for time of travel in compacted soil liners. Pp 456–467 in *Geotechnical Engineering Congress 1991*, ASCE Geotechnical Special Publication No. 27, New York.

BERAN, J., 1994. *Statistics for Long-Memory Processes*, Chapman & Hall, New York.

BORGARDI, I., KELLY, W.E., and BARDOSSY, A., 1989. Reliability model for soil liner: Initial design, *ASCE Journal of Geotechnical Engineering*, **115**(5), pp. 658–669.

BORGARDI, I., KELLY, W.E., and BARDOSSY, A., 1990. Reliability model for soil liner: Postconstruction, *ASCE Journal of Geotechnical Engineering*, **116**(10), pp. 1502–1520.

CHOWDURY, R., TANG, W.H., and SIDI, I., 1987. Reliability model of progressive slope failure, *Géotechnique* **37**(4), pp. 467–481.

DE FENETTI, B., 1970. *Theory of Probability*, transl. by A. Machi and A. Smith, John Wiley & Sons, New York.

DUNCAN, J.M., JAVETTE, D.F., AND STARK, T.D., 1991. The importance of a dessicated crust on clay settlements, *Soils and Foundations*, **31**(3), pp. 73–90.

EINSTEIN, H.H., LABRECHE, D.A., MARKOW, M.J., and BAECHER, G.B., 1978. Decision analysis applied to rock tunnel exploration, *Engineering Geology*, **12**(2), pp. 143–161.

EINSTEIN, H.H., and BAECHER, G.B., 1983. Probabilistic and statistical methods in engineering geology, Part 1. Explorations, *Rock Mechanics and Rock Engineering*, **16**(1), pp. 39–72.

FENTON, G.A., 1994. Error evaluation of three random field generators, *ASCE Journal of Engineering Mechanics*, **120**(12), pp. 2478–2497.

FENTON, G.A., and GRIFFITHS, D.V., 1993. Statistics of block conductivity through a simple bounded stochastic medium, *Water Resources Research*, **29**(6), pp. 1825–1830.

FENTON, G.A., 1990. *Simulation and Analysis of Random Fields*, Ph.D. Thesis, Princeton University, Princeton, New Jersey.

FENTON, G.A., and VANMARCKE, E.H., 1990. Simulation of random fields via local average subdivision, *ASCE Journal of Engineering Mechanics*, **116**(8), pp. 1733–1749.

FENTON, G.A., and VANMARCKE, E.H., 1991. Spatial variation in liquefaction risk assessment, pp. 594–607 in *Geotechnical Engineering Congress 1991*, ASCE Geotechnical Special Publication No. 27, Vol. I, New York.

FOLAYAN, J.I., HOEG, K., and BENJAMIN, J.R., 1970. Decision theory applied to settlement predictions, *ASCE Journal of Soil Mechanics and Foundations Division*, **96**(SM4), pp. 1127-1141.

FREEZE, R.A., MASSMANN, J., SMITH, L., SPERLING, T., and JAMES, B., 1990. Hydrogeological decision analysis: 1. A framework, *Ground Water*, **28**(5), pp. 738–766.

GILBERT, R.B., 1996. A model to design QA/QC programs for geomembrane liner seams, *ASCE Journal of Engineering Mechanics*, in press.

GILBERT, R.B., and TANG, W.H., 1995. Reliability-based design of waste containment systems, *Proceedings of Geoenvironment 2000*, ASCE Specialty Conference, New Orleans, Louisiana, pp. 499–513.

GRIFFITHS, D.V., and FENTON, G.A., 1993. Seepage beneath water retaining structures founded on spatially random soil, *Géotechnique*, **43**(4), pp. 577–587.

HACHICH, W., and VANMARCKE, E.H., 1983. Probabilistic updating of pore pressure fields, *ASCE Journal of Geotechnical Engineering*, **109**(3), pp. 373–385.

HALDAR, A., and TANG, W.H., 1979. A probabilistic evaluation of liquefaction potential, *ASCE Journal of Geotechnical Engineering*, **105**(GT2), pp. 145–163.

HALIM, I.S., and TANG, W.H., 1993. Site exploration strategy for geologic anomaly characterization, *ASCE Journal of Geotechnical Engineering*, **119**(2), pp. 195–213.

HALIM, I.S., and TANG, W.H., 1990. Bayesian method for characterization of geological anomaly, pp. 585–594 in *Proceedings of The First International Symposium on Uncertainty Modeling and Analysis*, '90 (ISUMA), Los Alamitos, California, IEEE-Computer Society Press.

HAMPTON, J.M., MOORE, P.G., and THOMAS, H., 1973. Subjective probability and its measurement, *J. Royal Statistical Soc.*, Series A, **136**, pp. 21–42.

HARR, M.E., 1977. *Mechanics of Particulate Media*, McGraw-Hill, New York.

HARR, M.E., 1987. *Reliability-Based Design in Civil Engineering*, McGraw-Hill, New York.

HOEG, K., and MURAKA, R.P., 1974. Probabilistic analysis and design of a retaining wall, *ASCE Journal of Geotechnical Engineering*, **100**(GT3), pp. 349–366.

LOENARDS, G.A., 1982. Investigation of failures. *ASCE Journal of Geotechnical Engineering*, **108**(GT2), pp. 185–246.

LUMB, P., 1974. Application of statistics in soil mechanics, pp. 44-112 in *Soil Mechanics: New Horizons*, I.K. Lee, ed., Newnes-Butterworth, London.

MADSEN, H.O., KWENK, S., and LIND, N.C., 1986. *Methods of Structural Safety,* Prentice-Hall, Inc., Englewood Cliffs, New Jersey.

MASSMANN, J., FREEZE, R.A., SMITH, L., SPERLING, T., and JAMES, B., 1991. Hydrogeologic decision analysis: 2. Applications to ground-water contamination. *Ground Water*, **29**(4), pp. 536–548.

MATSUO, M., and ASAOKA, A., 1982. Bayesian calibration of embankment safety under earthquake loading, *Structural Safety*, **2**(1), pp. 53–65.

MCGRATH, T.C., GILBERT, R.B. and MCKINNEY, D.C., 1996. Value and reliability of DNAPL-source location programs: A preliminary framework, *Proceedings of DNAPL*, ASCE Specialty Conference, Washington, in press.

MEYERHOF, G.G., 1976. Concepts of safety in foundation engineering ashore and offshore, pp. 501–515 in *Proceedings of the 1st International Conference on the Behavior or Offshore Structures*, Trondheim, Norway, Vol. 1.

MORRIS, P.A., 1974. Decision analysis expert use, *Management Science*, **20**(9), pp. 1233–1241.

NATIONAL RESEARCH COUNCIL, 1982. *Risk and Decision Making; Perspectives and Research*, Committee on Risk and Decision Making, NRC. National Academic Press, Washington, D.C.

OLSON, R.E., and DENNIS, N.D., 1982. Review and compilation of pile test results, axial pile capacity. *Geotechnical Engineering Report CR83-4*, University of Texas, Department of Civil Engineering, Austin, Texas.

PECK, R.B., 1969. Advantages and limitations of the observational method in applied soil mechanics, *Géotechnique*, **19**(2), pp. 171–187.

PECK, R.B., 1980. Where has all the judgement gone?, *Canadian Geotechnical Journal*, **17**, pp. 584–590.

PHOON, K.K., QUEK, S.T., CHOW, Y.K., and LEE, S.L., 1990. Reliability analysis of pile settlement, *ASCE Journal of Geotechnical Engineering*, **116**(11), pp. 1717–1735.

ROBERDS, W.J., 1991. Methodology for Optimizing Rock Slope Preventative Maintenance Programs, in *Proceedings of the ASCE Geotechnical Engineering Congress*, Geotechnical Special Publication No. 27, Vol. 1, Boulder, Colorado, pp 634–645.

ROSENBLUETH, E., 1975. Point estimates for probability moments, *Proceedings of National Academy of Sciences of the United States of America*, **72**(10), pp. 3812-3814.

SPETZLER, C.S., and STAEL VON HOLSTEIN, C-A., 1975. Probability encoding in decision analysis, *Management Science*, **22**(3), pp. 340–358.

TANG, W.H., 1971. A Bayesian evaluation of information for foundation engineering design, *First Intern. Conf. on Applications of Statistics and Probability to Soil and Structural Engrg.*, Hong Kong, pp 174–185.

TANG, W.H., 1984. Principles of probabilistic characterization of soil properties, *Probabilistic Characterization of Soil Properties*, D.S. Bowles and Hon-Kim Ko, eds., ASCE, New York, pp. 74–89.

TANG, W.H., 1988. Offshore Axial Pile Design Reliability, Final Report for Project PRAC 86-29B sponsored by the American Petroleum Institute. Copies of this report may be obtained from the American Petroleum Institute, Washington, D.C.

TANG, W.H., 1989. Uncertainties in offshore axial pile capacity, *Foundation Engineering: Current Principles and Practice*, F.H. Kulhawy, ed., ASCE, New York, pp. 833–847.

TANG, W.H., GILBERT, R.B., ANGULO, M., and WILLIAMS, R.S., 1994. Probabilistic observation method for settlement-based design of a landfill cover, *Vertical and Horizontal Deformations of Foundations and Embankments*, Yeung and Felio, eds., ASCE Geotechnical Special Publication No. 40, New York, pp. 1573–1589.

TANG, W.H., YUCEMEN, M.S., and ANG, A.H.-S., 1976. Probability-based short term design of soil slopes, *Canadian Geotechnical Journal*, **13**, pp. 201–215.

TANG, W.H., 1993. Recent developments in geotechnical reliability, pp. 3–28 in *Probabilistic Methods in Geotechnical Engineering*, K.S. Li and S-C.R. Lo, eds., A.A. Balkema, Rotterdam.

VANMARCKE, E.H., 1974. Decision Analysis in Dam Safety Monitoring, in *Proceedings of the Engineering Foundation Conference on Safety of Small Dams*, ASCE, New Hampshire, Aug 4-9, pp 127–148.

VANMARCKE, E.H., 1976. Probabilistic Modeling of Soil Profiles, *ASCE Journal of Geotechnical Engineering*, **103**(11), pp. 1227–1246.

VANMARCKE, E.H., 1976. Reliability of earth slopes, *ASCE Journal of Geotechnical Engineering*, **103**(11), pp. 1247–1265.

VANMARCKE, E.H., 1983. *Random Fields: Analysis and Synthesis*, M.I.T. Press, Cambridge, Massachusetts.

VANMARCKE, E.H., 1989. Reliability in Foundation Engineering Practice, in *Foundation Engineering: Current Principles and Practice*, Proc. ASCE Conference, Evanston, Illinios, pp 1658–1669.

VANMARCKE, E.H., HEREDIA-ZAVONI, E., and FENTON, G.A., 1993. Conditional simulation of spatially correlated earthquake ground, *ASCE Journal of Engineering Mechanics*, **119**(11), pp. 2333–2352.

VICK, S.G., 1992. Risk in geotechnical practice, *Geotechnique and Natural Hazards*, BiTech Publishers, Ltd., Richmond, British Columbia, pp. 41–62.

VICK, S.G., and BROMWELL, L.G., 1989. Risk analysis for dam design in karst, *ASCE Journal of Geotechnical Engineering*, **115**(6), pp. 819–835.

VICK, S.G., 1992. Risk in geotechnical practice, *Geotechnical News*, **10**, pp. 55–57.

WU, T.H., 1974. Uncertainty, safety and decision in civil engineering, *ASCE Journal of Geotechnical Engineering*, **100**(GT3), pp. 329–348.

WU, T.H., 1989. Variability of geological materials, pp. 221–239 in *The Art and Science of Geotechnical Engineering at the Dawn of the Twenty-First Century*, E.J. Cording *et al.*, eds., Prentice-Hall, Englewood Cliffs, New Jersey.

WU, T.H., and WONG, K.F., 1981. Probabilistic soil exploration: Case history. *ASCE Journal of Geotechnical Engineering*, **107**(GT12), pp. 1693–1711.

WU, T.H., LEE, I-M., POTTER, J.C., and KJOKSTAD, O., 1987. Uncertainties in evaluation of strength of a marine sand, *J. Geotechnical Engrg.*, **113**(7), pp. 719–738.

WU, T.H., KJEKSTAD, O., LEE, I.M., and LACASSE, S., 1989. Reliability analysis of foundation stability for gravity platforms in the North Sea, *Canadian Geotechnical Journal*, **26**, pp. 359–368.

YEGIAN, M.K., and WHITMAN, R.V., 1978. Risk analysis for ground failure by liquefaction, *ASCE Journal of Geotechnical Engineering*, **104**(GT7), pp. 921–938.

B.2 Conference Proceedings

Proceedings of International Conferences on Applications of Statistics and Probability to Soil and Structural Engineering (ICASP),
Hong Kong, 1971
Aachen, 1975
Sydney, 1979
Florence, 1983
Vancouver, 1987
Mexico City, 1991
Paris, 1995

Proceedings of the International Conferences on Structural Safety and Reliability (ICOSSAR),
Munich, 1977
Trondheim, 1981
Kobe, 1985
San Francisco, 1989
Innsbruck, 1993

Probability Theory and Reliability Analysis in Geotechnical Engineering,
D.A. Grivas, ed., Report of an NSF Workshop at Rensselaer Polytechnic Institute, 1966, RPI, New York.

The Practice of Geotechnical Engineering – Decision Making Under Uncertainty,
ASCE National Convention, Session 35, Atlanta Georgia, 1979.

Reliability Analysis and Geotechnical Engineering,
ASCE National Convention, Boston, Massachusetts, ASCE New York, 1979.

Proceedings, Seminar on Probabilistic Methods in Geotechnical Engineering,
Sept. 1982, Vicksburg, Mississipi.

Probabilistic Characterization of Soil Properties: Bridge Between Theory and Practice,
ASCE National Convention, Atlanta, Georgia, ASCE New York, 1984.

Selected Topics in Geotechnical Engineering – Lumb Volume,
K.S. Li, ed., Dept. of Civil Engineering, University College, University of New South Wales, Canberra, Australia, 1991.

Proceedings of Conference on Probabilistic Methods in Geotechnical Engineering,
Canberra, Australia, Feb. 1993, A.A. Balkema, Rotterdam.